Structure/Function Analysis of the Viral Potassium Channel Kcv

Mutagenesis studies of the two transmembrane domains

TECHNISCHE
UNIVERSITÄT
DARMSTADT

1. Table of contents

2. Chapter 1 - General Introduction

2.1. Ion Channels

Ion channels are transmembrane proteins, which form water filled pores through the biological lipid bilayer and allow in this way the passage of ions down the electrochemical gradient. The presence of ion channels can decrease the energy barrier for the transport of ions across the membrane from about 50 kcal* mol^{-1} (Parsegian 1969) down to just about 2 to 3 kcal* mol^{-1} (Berneche and Roux 2001). Ion channels are classified by means of their ion selectivity and gating mechanisms. Due to this classification, the family of ion channels can further be distinguished by their gating properties into: ligand-gated ion channels (LGICs), cyclic nucleotide gated channels (CNG channels), transient receptor potential channels (TRP channels), mechanosensitive ion channels (MS channels), light-gated channels, Chloride channels (ClCs), Voltage-gated sodium channels (Na_v channels), Voltage-gated calcium channels (VGCCs), Voltage-gated proton channels (H_v channels), Voltage-gated potassium channels (K_v channels) and other potassium channels (e.g. inwardly rectifying – Kir channels). Ion channels can be found in all forms of life and have an outstanding importance for a wide range of biological functions like the extreme acid resistance response of *Escherichia coli (E. coli)* (Iyer *et al.* 2002), for the communication in and between animal cells (Neher 1992), the cell turgor in plants (MacRobbie 2005) and others. Dysfunction of ion channels, so-called channelopathies, are usually linked with more or less fatal diseases like cystic fibrosis and epilepsy (ClCs), diabetes type 2 (probable Kir channels) or deafness (K_v channels) to name just a few (For a good overview see, for example, http://neuromuscular.wustl.edu/mother/chan.html). Therefore, a comprehensive understanding of the structure and function of ion channels is essentially required.

2.1.1. Potassium Channels

Potassium channels, as the name implies, are ion channels, which are highly selective for potassium ions (K^+); they conduct K^+ 10 to 1000 times better than sodium ions (Na^+) (Hille 2001). As already alluded, they are common in all kinds of life forms from bacteria up to humans. Common to all potassium channels is a homologue structural unit composed of two transmembrane domains (TMD) connected by a pore loop (P loop) with a highly conserved

signature sequence **TxxTxG(Y/F)G**; the latter is responsible for the high selectivity of the channels (Miller 1992, Jan and Jan 1992).

Usually potassium channels are tetrameric proteins (MacKinnon 1991) meaning that four subunits group together to form the pore region. A top view on an exemplary channel tetramer from the bacterial potassium channel KcsA is shown in Figure 1A and the structure of KcsA in side view is shown in Figure 1B. The four subunits generate a central pore for K^+ transport.
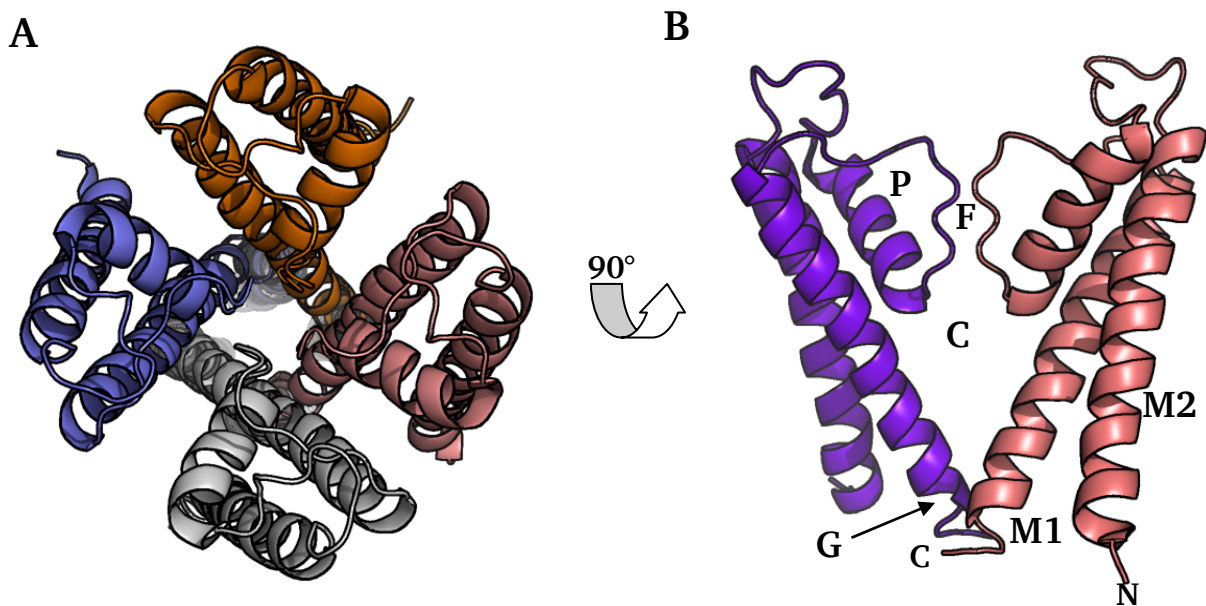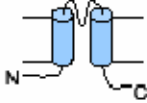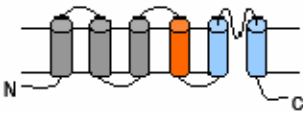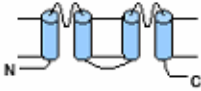
Figure 1: Structure of the bacterial potassium channel KcsA. Shown is **(A)** a cartoon of the bacterial potassium channel KcsA as a tetramer in top view (PDB-Code: 3EFF). Each of the four subunits is coloured in a different colour. In **(B)** are two out of four subunits shown as a cartoon in side view with truncated cytoplasmatic C-termini and with the two transmembrane helices (M1 and M2), the pore loop (P) and the three main functional areas: filter region (F), cavity (C) and gate (G).

Exceptions of this tetrameric architecture are the so-called tandem pore domain potassium channels, which are functional as dimers as noted below.

All K^+ channels can be classified into different families according to the number of helices in each subunit or the number of subunits. The architecture of tetrameric channels comprises the 2TMD and the 6TMD motif channels. In 2TMD motif channels one subunit consist of two transmembrane domains connected by the P loop ($TMD_1 - P - TMD_2$). In 6TMD motif channels one subunit consists of six transmembrane helices, where the P loop is located between TMD5 and TMD6 ($TMD_{1-5} - P - TMD_6$). Both channel types are functional as tetramers. The tandem pore domain potassium channels exhibit two pore domains, which are

arranged in tandem. The functional channels are built of a combination of the aforementioned motifs; one subunit either consists of two connected 2TMD motifs or of one 2TMD motif combined with a 6TMD motif. Therefore, each subunit contains already two pore domains; hence, the channels are functional as dimers.

Table 1: Overview over the different structure types and families of potassium channels (according to Hertel 2005).

Potassium Channel – Subtypes	Example	Organism
2TMD Motif		
Kir (inward rectifier)	KirBac1.1	*Burkholderia pseudomallei*
	Kir6.2	*Homo sapiens*
Channel homologues from Prokaryots	KcsA	*Streptomyces lividans*
	MthK	*M. thermoautotrohicum*
Channel homologues from algea viruses	Kcv	Chlorella Virus PBCV–1
	Kesv	Ectocarpus Virus EsV–1
6TMD Motif		
Kv (Shaker typ)	Shaker (Kv1)	*Drosophila melanogaster*
EAG (ether–à–gogo)	EAG	*Caenorhabditis elegans*
	hERG	*Homo sapiens*
Slo (BK channel)	mSlo	*Homo sapiens*
HCN (Hyperpolarization–activated cyclic nucleotide gated channels)	HCN2	*Homo sapiens*
Plant channels	KAT1	*Arabidopsis thaliana*
	AKT1	*Arabidopsis thaliana*
Two Pore Channels		
2TMD Motif + 6TMD Motif	Tok1	*Saccharomyces cerevisiae*
2x 2TMD Motifs	Cetk1	*Caenorhabditis elegans*

The aforementioned signature sequence with the consensus sequence **TxxTxG(Y/F)G** is responsible for the selectivity of the potassium channels. This is due to electrostatic interactions between the oxygen atoms of the amino acid carboxyl groups with the K^+ ions (Doyle *et al*. 1998). The oxygen atoms allocate the necessary interaction partners between protein and ion, so that the hydration shell of the ions can be removed without spending energy. From this it follows, that transition of ions occurs only if the ions have the right size to fit into the pore (Morais-Cabral *et al.* 2001). The sketch in Figure 2 shows that ions, which do not perfectly fit into this ensemble, cannot be stabilised in the pore. This disability of the carboxyl groups to mimic the hydration shell of ions, other than K^+ and Rb^+, yields in a meticulous selectivity of the channel.
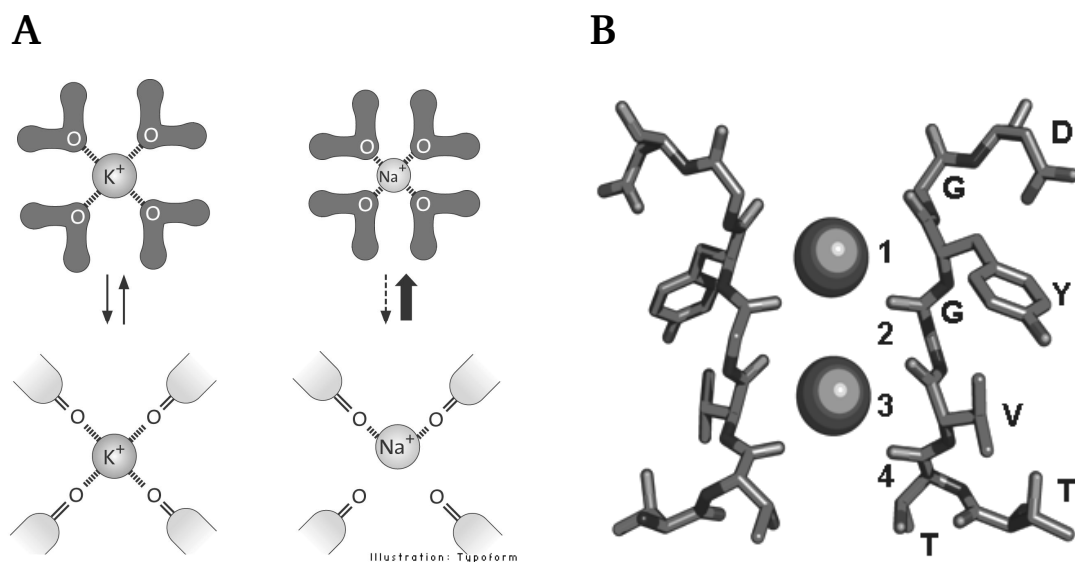
Figure 2: Top and side view of the pore from a potassium channel. (A) Shown are a cartoon of a potassium ion (upper left side) and a sodium ion (upper right side) with hydration shell. The pore of a potassium channel is able to stabilise the K^+ (lower left side, top view) but not the Na^+ (lower right side, top view) (according to http://www.bio.miami.edu). **(B)** Side view of the pore from two subunits of KcsA as ball-stick-model with the four potassium ion binding sites (numbered from 1 to 4 with two bound potassium ions) in the pore with partially highlighted signature sequence.

In addition to the selective transport of ions, the so-called permeation, a second process, namely gating, is of vital importance for a proper channel function. The molecular basis of gating is that channels have at least two functional conformations: an open and a closed state (Neher and Sakmann 1976). The exact function and position of the gates, i.e. the structures, which open and close a channel, are still ambiguous.

Currently there are two hypotheses discussed for the gating of K^+ channels:

1. Figure 3 illustrates the first hypothesis. It focuses on a bundle crossing of the second TMDs of each channel subunit on the site of the cytosol, which form a gate. This hypothesis is supported by the crystal structure of two bacterial ion channels namely KcsA in the closed (Perozo *et al.* 1999) and MthK in the open conformation (Jiang *et al.* 2002a).

Closed   Open
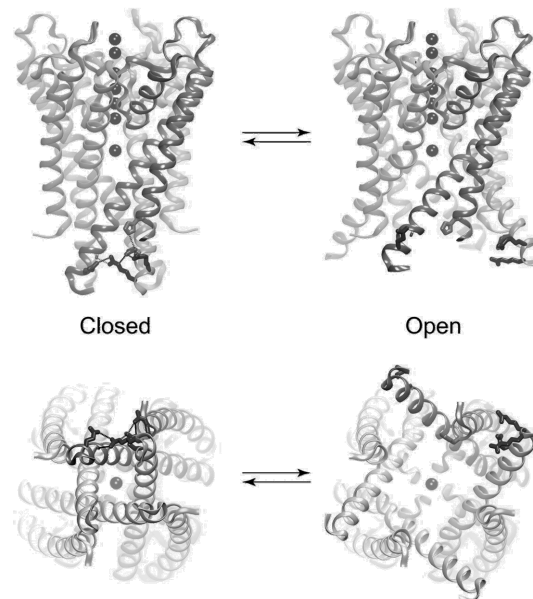
Figure 3: Model of the opening and closing of KcsA. Shown is a model of the open-to-closed transition of the four subunits of the bacterial channel KcsA as a cartoon in side (upper part) and top view (lower part) (according to Thompson *et al.* 2008).

2. The second hypothesis proposes a double function of the selectivity filter (Cordero-Morales *et al.* 2006 and 2007). According to this view, the selectivity filter is responsible for both permeation and gating. Mutational studies in the selectivity filter from the shaker potassium channel for example support this hypothesis. These mutations influence not only the selectivity of the channel but also the open probability and, hence, the gating processes (Zheng and Sigworth 1997, Lu *et al.* 2001).

Recent studies revealed that both hypotheses are not mutually exclusive and can occur simultaneously in ion channels. For example, KcsA, the model system for both processes of the bundle crossing (Perozo *et al.* 1999) and gating, exhibits in addition to the cytosolic gate a second gate in the selectivity filter (Blunck *et al.* 2006, Cuello *et al.* 2010).

2.1.2. Viral Potassium Channel Kcv

Kcv (**K**$^+$ channel **C**hlorella **V**irus) is the potassium channel from the chlorella virus PBCV-1 (*Paramecium bursaria* **C**hlorella **V**irus Type **1**). As implied by the name the virus infects Chlorella of the strain NC64A, a worldwide common unicellular alga from fresh water, which lives endosymbionticaly in *Paramecium bursaria*. This endosymbiontic lifestyle protects the algae against a viral infection but as soon as the algae are unprotected, PBCV-1 will infect and kill them immediately.

PBCV-1 belongs to the genus *Chloroviruses* a member of the family of *Phycodnaviridae*. It has a linear 330 kilobase (kb) long, double-stranded DNA genome (Van Etten *et al.* 2002), which encodes for approximately 375 proteins.

Kcv was the first known viral potassium channel and for a long time with a size of only 94 amino acids also the smallest known potassium channel (Plugge *et al.* 2000). Since then over 40 homologues of Kcv were isolated from different strains of Chlorella viruses (Kang *et al.* 2004) and also shorter potassium channels were found, like the 82 amino acid short potassium channel of ATCV-1 (*Acanthocystis turfacea* **C**hlorella **V**irus Type **1**) (Gazzarrini *et al.* 2009).

As mentioned in the previous chapter one of the basic channel structure types are the 2TMD motif channels with the overall structure of $TMD_1 - P - TMD_2$. Like all members of this subtype Kcv is functional as a tetramer (Figure 4A) (Shim *et al.* 2007, Pagliuca *et al.* 2007, Chatelain *et al.* 2009).

Kcv exhibits an only 12 amino acids long N-terminus; a cytoplasmic C-terminus is missing completely (Figure 4B). Complex potassium channels, in contrast, exhibit often large and complex cytoplasmic domains. For example, the bacterial channel KcsA belongs to the smallest potassium channels but exhibits already a 40 amino acid long cytoplasmatic C-terminus, which is important for gating (Cortes *et al.* 2001). The human potassium channel HERG (human eag-related gene), an even more complex channel of the 6TMD motif type, contains for comparison a 398 amino acid long cytoplasmatic N-terminus (Schönherr and Heinemann 1996).

Despite the small size of Kcv, the viral channel exhibits nonetheless many of the structural and functional hallmarks of the much more complex potassium channels listed in Table 1. One of these functional hallmarks is the pore region with the selectivity filter; it exhibits also the characteristic signature sequence **TxxTxGFG.** Hence, Kcv shows selectivity for monovalent

cations in the characteristic manner: Rb^+ $K^+ > Cs^+ >> Na^+ >> Li^+$. It is blocked by typical potassium channel blockers and in spite of its small size, it is still gated (Gazzarrini *et al.* 2003, Moroni *et al.* 2002, Abenavoli *et al.* 2009; Pagliuca *et al.* 2007).

Therefore, Kcv with the overall structure of $TMD_1 - P - TMD_2$ turns out to be to be the pore module of all potassium channels. For this reason Kcv is a perfect model system to study structure/function relationships with the goal to understand functional principles in potassium channels per se. This may help in the future to cure channelopathies.
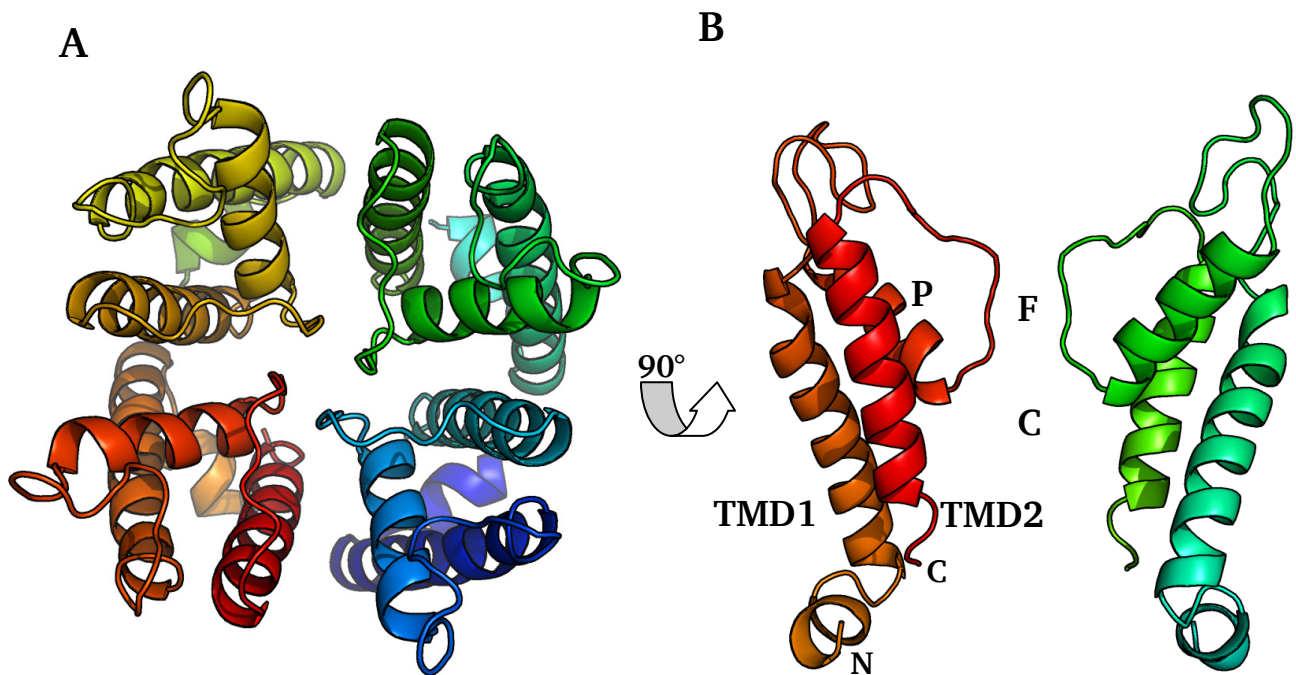
Figure 4: Structure of the viral potassium channel Kcv. Shown is **(A)** a cartoon of the viral potassium channel Kcv as a tetramer in top view. Each subunit is coloured in a different colour. In **(B)** are two out of four subunits from Kcv shown as a cartoon in side view with the two transmembrane domains (TMD1 and TMD2), the pore loop (P) and the two main functional areas: the filter region (F) and the cavity (C) (according to Tayefeh *et al.* 2009).

2.2. Interactions

As mentioned before, ion channels exhibit two distinct conformations, namely an open (conducting) state and a closed (non-conducting) state (Neher and Sakmann 1976). The switching between both conditions is called gating and controls the passage of ions through the channel.

Several processes can contribute to the regulation of gating like the binding of ligands or changes in membrane voltage. In any case, conformational changes within a protein are basic requirements to switch the protein from one to another functional state. These conformational changes lead to a partial channel movement within the lipid bilayer. For example, the bacterial potassium channel KcsA undergoes a global twisting motion during gating, and this twisting starts in the middle of the second transmembrane domain (Shimizu *et al.* 2008).

Other examples are the voltage-dependent delayed rectifier K^+ channels, which were first postulated by Hodgkin and Huxley (1952). These channels belong to the 6TMD motif channels where the fourth TMD (S4) contains several positive charged amino acids. These charged amino acids sense changes in membrane voltages and respond to changes in the electrical field with a movement of the voltage sensor (S4) within the membrane (Hille 2001). There are several hypotheses about the stabilisation and movement of this highly charged transmembrane segment in the hydrophobic membrane, which are summarised in Figure 5.
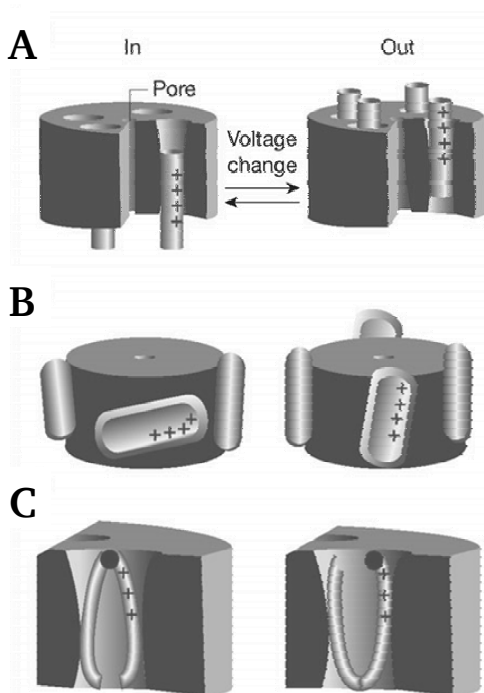
Figure 5: Different models of the voltage sensor movement of voltage-dependent ion channels. Pictured are three different models for the movement of the voltage sensor namely **(A)** the helical-screw model, **(B)** the paddle model and **(C)** the transporter-like model (according to Blaustein and Miller 2004).

Figure 5A depicts the helical-screw model, which suggests that the positive charges in S4 make electrostatic contacts with negative charges in the S2 (second TMD) and S3 (third TMD) domain. These interactions lead to a rotation and sliding of the S4 segment along the rest of the channel protein (Catterall 1986, Grabe *et al.* 2007, Guy and Seetharamulu 1986, Keynes and Elinder 1999, Lecar *et al.* 2003, Tombola *et al.* 2007). The paddle model in Figure 5B in contrast suggests that the S4 segment and the extracellular part of the S3 segment are a functional unit, which moves together across the interface between the lipid bilayer and the core of the channel protein (Jiang *et al.* 2003a, Jiang *et al.* 2003b, Long *et al.* 2005a, Long *et al.* 2005b, Long *et al.* 2007). Starace and Benzilla (2004) proposed an alternative transporter-like model, which is shown in Figure 5C. In this model, the S4 voltage sensor separates the internal and external solutions with a narrow gate, which produces a highly focused electric field due to several charges (Starace and Benzilla 2004).

Irrespective of the model, all conformational changes are linked to two important kinds of interactions namely the protein-protein-interactions between different subunits or proteins and protein-lipid-interactions between the protein and the surrounding lipid environment. These two key interactions will be explained in more detail below.

2.2.1. Protein-Protein-Interactions

Protein-protein-interactions are defined as the interactions between proteins or protein subunits. They are mediated via non-covalent interactions between the main-chain atoms (Pal and Chakrabarti 1998) or side chain atoms (Singh and Thornton 1993) of amino acid residues. These interactions are: van der Waals forces, hydrogen bonds, salt bridges and hydrophobic effects. Even though they are individually weak, they are nonetheless numerous in a protein and can, therefore, contribute substantially to the overall stabilisation of the proteins (Burley and Petsko 1988). For the same reason, they can also modify the behaviour and function of proteins by triggering conformational changes. This kind of changes in proteins, which are due to a modification of non-covalent interactions, has already been shown in numerous cases to be of vital importance in signal transduction cascades in cells (Pawson and Nash 2000).

For these signal transduction cascades and for many other processes, like cell cycle regulation, mitochondrial enzymes or cytoskeleton interactions, modular protein domains are critical elements, which mediate the protein-protein interactions, as for example 14-3-3 (Ferl 1996), ANK repeats (repeat of an 33 amino acids long motif, named after ankyrin proteins) (Sedgwick and Smerdon 1999) and dozen of others. These protein-protein-interaction domains, so-called binding interfaces, are normally around $600 - 1300$ Å^2 in size (Clackson and Wells 1995) and are characterised by a specific orientation of the involved amino acids with defined interplanar angles (Bhattacharyya *et al.* 2002). However, there are still uncertainties if the geometric arrangement of amino acid residues is only determined by the tertiary structure of the protein itself or also by the location of the amino acid residue in a given secondary structure (Bhattacharyya *et al.* 2002).

2.2.2. Protein-Lipid-Interaction

Depending on the characteristics of the proteins, they are resident and functional either in a hydrophilic environment or in the hydrophobic environment of membranes. In the case of transmembrane proteins, the interactions with the lipid environment are of great importance. Indeed, for several membrane proteins, including ion channels, it was already shown, that the lipid composition can modulate the stability and functionality of these proteins (Yau *et al.* 1998, Killian and von Heijne 2000, Killian 2003, Domene *et al.* 2003). The factors, which

dominate lipid-protein-interactions, are the different charged lipid headgroups, the saturation grades of the lipids and the variable lengths of the hydrophobic domains of the lipids relative to the length of the transmembrane domains.

It has been shown, that the charge of the phospholipid headgroups can influence the stability of proteins in the membrane. The stability of the bacterial potassium channel KcsA for example strongly depends on the charge of the phospholipids (Raja *et al.* 2007). Also the open probability depends on the lipids. As shown for KcsA, the open probability is relatively low in zwitterionic phosphatidylcholin (PC), but increases significantly with an increasing content of anionic lipids like, for example, phosphatidylserin (PS) (Marius *et al.* 2008). Other examples for the strong influence of lipids are: the inwardly rectifying potassium channel KATP (ATP-sensitive potassium channel), whose function is modulated by phosphatidylinositol (PI) (Fan and Makielski 1997); the connexin channels, which are inactive in pure PC membranes but active in the presence of about 60 % of anionic lipids like PS (Locke and Harris 2009) or the MscL channel (mechanosensitive channel of large conductance), where the presence of anionic lipids increases the transport rate of small molecules (Powl *et al.* 2008). The interactions of lipids with proteins can be very strong and specific, because these interactions often correspond with clusters of charged amino acid residues. This can be seen, for example, in MscL, where the binding of anionic lipids occurs in a cluster of three positively charged amino acid side chains (Powl *et al.* 2008). Therefore, lipids can even be co-purifyed with the protein and the lipids can be seen in the crystals in distinct pockets (Bertero *et al.* 2003). Such non-annular lipids have been recently found in KcsA where the binding of the lipids at specific protein binding sites between the subunits (Figure 6) greatly increases the stability of the channel in the tetrameric form (Triano *et al.* 2010).
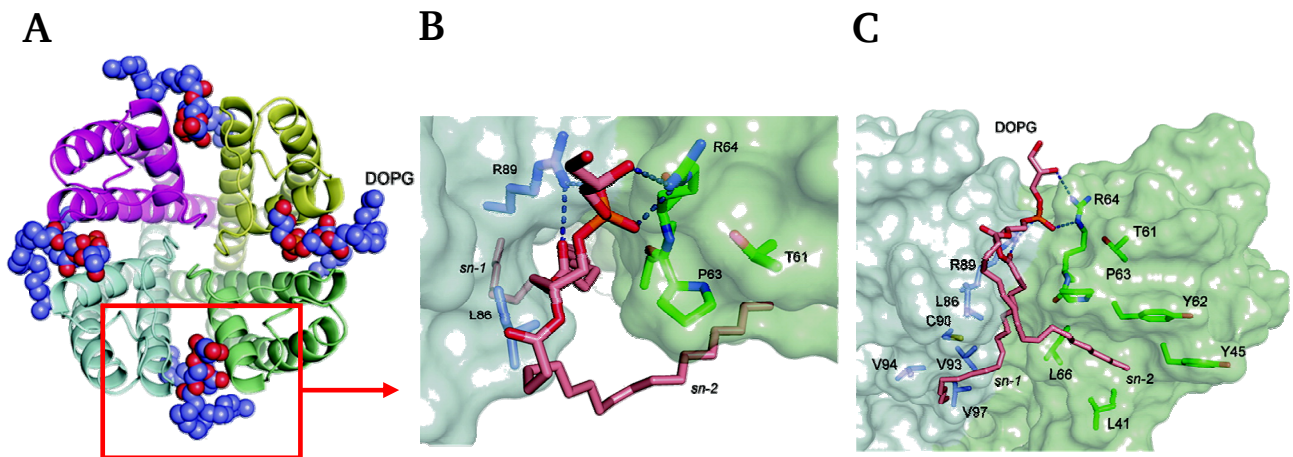
Figure 6: Molecular models of the non-annular lipids between the subunits of KcsA. Shown are **(A)** a cartoon of KcsA (PDB-Code: 1K4D) in top view with four DOPG molecules (synthetic lipid, dioleoylphosphatidylglycerol), which are bound to the non-annular protein sites between the four subunits. The scaffolds of the drawn DOPG molecules were the partial lipid structure, which appeared in the protein crystal. The close-up of the intersubunit non-annular sites in **(B)** top and **(C)** side view of two subunits includes the bound DOPG and the main amino acid residues, which are involved in the interaction with the phospholipids with hydrogen bounds marked as blue dashed lines (according to Triano *et al.* 2010).

Generally, the lipids are not buried within the structure of the proteins, but surround the surface of the TMDs, as shown in Figure 7, to solvate the proteins in the same way, as water molecules would surround water-soluble proteins (Lee 2009). Thereby, only the first "shell" of lipids, which surrounds the protein, is highly distorted to match the protein surface (Figure 7). All further lipids are arranged normally, e.g. nondistorted.
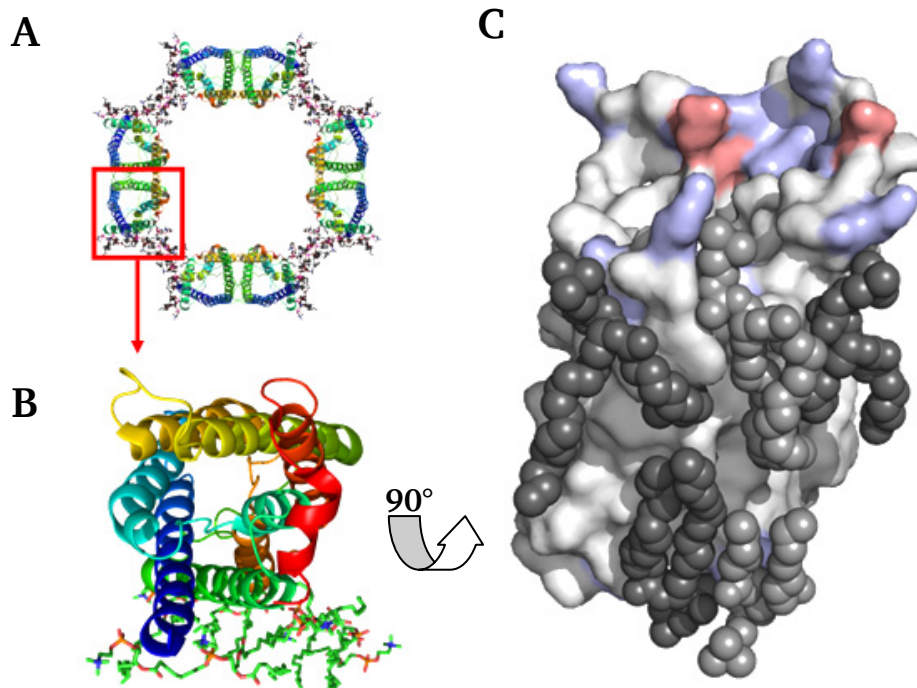
Figure 7: Structure of lens Aquaporin-0 (AQP0). Shown are **(A)** a top view of a biological assembly image of the electron crystallographic structure of lens Aquaporin-0 (AQP0) in a closed pore state (PDB-Code: 2B6O, resolution 1.9Å). The **(B)** top view of the cartoon of one asymmetric unit shows the existence of annular lipids. The **(C)** side view of the surface plot (positive amino acids in blue, negative amino acids in red) shows the bound annular lipids (gray, space-filling format, not all lipids are shown), which are highly distorted to match the protein surface (image A+B according to Gonen *et al.* 2005).

Depending on the lipid composition of the membrane, different physical properties of the lipid bilayer can change, such as: **i.** the pressure profile across the membrane, **ii.** the properties of spontaneous curvature, which are important for the vertical movement of proteins in the membrane, **iii.** the fluidity and **iv.** the hydrophobic thickness (Lee 2006).

The hydrophobic thickness of the membrane influences also the amino acid composition of the TMDs. Figure 8 shows how the amino acid composition of transmembrane segments is adapted to the special requirements of the lipid bilayer. This means that amino acids in the centre of transmembrane segments, which are exposed to the lipids, are mostly hydrophobic to fit the hydrophobic core of the membranes. Hydrophilic and charged amino acids are more common at the ends of the segments, where they can interact with the phospholipids headgroups (Killian and von Heijne 2000, Planque and Killian 2003). Aromatic residues, depending on their chemical properties, can often be found within the transmembrane segments as well as in the interfacial regions (Killian and von Heijne 2000). Tryptophan (Trp), for example, contains a large hydrophobic aromatic ring system together with an amide

group, which gives the side chain a polarity. Therefore, Trp can interact very well with the polar-apolar interface. A contrast to this is the ring system of phenylalanine (Phe), which is completely hydrophobic; hence, it is mostly found in the transmembrane regions of the proteins (Wallin *et al.* 1997).
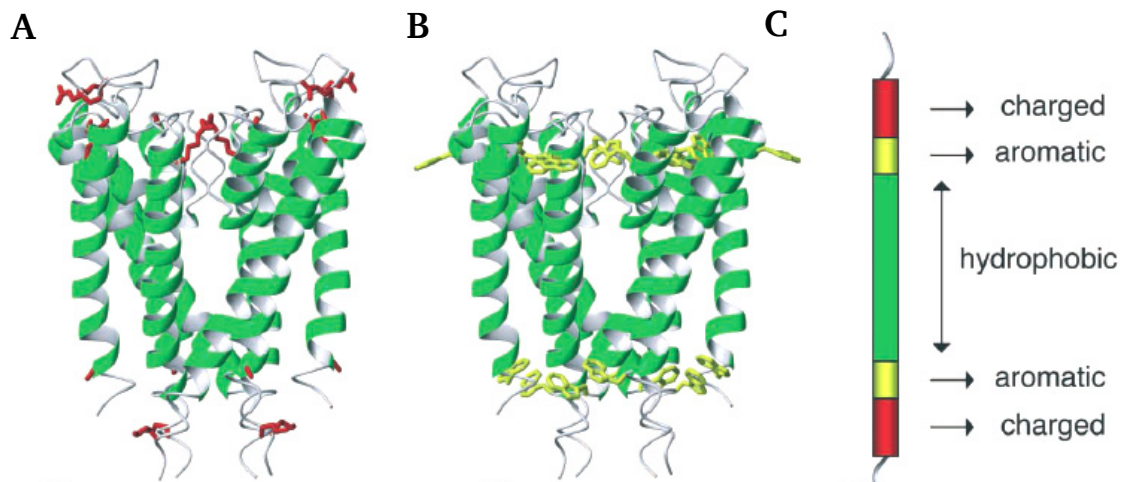
Figure 8: Distribution of charged and aromatic amino acids in the transmembrane segments of the bacterial potassium channel KcsA. Shown is the structure of KcsA as a cartoon with highlighted **(A)** arginine or **(B)** tryptophan residues of the transmembrane segments as stick model. The distribution of the amino acids shows a good agreement compared with **(C)** the general model for the distribution of amino acids in transmembrane segments of transmembrane proteins (according to Planque and Killian 2003).

The length of the hydrophobic core of the lipids influences not only the amino acid flavour but also the length of the transmembrane segments, since the TMD has to span through the membrane. Because of this feature, it has been shown that the length of TMDs can, indeed, function as an intracellular sorting signal for the correct insertion of proteins into the respective cell compartments (Rayner and Pelham 1997, Ronchi *et al.* 2008, Balss *et al.* 2008). A deviation of the hydrophobic length of the transmembrane domain from the thickness of the bilayer, results in a so-called hydrophobic mismatch. Because this mismatch is energetically unfavourable, different avoiding strategies are available (Planque and Killian 2003). Figure 9 sketches one of these avoiding mechanisms, the so-called snorkeling effect, which will be relevant for this work (Chamberlain *et al.* 2004). This effect is specific to some amino acids, namely lysine (Lys), arginine (Arg), tryptophan (Trp), phenylalanine (Phe) and tyrosine (Tyr). The side chains of these amino acids prefer either the polar headgroups (snorkeling of Lys, Arg, Trp and Tyr) or the hydrophobic core (anti-snorkeling of Phe, Trp and Tyr) and can,

therefore, increase (Strandberg and Killian 2003) or decrease (Liang *et al.* 2005) the hydrophobic length of the protein if the residues are positioned near the water-lipid-interface. For an increase of the hydrophobic length of a transmembrane segment, the amino acids (Lys, Arg, Trp and Tyr) extend their side chains perpendicular to the membrane and with this towards the polar lipid headgroups. With this snorkeling, they avoid the hydrophobic membrane core and as a result stretchs the TMD. For a decrease of the hydrophobic length, the aromatic amino acids (Phe, Trp and Tyr) behave in the opposite way (anti-snorkling); these amino acids extend their side chains perpendicular to the lipid bilayer towards the hydrophobic core in order to avoid the polar interface regions (Liang *et al.* 2005). The ability of the amino acids to snorkel or anti-snorkel depends on the properties of their side chains. A summary of the snorkeling or anti-snorkeling behaviour is given in Table 2.
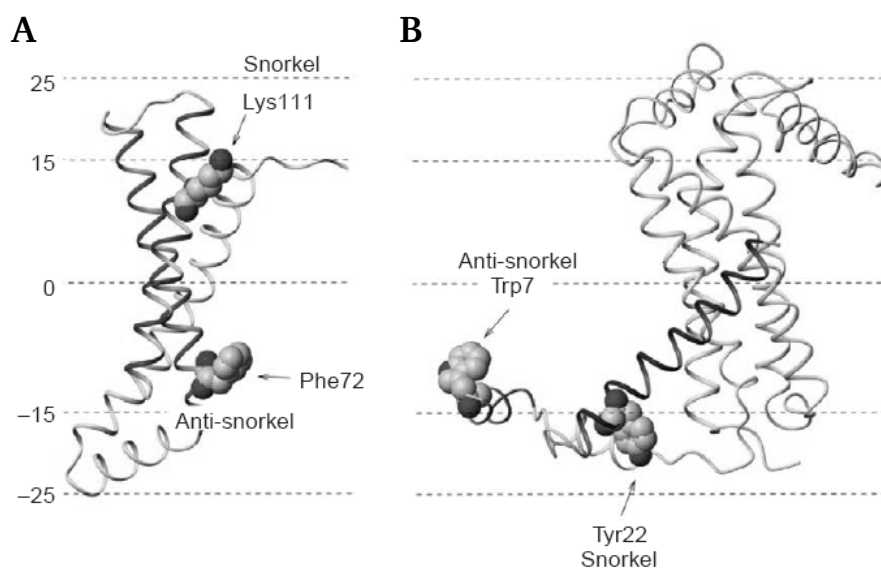
Figure 9: Snorkeling and anti-snorkeling effects in membrane proteins. Shown are examples of snorkeling and anti-snorkeling effects of amino acids in **(A)** the subunit SdhC of succinate dehydrogenase and in **(B)** the cytochrome b6 and PetL subunits of the cytochrome b6f complex. The transmembrane segment spans the region of ± 15 Å (according to Liang *et al.* 2005).

The snorkeling of amino acids is an energy consuming process and costs between 0.07 and 0.7 kcal*mol^{-1}. Therefore, not every amino acid that is able to snorkel shows this behaviour. Nevertheless, it is a common process to overcome hydrophobic mismatches (Strandberg and Killian 2003).

Table 2: Summary of the snorkeling and anti-snorkeling behaviours of different amino acid residues in the transmembrane and interface region of a membrane (from Liang *et al.* 2005).

Region	Polar	Hydrophobic	Amphipathic
Transmembrane Region	Snorkel	Anti-snorkel	Snorkel
Interface Region	Snorkel	Anti-snorkel	Anti-snorkel

In summary, protein-lipid interactions have a strong influence on different protein properties like: the specific functionality of proteins depending on different lipids (e.g. Raja *et al.* 2007), the primary structure of transmembrane segments to span the hydrophobic membrane core (e.g. Planque and Killian 2003) or the proper folding and sorting of the proteins depending on the length of their transmembrane segments (e.g. Rayner and Pelham 1997). Finally, the pleiotropic effects of the direct protein–lipid interactions seem to be crucial for the translocon-mediated membrane insertion (Liang *et al.* 2005).

2.3. References

Abenavoli A, DiFrancesco ML, Schroeder I, Epimashko S, Gazzarrini S, Hansen UP, Thiel G, Moroni A (2009) Fast and slow gating are inherent properties of the pore module of the K$^+$ channel Kcv. *J Gen Physiol.* 134:219-29. doi:10.1085/jgp.200910266

Balss J, Papatheodorou P, Mehmel M, Baumeister D, Hertel B, Delaroque N, Chatelain FC, Minor DL, Van Etten JL, Rassow J, Moroni A, Thiel G (2008) Transmembrane domain length of viral K$^+$ channels is a signal for mitochondria targeting. *PNAS* 105:12313-12318. doi:10.1073/pnas.0805709105

Bhattacharyya R, Samanta U, Chakrabarti P (2002) Aromatic–aromatic interactions in and around α-helices. *Protein Engineering* 15:91-100

Bernèche S and Roux B (2001) Energetics of ion conduction through the K$^+$ channel. *Nature* 414:73-77. doi:10.1038/35102067

Bertero MG, Rothery RA, Palak M, Hou C, Lim D, Blasco F, Weiner JH, Strynadka NC (2003) Insights into the respiratory electron transfer pathway from the structure of nitrate reductase A. *Nat Struct Biol.* 10:681-7. doi:10.1038/nsb969

Blaustein RO, Miller C (2004) Ion channels: Shake, rattle or roll? *Nature* 427:499-500. doi:10.1038/427499a

Blunck R, Cordero-Morales JF, Cuello LG, Perozo E, Bezanilla F (2006) Detection of the Opening of the Bundle Crossing in KcsA with Fluorescence Lifetime Spectroscopy Reveals the Existence of Two Gates for Ion Conduction. *JGP* 128:569-581. doi:10.1085/jgp.200609638

Burley SK and Petsko GA (1988) Weakly polar interactions in proteins. *Adv Protein Chem.* 39:125-89.

Catterall WA (1986) Voltage dependent gating of sodium channels: correlating structure and function. *Trends Neurosci.* 9:7–10. doi:10.1016/0166-2236(86)90004-4

Chamberlain AK, Lee Y, Kim S, Bowie JU (2004) Snorkeling preferences foster an amino acid composition bias in transmembrane helices. *J Mol Biol.* 339:471-9. doi:10.1016/j.jmb.2004.03.072

Chatelain FC, Gazzarrini S, Fujiwara Y, Arrigoni C, Domigan C, Ferrara G, Pantoja C, Thiel G, Moroni A, Minor DL Jr. (2009) Selection of inhibitor-resistant viral potassium channels identifies a selectivity filter site that affects barium and amantadine block. *PLoS One* 4:e7496. doi:10.1371/journal.pone.0007496

Clackson T and Wells JA (1995) A Hot Spot of Binding Energy in a Hormone-Receptor Interface. *Science* 267:383-386. doi: 10.1126/science.7529940

Cordero-Morales JF, Jogini V, Lewis A, Vásquez V, Cortes DM, Roux B, Perozo E (2007) Molecular Driving Forces Determining Potassium Channel Slow Inactivation. *Nature Structural & Molecular Biology,* 14:1062-1069. doi:10.1038/nsmb1309

Cordero-Morales JF, Cuello LG, Zhao Y, Jogini V, Cortes DM, Roux B, Perozo E (2006) Molecular determinants of gating at the potassium-channel selectivity filter. *Nature Structural & Molecular Biology* 13:311 – 318. doi:10.1038/nsmb1069

Cortes DM, Cuello LG, Perozo E (2001) Molecular Architecture of Full-Length KcsA - Role of Cytoplasmic Domains in Ion Permeation and Activation Gating. *JGP* 117:165-180. doi:10.1085/jgp.117.2.165

Cuello LG, Jogini V, Cortes DM, Pan AC, Gagnon DG, Dalmas O, Cordero-Morales JF, Chakrapani S, Roux B, Perozo E (2010) Structural basis for the coupling between activation and inactivation gates in K$^+$ channels. *Nature* 466:272-5. doi:10.1038/nature09136

Domene C, Bond P, Sansom MSP (2003) Membrane protein simulation: ion channels and bacterial outer membrane proteins. *Adv. Protein Chem.* 66:159-193

Doyle DA, Morais CJ, Pfuetzner RA, Kuo A, Gulbis JM, Cohen SL, Chait BT, MacKinnon R (1998) The structure of the potassium channel: molecular basis of K+ conduction and selectivity. *Science* 280:69-77

Fan Z, Makielski JC (1997) Anionic phospholipids activate ATP-sensitive potassium channels. *J Biol Chem.* 272:5388-95. doi:10.1074/jbc.272.9.5388

Ferl RJ (1996) 14-3-3 PROTEINS AND SIGNAL TRANSDUCTION. *Annual Review of Plant Physiology and Plant Molecular Biology* 47:49-73. doi:10.1146/annurev.arplant.47.1.49

Gazzarrini S, Severino M, Lombardi M, Morandi M, DiFrancesco D, Van Etten JL, Thiel G, Moroni A (2003) The viral potassium channel Kcv: structural and functional features. *FEBS Lett.* 552:12-16

Gazzarrini S, Kang M, Abenavoli A, Romani G, Olivari C, Gaslini D, Ferrara G, van Etten JL, Kreim M, Kast SM, Thiel G, Moroni A (2009) Chlorella virus ATCV-1 encodes a functional potassium channel of 82 amino acids. *Biochem J.* 420:295-303.

Gonen, T, Cheng Y, Sliz P, Hiroaki Y, Fujiyoshi Y, Harrison SC, Walz T (2005) Lipid-protein interactions in double-layered two-dimensional AQP0 crystals. *Nature* 438:633-638. doi:10.1038/nature04321

Grabe M, Lai HC, Jain M, Jan YN, Jan LY (2007) Structure prediction for the down state of a potassium channel voltage sensor. *Nature* 445:550-553. doi:10.1038/nature05494

Guy HR, Seetharamulu P, Molecular model of the action potential sodium channel. *Proc. Natl. Acad. Sci.* USA 83:508–512.

Hille B (2001) Ion channels of excitable membranes. 3. Edition, Sinauer Associates Inc., Sunderland

Iyer R, Iverson TM, Accardi A, Miller C (2002) A biological role for prokaryotic ClC chloride channels. *Nature* 419:715-718. doi:10.1038/nature01000

Jan LY and Jan YN (1992) Structural elements involved in specific K+ channel functions. *Annu. Rev. Physiol.* 54:537-555

Jiang Y, Lee A, Chen J, Cadene M, Chait BT, MacKinnon R (2002a) Crystal structure and mechanism of a calcium-gated potassium channel. *Nature* 417:515-522. doi:10.1038/417515a

Jiang Y, Lee A, Chen J, Ruta V, Cadene M, Chait BT, MacKinnon R (2003a) X-ray structure of a voltage-dependent K^+ channel. *Nature* 423:33–41. doi:10.1038/nature01580

Jiang Y, Ruta V, Chen J, Lee A, MacKinnon R (2003b) The principle of gating charge movement in a voltage-dependent K^+ channel. *Nature* 423:42–48. doi:10.1038/nature01581

Kang M, Moroni A, Gazzarrini S, DiFrancesco D, Thiel G, Severino M, VanEtten JL (2004b) Small potassium ion channel proteins encoded by chlorella viruses. *PNAS* 101:5318-5324

Keynes RD, Elinder F (1999) The screw-helical voltage gating of ion channels. *Proc. Biol. Sci.* 266:843–852. doi:10.1098/rspb.1999.0714

Killian JA (2003) Synthetic peptides as models for intrinsic membrane proteins. *FEBS Lett.* 555:134-138

Killian JA, von Heijne G (2000) How proteins adopt to a membrane-water interface. Trends Biochem. Sci. 25:429-434

Lecar H, Larsson HP, Grabe M (2008) Electrostatic model of S4 motion in voltage-gated ion channels. Biophys. J. 85:2854–2864. doi:10.1016/S0006-3495(03)74708-0

Lee AG (2006) How lipids affect the activities of integral membrane proteins. Biochimica et Biophysica Acta (BBA) – Biomembranes 1666:62-87. doi:10.1016/j.bbamem.2004.05.012

Lee AG (2009) The effects of lipids on channel function. *J Biol.* 2009 8(9):86. doi:10.1186/jbiol178.

Liang J, Adamian L, Jackups RJ (2005) The membrane–water interface region of membrane proteins: structural bias and the anti-snorkeling effect. *TRENDS in Biochemical Sciences* 30:355-357

Locke D, Harris AL (2009) Connexin channels and phospholipids: association and modulation. *BMC Biol.* 7:52. doi:10.1186/1741-7007-7-52.

Long SB, Campbell EB, Mackinnon R (2005a) Crystal structure of a mammalian voltage-dependent Shaker family K^+ channel. *Science* 309:897–903. doi:10.1126/science.1116269

Long SB, Campbell EB, Mackinnon R (2005b) Voltage sensor of Kv1.2: structural basis of electromechanical coupling. *Science* 309:903–908. doi:10.1126/science.1116270

Long SB, Tao X, Campbell EB, Mackinnon R (2007) Atomic structure of a voltage-dependent K^+ channel in a lipid membrane-like environment. *Nature* 450:376–382. doi:10.1038/nature06265

Lu H, Marti T, Booth PJ (2001) Proline Residues in Transmembrane - Helices Affect the Folding of Bacteriorhodopsin. *J. Mol. Biol.* 308:437-446

MacKinnon R (1991) Determination of the subunit stoichiometry of a voltage-activated potassium channel. *Nature* 350:232-235

MacRobbie EAC (2005) Control of Volume and Turgor in Stomatal Guard Cells. *Journal of Membrane Biology* 210:131-42. doi:10.1007/s00232-005-0851-7

Marius P, Zagnoni M, Sandison ME, East JM, Morgan H, Lee AG (2008) Binding of anionic lipids to at least three nonannular sites on the potassium channel KcsA is required for channel opening. *Biophys J.* 94:1689-98. doi:10.1529/biophysj.107.117507.

Miller C (1992) Ion channel structure and function. *Science* 258:240-241

Morais-Cabral JH, Zhou Y, MacKinnon R (2001) Energetic optimization of ion conduction rate by the K^+ selectivity filter. *Nature* 414:37-42. doi:10.1038/35102000

Moroni A, Viscomi C, Sangiorgio V, Pagliuca C, Meckel T, Horvath F, Gazzarrini S, Valbuzzi P, Van Etten JL, DiFrancesco D, Thiel G (2002) The short N-terminus is required for functional expression of the virus-encoded miniature K$^+$ channel Kcv. *FEBS Lett.* 530:65-69

Neher E (1992) Ion channels for communication between and within cells. *EMBO* 11:1673 - 1679

Neher E and Sakmann B (1976) Single-channel currents recorded from membrane of denervated frog muscle muscle fibres. *Nature* 260:799-802

Pagliuca C, Goetze TA, Wagner R, Thiel G, Moroni A, Parcej D (2007) Molecular Properties of Kcv, a Virus Encoded K+ Channel. *Biochemistry* 46:1079–1090. doi:10.1021/bi061530w

Pal D and Chakrabarti P (1998) Different types of interactions involving cysteine sulfhydryl group in proteins. *J Biomol Struct Dyn.* 15:1059-72.

Parsegian (1969). Energy of an ion crossing a low dielectric membrane: solutions to four relevant electrostatic problems. *Nature* 221:844-846. doi:10.1038/221844a0

Pawson T and Nash P (2000) Protein–protein interactions define specificity in signal transduction. *Genes & Dev.* 14:1027-1047. doi: 10.1101/gad.14.9.1027

Perozo E, Cortes DM, Cuello LG (1999) Structural Rearrangements Underlying K$^+$-Channel Activation Gating. *Science* 285:73-78

Planque MRR, Killian JA (2003) Protein/lipid interactions studied with designed transmembrane peptides: role of hydrophobic matching and interfacial anchoring. *Molecular Membrane Biology* 20:271-284

Plugge B, Gazzarrini S, Nelson M, Cerana R, Van Etten JL, Derst C, DiFrancesco D, Moroni A, Thiel G (2000) A potassium channel protein encoded by chlorella virus PBCV-1. *Science* 287:1641–1644

Powl AM, East JM, Lee AG (2008) Importance of direct interactions with lipids for the function of the mechanosensitive channel MscL. *Biochemistry* 47:12175-84. doi:10.1021/bi801352a

Raja M, Spelbrink REJ, de Kruijff B, Killian JA (2007) Phosphatidic acid plays a special role in stabilizing and folding of the tetrameric potassium channel KcsA. *FEBS Letters* 581:5715-5722. doi:10.1016/j.febslet.2007.11.039

Rayner JC and Pelham HRB (1997) Transmembrane domain-dependent sorting of proteins to the ER and plasma membrane in yeast. *The EMBO Journal* 16:1832 – 1841 doi:10.1093/emboj/16.8.1832

Ronchi P, Colombo S, Francolini M, Borgese N (2008) Transmembrane domain–dependent partitioning of membrane proteins within the endoplasmic reticulum. *JCB* 81:105-118. doi:10.1083/jcb.200710093

Schönherr R and Heinemann SH (1996) Molecular determinants for activation and inactivation of HERG, a human inward rectifier potassium channel. *J Physiol.* 493:635–642.

Shim JW, Yang M, Gu LQ (2007) In vitro synthesis, tetramerization and single channel characterization of virus-encoded potassium channel Kcv. *FEBS Letters* 581:1027-1034. doi:10.1016/j.febslet.2007.02.005

Shimizu H, Iwamoto M, Konno T, Nihei A, Sasaki YC, Oiki S (2008) Global Twisting Motion of Single Molecular KcsA Potassium Channel upon Gating. *Cell* 132:67-78. doi:10.1016/j.cell.2007.11.040

Singh J and Thornton JM (1993) Atlas of protein side-chain interactions. Vols. I and II. *Acta Cryst.* D49:355-356

Sedgwick SG, Smerdon SJ (1999) The ankyrin repeat: a diversity of interactions on a common structural framework. *Trends in Biochemical Sciences* 24:311-316 doi:10.1016/S0968-0004(99)01426-7

Spergel DJ (2007) Calcium and Small-Conductance Calcium-Activated Potassium Channels in Gonadotropin-Releasing Hormone Neurons before, during, and after Puberty. *Endocrinology* 148:2383-2390. doi:10.1210/en.2006-1693

Starace DM, Bezanilla F (2004) A proton pore in a potassium channel voltage sensor reveals a focused electric field. *Nature* 427:548-553. doi:10.1038/nature02270

Strandberg E, J. Antoinette Killian JA (2003) Snorkeling of lysine side chains in transmembrane helices: how easy can it get? *FEBS Letters* 544:69-73.

Tayefeh S, Kloss T, Thiel G, Hertel B, Moroni A, Kast SM (2007) Molecular Dynamics Simulation of the Cytosolic Mouth in Kcv-Type Potassium Channels. *Biochemistry* 46:4826-4839. doi:10.1021/bi602468r

Tayefeh S, Kloss T, Kreim M, Gebhardt M, Baumeister D, Hertel B, Richter C, Schwalbe H, Moroni A, Thiel G, Kast SM (2009) Model development for the viral potassium channel. *Biophys J* 96:485–498. doi:10.1016/j.bpj.2008.09.050

Thompson AN, Posson DJ, Parsa PV, Nimigean CM (2008) Molecular mechanism of pH sensing in KcsA potassium channels.
PNAS 105:6900-6905. doi:10.1073/pnas.0800873105

Tombola F, Pathak MM, Gorostiza P, Isacoff EY (2007) The twisted ion-permeation pathway of a resting voltage-sensing domain.
Nature 445:546–549. doi:10.1038/nature05396

Triano I, Barrera FN, Renart ML, Molina ML, Fernández-Ballester G, Poveda JA, Fernández AM, Encinar JA, Ferrer-Montiel AV, Otzen D, González-Ros JM (2010) Occupancy of Nonannular Lipid Binding Sites on KcsA Greatly Increases the Stability of the Tetrameric Protein. *Biochemistry Article ASAP*. doi:10.1021/bi1003712

Van Etten JL, Graves MV, Müller DG, Boland W, Delaroque N (2002) Phycodnaviridae – large DNA algal viruses. *Arch. Virol.* 147:1479-1516

Wallin, E, Tsukihara T, Yoshikawa S, von Heijne G, Elofsson A. (1997) Architecture of helix bundle membrane proteins: An analysis of cytochrome c oxidase from bovine mitochondria. *Protein Sci.* 6:808-15.

Yau WM, Wimley WC, Gawrisch K, White SH (1998) The preference of tryptophan for membrane interfaces. *Biochemistry* 37:14713-14718

Zheng J und Sigworth FJ (1997) Selectivity Changes during Activation of Mutant Shaker Potassium Channels. *J. Gen. Physiol.* 110:101-117

Chapter 2 - Computational Studies and Site Directed Mutagenesis reveals that Snorkeling Effects in the Viral Potassium Channel Kcv are nonessential for a proper Channel Function.

3.1. Abstract

Potassium channels are crucial for many biological functions like cell-cell-communication (Neher 1992) or osmoregulation (Schroeder *et al.* 1989). They are common in all life forms form bacteria to humans. Also some viruses contain channel proteins, which are generally very small but still functional. One example of these miniature channel proteins is the viral potassium channel Kcv from the Chlorella virus PBCV-1; with only 94 amino acids, it is one of the smallest known potassium channels. In spite of the small size, it contains essential structural and functional hallmarks of more complex potassium channels. Structurally Kcv is not more than the pore module of potassium channels. Because of its structural simplicity, this protein offers a good model system for the analysis of basic structure/function correlates in K^+ channel proteins.

One interesting feature in the structure of Kcv is a lysine at position 29 (Lys29) in the C-terminal end of the first transmembrane domain (TMD1). This is a highly conserved amino acid in viral K^+ channels and is present in nearly all other K^+ channels isolated from viral origin. This amino acid is located close to the water/lipid interface. Lysines in the interface of TMDs frequently stretch their charged side chains away from the hydrophobic membrane core towards the polar phospholipid headgroups. This so-called snorkeling can increase the hydrophobic length of TM segments.

Computational studies of the Kcv protein in a lipid bilayer by molecular modelling and molecular dynamics (MD) simulations, however, revealed other than expected that the protein structure is very unstable with a protonated lysine. The protein model is only stable and able to conduct K^+ ions when Lys29 is deprotonated i.e. not charged. This may indicate that the pK_a of Lys29 is strongly shifted to lower pH values in the context of the lipid environment compared to its pK_a in water. Hence, the lysine may in reality be deprotonated. To examine this possibility and to investigate the structural contribution of this amino acid on function, we mutated Lys29 into all possible amino acids. The functional analysis of these mutants supports the view that position 29 in Kcv can be occupied by a non-charged amino acid without a consequence for function. However, the same mutation in the corresponding position in other

vial ion channels revealed that Kcv seems to be an exception because other viral ion channels require a protonated amino acid in this specific position

3.2. Introduction

Potassium channels are a family of membrane proteins, which catalyse the selective diffusion of K^+ ions across membranes (Hille *et al.* 2001). With this function, K^+ channels are involved in many physiological processes (Ashcroft 2000). The simplest K^+ channels, the two transmembrane domain (2TMD) channels, are tetramers in which the monomers are made of two transmembrane domains (Ho *et al.* 1993). These are connected via the pore helix, which comprises the selectivity filter (Miller 1992, Jan and Jan 1992, Heginbotham *et al.*1994). Cytoplasmic domains on the C- and N-terminus often harbor binding domains for regulatory ligands (Haider *et al.* 2005, Wollmuth and Sobolevsky 2004). A combination of structural information, computer simulations and functional studies has uncovered in the last decade many key structure/function correlations, which are able to explain details on the operation of these proteins on the atomic level. It was found that the architecture of the selectivity filter determines the ability of the protein to discriminate between different cations and still transports K^+ with a high velocity (Hille 2001). Further structural details have provided evidence for structural changes, which underlay the gating of the channels (Doyle 2004). In addition, the importance of the inner transmembrane domain was highlighted because conformational changes of this domain seem to be important for the gating of the channel (Perozo *et al.* 1999, Kuo *et al.* 2003). Recently it became evident that also the outer transmembrane domain could be relevant in the function of these channels (Gazzarrini *et al.* 2004).

An interesting system to uncover more structure/function correlates in K^+ channels is present in the form of the viral K^+ channel Kcv. This channel has structural and functional hallmarks of all complex K^+ channels (Plugge *et al.* 2000, Tayefeh *et al.* 2007). It is made as a tetramer and is able to selectively transport K^+ (Pagliuca *et al.* 2007, Shim *et al.* 2007); it is sensitive to typical K^+ channel blockers and it is gated (Moroni *et al.* 2002, Abenavoli *et al.* 2009, Pagliuca *et al.* 2007). What makes Kcv_{PBCV-1} so interesting is its small size; a channel monomer is composed of only 94 amino acids (Plugge *et al.* 2000). A recently discovered K^+ channel from another virus, Kcv_{ATCV-1}, is, with only 82 amino acids, even smaller (Gazzarrini *et al.* 2009).

With these few amino acids, the viral channel represents not more than the pore module of all K^+ channels namely two transmembrane domains, which are connected via the pore helix and the selectivity filter.

Previous studies have already revealed the importance of the outer transmembrane domain on Kcv function. In natural occurring orthologs of Kcv_{PBCV-1} it was found that a single amino acid exchange of valine at position 19 to phenylalanine (Kcv-V19F) in the first transmembrane domain (TMD1) made the channel more susceptible for a block by Cs^+ and it altered the voltage dependency of the channel (Gazzarrini *et al.* 2004, Kang *et al.* 2004). The impact of the amino acid in position 19 was synergistically coupled to other amino acid positions, implying long distance relations between sites in TMD1 and other parts of the protein including the pore. More support for the functional importance of TMD1 was obtained from experiments in which this domain was extended at the upstream part of TMD1. This manipulation resulted in a gain of time dependent channel activation at negative voltages (Hertel *et al.* 2006). Finally examinations of the salt bridge patterns in the Kcv protein revealed functionally essential dynamic making and breaking of salt bridges between the inner and outer transmembrane domain at the cytoplasmic entry to the channel cavity (Hertel *et al.* 2009). Altogether, the results of these experiments suggest that the structure of the outer transmembrane domain has implications for the function of these channel proteins.

Scrutiny of the structure of TMD1 of Kcv shows that this domain has at the down stream end, towards the outer aqueous face, the basic amino acid lysine (Tayefeh *et al.* 2007 and 2009). This is typical for many transmembrane proteins, which reveal with a high frequency, charged residues at the outer flanks of TM helices (Ulmschneider and Sansom 2001). In particular, Lys and arginine (Arg), the amino acids with long, positively charged side chains, often occur in the interfacial region between membrane and aqueous solution. From this position deep in the hydrophobic part of the bilayer, they can perform what is known as "snorkeling". This allows a high degree of flexibility in the positioning of side chains at the interface and, hence, more freedom in the localisation and dynamics of the helices in the bilayer (Strandberg and Killian 2003).

Recent computational and experimental studies on the role of the lysine in Kcv_{PBCV-1} revealed a surprising result. In molecular dynamics simulations it was found that a protonated Lys resulted in very vivid snorkeling activity with the result that the protein structure became very

unstable and that the protein failed to transport ions (Tayefeh *et al.* 2009). Only modeling of the protein with a deprotonated Lys gave a stable channel protein, which transported ions. The data prompted the view that the lysine at position 29 (K29) in Kcv$_{PBCV-1}$ may not be charged in the functional channel. This hypothesis was supported by an analysis of site directed mutants, which showed that K29 can be replaced by Ala, serine (Ser) or tryptophan (Trp) without impairing channel function in HEK293 cells (Tayefeh *et al.* 2009).

In the present study, we continue to examine the functional role of this amino acid in the structure/function context of viral K$^+$ channels. We find that in Kcv$_{PBCV-1}$ K29 can be replaced by all possible amino acids with the exception of proline (Pro) without loosing channel function. This implies that the function of the channel is insensitive to the nature of the amino acid in this position. On the other hand, a comparison of Kcv$_{PBCV-1}$ with other viral K$^+$ channels shows that this position is very conserved. Functional studies using two other viral K$^+$ channels showed that Lys in this position is indeed essential for making a functional channel. Collectively the data show that the contribution of a single amino acid to the structure/function correlation of a channel protein can only be understood in the context of the entire channel protein.

3.3. Material and Methods

3.3.1. Heterologous Expression Systems

HEK293 cells (human embryonic kidney 293 cell) were used for the electrophysiological measurements (Graham *et al.* 1977). The yeast strain SGY1528 with the genotype Mat *a ade* 2–1 *can* 1–100 *his* 3–11,15 *leu* 2–3,112 *trp* 1–1 *ura* 3–1 *trk* 1::HIS3 *trk* 2::TRP1 (Tang *et al.* 1995) was used for the complementation assay. Dr. Minor (UCSF, USA) kindly provided the yeast strain.

3.3.2. Constructs and Mutagenesis

The genes from Kcv$_{PBCV-1}$ and its orthologs Kcv$_{ATCV-1}$ and Kcv$_{MT325}$ were cloned either in the pEGFP-N2 vector (Clontech-Takara Bio Europe, Saint-Germain-en-Laye, France) for electrophysiological measurements in HEK293 cells or in a modified pYES2 vector (Invitrogen

GmbH, Karlsruhe, Germany) for the yeast complementation assay (Minor *et al.* 1999). In the pEGFP-N2 vector, the genes were cloned in the BglII and EcoRI site without their stop codons in frame with the downstream enhanced green fluorescent protein (EGFP) to get the fusion proteins. For the yeast experiments, the genes were cloned with their stop codons into the EcoRI and XhoI site of the pYES2 vector.

For the insertion of the site-directed mutations, the QuikChange Site-directed Mutagenesis method (Stratagen) was used, and the resulting constructs were checked by DNA sequencing.

3.3.3. Electrophysiological Measurements

HEK293 cells were grown in 35 mm culture dishes at 37 °C in 5 % CO_2 for 1 – 2 days until they were 70 % confluent. Thereafter the cells were transiently transfected with the different constructs from Kcv_{PBCV-1} and its orthologs Kcv_{ATCV-1} and Kcv_{MT325} in pEGFP-N2 with the help of the liposomal transfection reagent TurboFect^{TM} (Fermentas, St. Leon Rot). After 1 day of growth, the cells were washed with phosphate buffered saline, dispersed with Accutase$^{®}$ (SIGMA-ALDRICH, Schnelldorf, Germany), sowed in lower density in new 35 mm culture dishes and allowed to settle down over night.

For the single cell patch-clamp measurements, the culture medium was replaced by the different solutions for research. The measurements were performed in the whole-cell configuration according to standard methods (Hamill *et al.* 1981) using an EPC-9 patch-clamp amplifier (HEKA, Lambrecht, Germany). The holding voltage was 0 mV and the testing voltages were between +60 and -160 mV. The data were gathered and analysed with the Pulse software (HEKA, Lambrecht, Germany).

The measurements were performed at room temperature in the following bath solutions: 1.8 mM $CaCl_2$, 1 mM $MgCl_2$ and 5 mM 4-(2-hydroxyethyl)-1-piperazineethanesulfonic acid (HEPES, pH 7.4) and either 100 mM KCl or 100 mM NaCl or 100 mM KCl together with 10 mM $BaCl_2$. The osmolarity of all solutions was adjusted with mannitol to 330 mOsmol. The used pipette solution contained 130 mM D-potassium-gluconic acid, 10 mM NaCl, 5 mM HEPES, 0.1 mM guanosine triphosphate (Na salt), 0.1 μM $CaCl_2$, 2 mM, $MgCl_2$, 5 mM phosphocreatine and 2 mM adenosine triphosphate (Na salt, pH 7.4).

The fast exchange of the different bath solutions in the chamber in approximately one minute was guaranteed by using a perfusion pipette, which was placed near to the cell of interest.

3.3.4. *Saccharomyces cerevisiae* Complementation Assay

The yeast complementation assays were done as described in Minor *et al.* 1999. The used yeast strain SGY1528 lacks an endogenous K^+ uptake system. Therefore, the yeasts are not able to grow on media with potassium concentrations lower than 10 mM K^+. For the yeast complementation assay on plates, non-selective media (100 mM K^+ agar plates) and selective media (1 mM and 0.5 mM K^+ agar plates) were used. The plates were incubated for about three days at 30 °C. For the experiments with liquid cultures 0.5 mM K^+ selective media was used and the optical density was measured at 600 nm (OD_{600}). Therefore, 0.5 mM K^+ selective media was inoculated with a yeast suspension (prepared and washed in the same manner as for the plates) to a final OD_{600} of 0.1 and incubated directly in 2 ml cuvettes sealed with laboratory film at 30 °C and 230 rpm. After 0 h and 24 h the OD_{600} was measured using a spectrophotometer.

3.3.5. Homology Model Structure Analysis

The homology model of Kcv is based on the tetrameric form of the KirBac1.1 (PDB-Code: 1P7B) x-ray template structure (Tayefeh *et al.* 2009). The structure calculations, the 3D modelling, the MD simulations and the structural, thermodynamic and dynamical evaluations were done as described in Tayefeh *et al.* (2009).

3.4. Results

Previous studies have shown that Kcv$_{PBCV-1}$ has a lysine at position 29 (K29) in the outer transmembrane domain (TMD1) at the interface between the membrane and the outer aqueous solution. Experimental and computational studies show that the channel is functional when this Lys is neutralised in the mutant Kcv$_{PBCV-1}$-K29A; in model simulations (Figure 10) it occurred that the channel was only functional when K29 was deprotonated (Tayefeh *et al.* 2009).
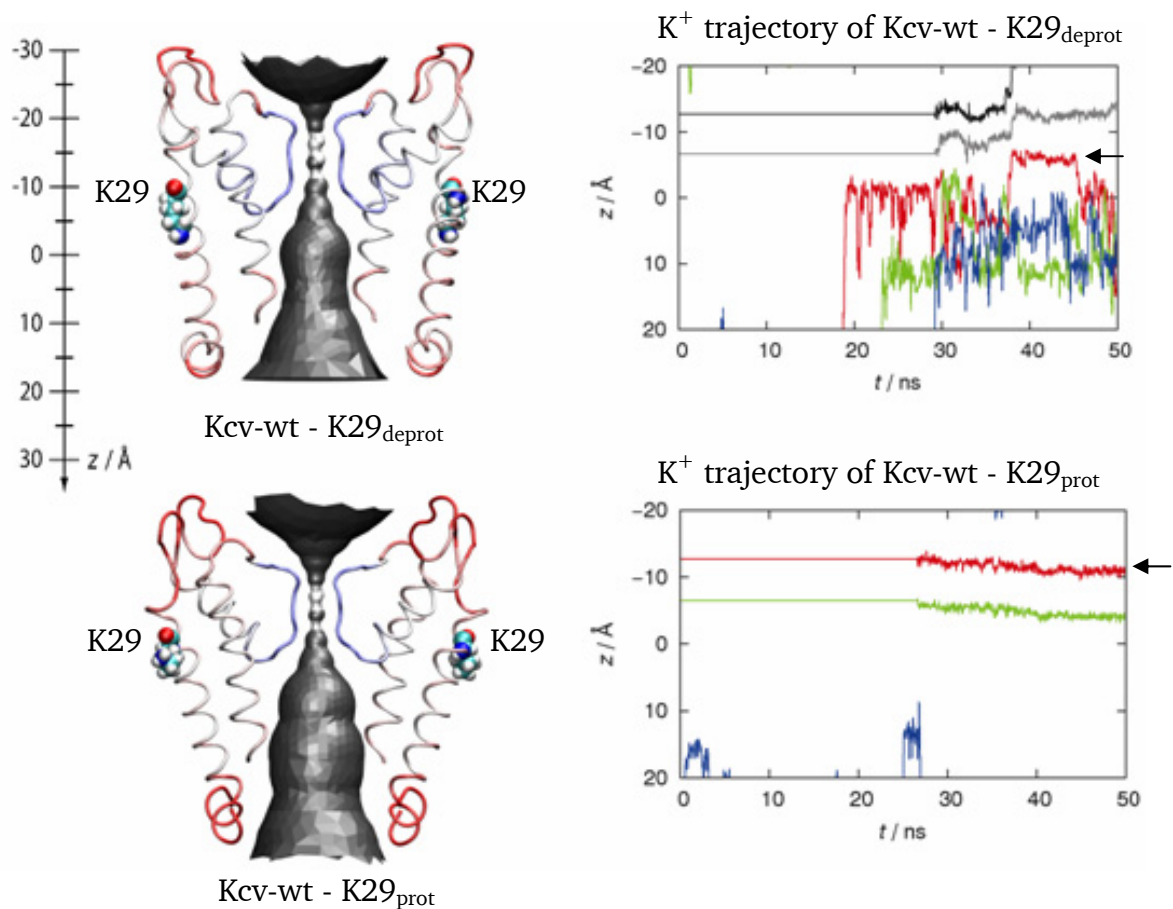
Figure 10: Simulation model and corresponding K$^+$ trajectory of Kcv$_{PBCV-1}$-wt with protonated and deprotonated lysine at position 29. On the left side are the HOLE analysis and the backbone atomic b-factors (blue: <10 Å$^\circ{}^2$; red: >20 Å$^\circ{}^2$) of the two models of Kcv$_{PBCV-1}$-wt with deprotonated (upper structure) or protonated (lower structure) lysine at position 29 (K29) shown. On the right site are the corresponding K$^+$ trajectories shown, which display the z coordinates of K$^+$ ions over 6 ns simulation time. The simulations of Kcv$_{PBCV-1}$-wt reveal the spontaneous ion transitions through the entire pore. This event was observed only when the lysine was deprotonated (upper part). The black arrow in the upper graph highlights a spontaneous ion transition. Protonation of K29 (lower part) completely prevents ion transition, which is distinguishable by the motionlessness of the K$^+$ ions (see arrow in the lower graph). Average structures of the homology model derived from a symmetrising annealing protocol (according to Tayefeh *et al.* 2009).

A closer analysis of the spatial arrangement of both structures of the simulation models revealed that the protonation of the lysine leads to the entering of water into the membrane and, therefore, to a breakdown of the TM helix as shown in Figure 11.
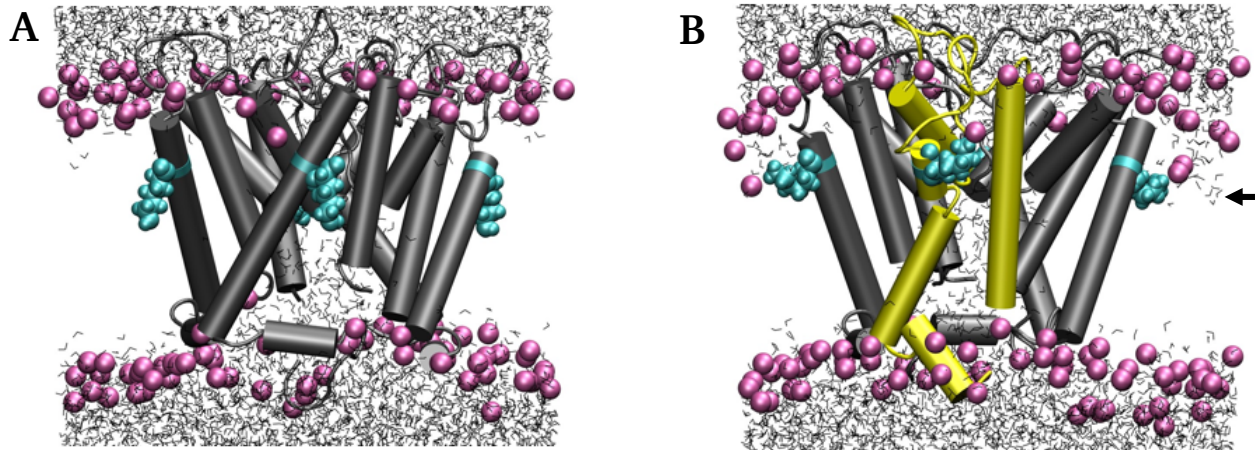
Figure 11: Snapshot of the computer simulations of the homology model from Kcv$_{PBCV-1}$-wt with protonated and deprotonated lysines at position 29. The snapshots at t = 39 ns (i.e., 9 ns after filter constraints were removed) of Kcv$_{PBCV-1}$-wt with **(A)** deprotonated or **(B)** protonated lysines, where water enters the membrane (black arrow). The α-helices are depicted as tubescylinders. Color code: magenta = lipids (only P atoms are shown), cyan = Lys29, grey = water and yellow = regions with the largest helix loss) (according to Tayefeh *et al.* 2009).

To examine the contribution of this position for channel function further, we used a yeast complementation system. The yeast mutant SGY1528 is deprived of its endogenous K$^+$ uptake systems and hence, only able to survive in medium with high K$^+$ supply. In a medium with low K$^+$ concentration yeast growth can be rescued when the cells are supplied with a functional K$^+$ channel (Tang *et al.* 1995), which is properly sorted to the plasma membrane (Balss *et al.* 2008).
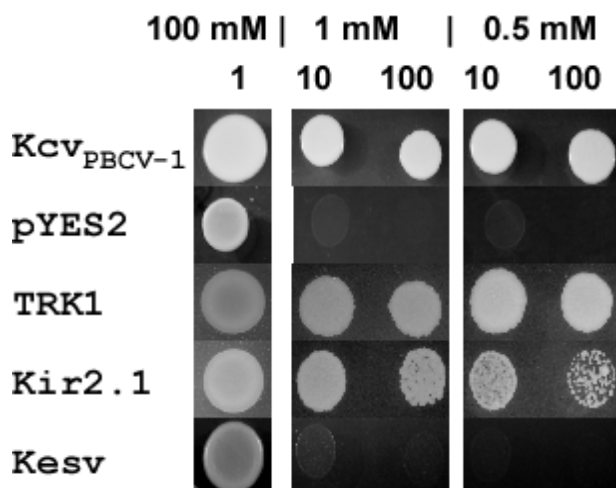
Figure 12: The Yeast Complementation Assay. Shown is a yeast strain, which lacks a functional K$^+$ uptake system. Only yeasts, which express a functional K$^+$ uptake system (TRK, Kir2.1 or Kcv) are able to survive on selective media. The empty vector pYES2 or functional channels, which are not sorted to the plasma membrane (Kesv), are not able to rescue the yeast growth. The 100 mM KCl media serve as a control if the heterologous expressed proteins are toxic for the yeasts, hence, all yeast have to growth under this conditions.

To test, which type of amino acids is tolerated in Kcv_{PBCV-1} for giving a functional channel, K29 was mutated into all possible amino acids. The results in Figure 13 show that all mutants were able to grow on a medium with 100 mM K^+; none of the mutations was deleterious for yeast growth. Surprisingly also on a selective medium with 1 or 0.5 mM K^+ all the mutants with the exception of one, the exchange of lysine to proline (Kcv_{PBCV-1}-K29P), were growing. The result of this experiment means that Kcv_{PBCV-1} tolerates quasi any amino acid in this position without loosing function; only proline is not tolerated. Since proline is the amino acid with the strongest propensity for terminating α-helices, we can assume here, that the only real function of this position is to guarantee a proper α-helix (Hertel 2005)
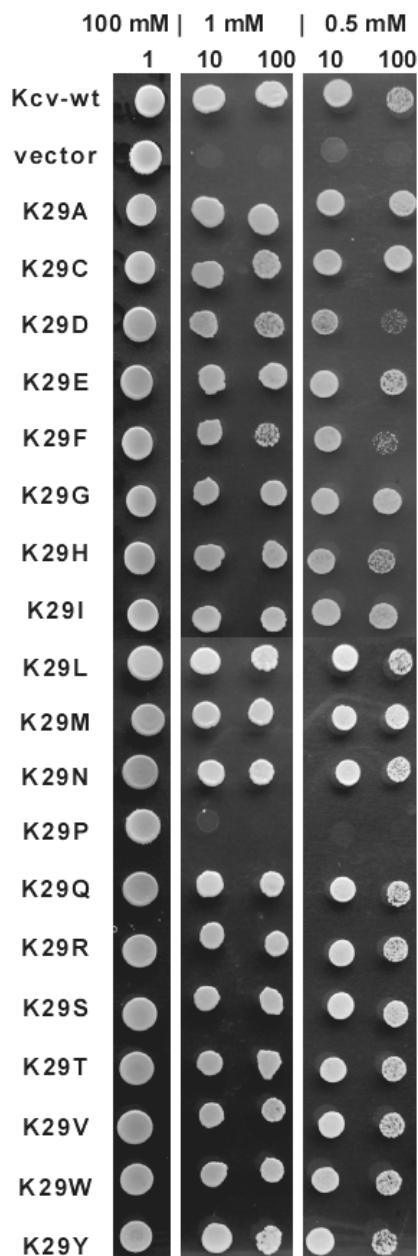
Figure 13: Yeast complementation assay of the scanning of the lysine at position 29 in the first TMD of Kcv. Shown is the yeast complementation assay for the Lys29 in the first TMD where the Lys29 was substituted to all possible amino acids. The assay was done with three different potassium concentrations in the media: 100 mM KCl as control and 1 mM as well as 0.5 mM KCl as selective conditions. The yeast mutants as well as Kcv-wt and the empty vector as controls were spotted in different dilutions: 1 (undiluted), 1:10, 1:100 and 1:1000. The test results are partly shown in the figure.

While the data in Figure 13 imply that all amino acids, with exception of Pro, are able to substitute for K29 in Kcv$_{PBCV-1}$, they nonetheless reveal differences in the efficiency to rescue growth. In order to quantify this difference in rescue efficiency we performed growth experiments of the different mutants; the rescue efficiency was estimated from the optical density, which the growth medium achieved after 24 h. The data in Figure 14 provide the same general picture that was seen on the agar plates. All the constructs with exception of K29P were able to rescue growth; some amino acids were more effective in stimulating growth than others. In an attempt to extract structural information from these data we examined the correlation between the yeast growth data and different properties of amino acids such as hydrophobicity, volume etc. A complete list of the tested properties is given in the Appendix in Table 8; the correlation coefficients show that there is no apparent correlation between the assay data and any of the amino acid properties tested. This means that a single structural feature of the amino acid in this position of the Kcv$_{PBCV-1}$ channels is not sufficient to explain the data.
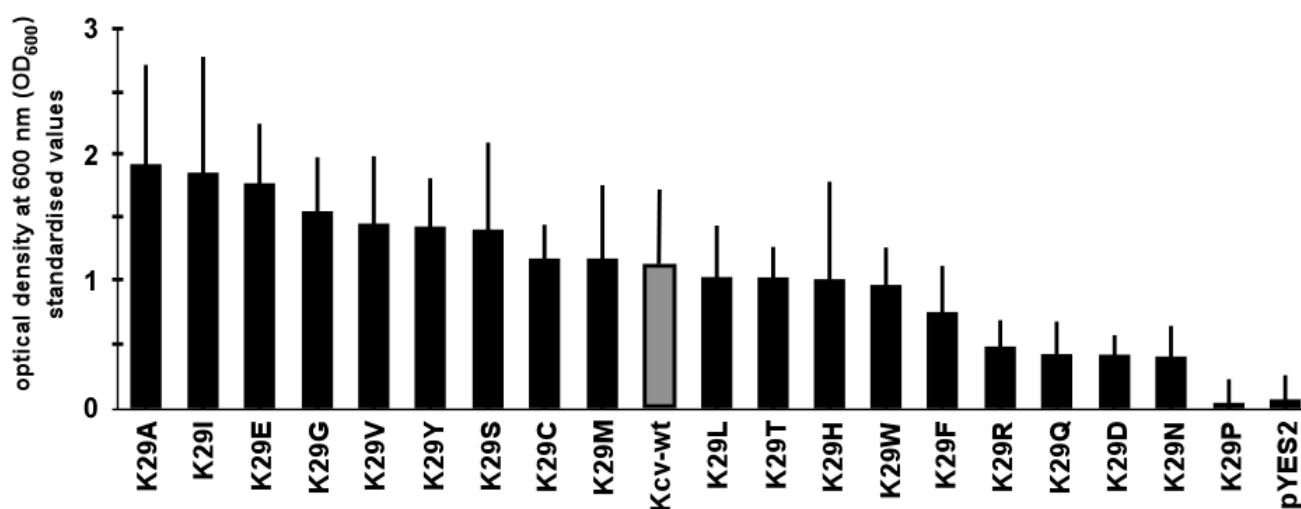
Figure 14: Comparison of the ability of the different Lys29 mutants to rescue yeast growth. Shown are the different optical densities at 600 nm (OD$_{600}$) of the empty vector pYES2 as a control and the different Kcv-K29 mutants (black bars) and of Kcv wildtype (Kcv-wt, grey bar) after 24 h of growth in liquid 0.5 mM selective media. With exception of K29P are all mutants able to rescue yeast growth. The OD$_{600}$ values are normalised to the density at the start of the experiment (with standard deviation).

When we align all the viral Kcv type channels (Figure 15), we realise that they all have in this position a Lys or an Arg. In the context of the experimental results, it is indeed remarkable to find that natural occurring orthologs of Kcv$_{PBCV-1}$ have either a Lys or an Arg in this very

position. This high degree of conservation implies that the charge at this site is more important than anticipated from the aforementioned experiments.

```
                    N     TM1      |                                              Pore helix                              TM2                    C

NC64A-    PBCV-1      -MLVFSKFLTRTEPFMIHLFILAMFVMIYKFFPGGFENNFS-----VANPDKKASWIDCLYFGVTTHSTVGFGDILPKTTGAKLCTIAHIVTVFFIVLTL----------   94
Viruses   MA-1D       -MLVFSKFLTRTEPFMIHLVVLAMFVTIYRFFPGGFENNFS-----VANPDKKASWIDCLYFGVTTHSTVGFGDILPKTTGAKLCTIAHIVTVFFIVLTL----------   94
          NY-2A       -MLVFSKFLMKTEPFMIHLVVLAMFVTIYRFFPGGFENNFS-----VANPDKKASWIDCLYFGVTTHSTVGFGDILPTSTGAKLCTIAHIVTVFFIVLTL----------   94
          NY-2B       -MLVFSKFLTRTEPFMIHLVVLAMFVTIYRFFPGGFENNFS-----VANPDKKASWIDCLYFGVTTHSTLGLGDILPRTTGAKFCTIAHVCIVFFIVLTL----------   94

ATC-      AlkaliCanal -MLLL---------LIHVGILVFFTTVIKMLPGGMFSNT--------DP-----SWVDCLYFSASTHTTVGYGDLTPKSPVAKLVATAHMMIVFAIVVSSFTFPW------   82
Viruses   AlkaliSmith -MLLL---------LIHVGILVFFTTVIKMLPGGMFSNT--------DP-----SWVDCLYFSASTHTTVGYGDLTPKSPVAKLVATAHMMIVFAIVVSSFTFPW------   82
          ATCV-1      -MLLL---------IIHIIILIVFTAIYKMLPGGMFSNT--------DP-----TWVDCLYFSASTHTTVGYGDLTPKSPVAKLTATAHMLIVFAIVISGFTFPW------   82
          AlkaliNPS   -MLLL---------LIHLSILVIFTAIYKMLPGGMFSNT--------DP-----TWVDCLYFSASTHTTVGYGDLTPKSPVAKLTATAHMLIVFAIVISGFTFPW------   82
          AlkaliNTS   -MLLL---------IIHLSILVIFTAIYKMLPGGMFSNT--------DP-----TWVDCLYFSASTHTTVGYGDLTPKSPVAKLTATAHMLIVFAIVISGFTFPW------   82

PbI-      MT325       -MSIL---------GVHFAILLLFAALYKFFPGGFENNFKRGDGSKEPV----SWMDAIYVSAATHTTTGFGDIVADSRAAKFAVTAHMLIVFSIVVLGLKPELITNLI---   95
Viruses   CVM-1       -MSIL---------GVHFAILLLFAALYKFFPGGFANNFKRSDGSKEPV----SWMDAIYVSAATHTTTGFGDIVADSRAAKFAVTAHMLIVFSIVVLGLKPELITNLYKIM   98
```

Figure 15: **Alignment of viral potassium channels of different viruses of the family of Phycodnaviridae.** Highlighted in black are the positions, which are corresponding to the lysine at position 29 in Kcv$_{PBCV-1}$. The vertical-bar above the alignment sketches the secondary structure of Kcv$_{PBCV-1}$.

Next, we tested therefore if the equivalent position in Kcv_{ATCV-1} and Kcv_{MT325} is in the same way tolerant to mutations as Kcv_{PBCV-1}. Kcv_{ATCV-1} and Kcv_{MT325} are two functional viral potassium channels (Gazzarrini *et al.* 2007 and 2009). Figure 16 shows yeast rescue experiments with the respective mutants. Yeast mutants expressing the mutant Kcv_{ATCV-1}-K19A and Kcv_{MT325}-K19A are both growing on medium with high K^+ concentration meaning that the chan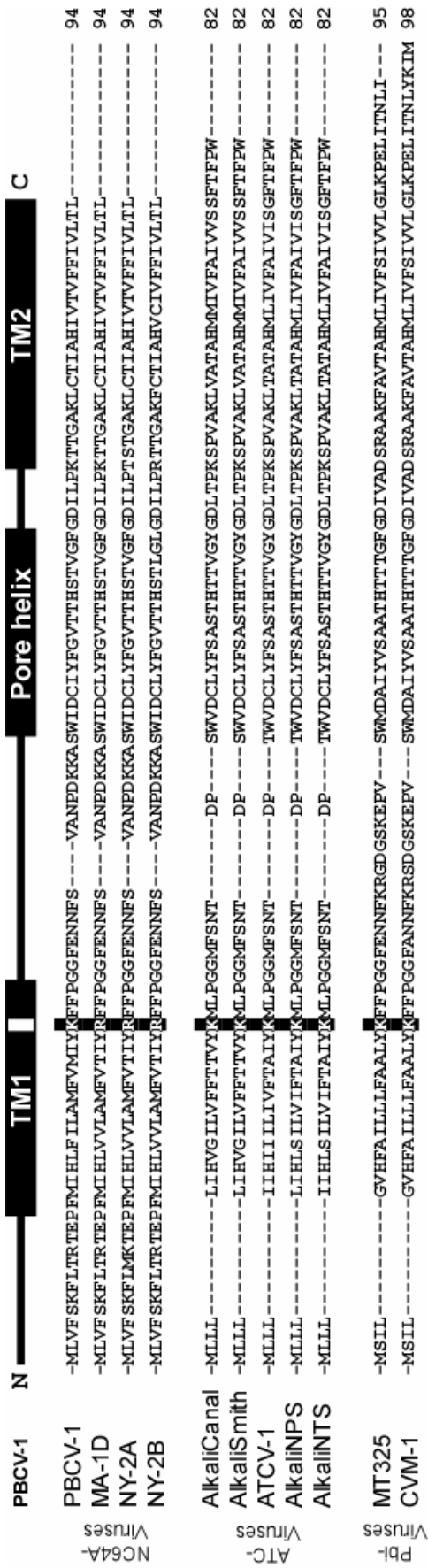nel is not deleterious for the cells. A growth test on selective medium on the other hand shows that neither of the two mutants is able to rescue the K^+ uptake deficient yeast mutants. This implies that a neutralisation of the charge renders these channels inactive.
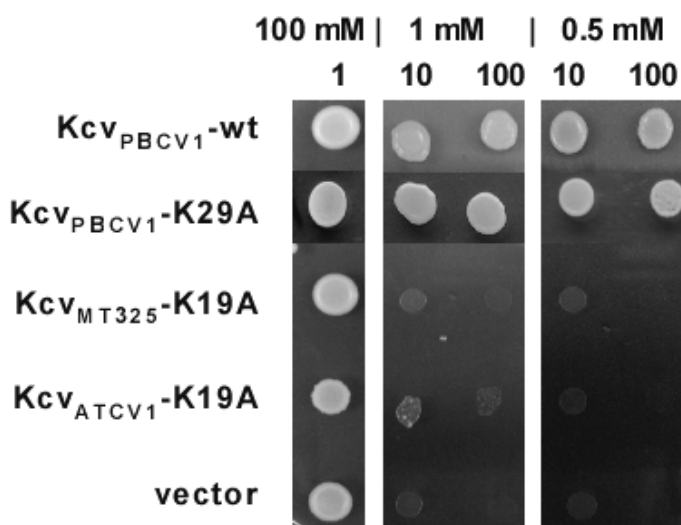
Figure 16: Yeast complementation assay of Kcv_{PBCV-1}-K29A and the equivalent position of Kcv_{PBCV-1}-K29 in Kcv_{ATCV-1} and Kcv_{MT325}. Shown is a yeast complementation assay of the mutants Kcv_{PBCV-1}-K29A, Kcv_{MT325}-K19A, Kcv_{ATCV-1}-K19A and the positive (Kcv_{PBCV-1}-wt) and negative (empty vector) control. These mutations equal the mutation Kcv_{PBCV-1}-K29A as shown in Figure 15. The yeast complementation assay was down as described in Figure 13.

The results of these experiments suggest that Kcv_{PBCV-1} tolerates a neutralisation of the charged amino acid in TMD1 while the other two Kcv channels do not (Figure 16). To test this further we measured the activity of a chimera of GFP with Kcv_{ATCV-1} or its mutants in HEK293 cells. The data in Figure 17 show a representative recording of mock-transfected HEK293 cells and a cell transfected with Kcv_{ATCV-1}-GFP. The mock-transfected, like un-transfected cells, shows the typical low conductance over a wide voltage range. Cells transfected with Kcv_{ATCV-1}-wt exhibit a clearly different current response to the standard voltage protocol. These cells have an elevated quasi-linear conductance at voltages between ca. +60 and -60 mV. At more hyperpolarised voltages the current/voltage (I/V) relation shows a pronounced negative conductance. In this respect the I/V relation of Kcv_{ATCV-1} is similar to that measured in *Xenopus* oocytes and the negative slope can be attributed to a fast gating of the channel at negative voltages. The typical Kcv_{ATCV-1} type I/V relation has been recorded in 6 out of 13 cells (= 46.15 %) revealing positive expression of the channel. In comparison, 65 % of the HEK293

cells transfected with Kcv$_{PBCV-1}$::GFP showed a characteristic Kcv channel activity (Hertel *et al.* 2009).
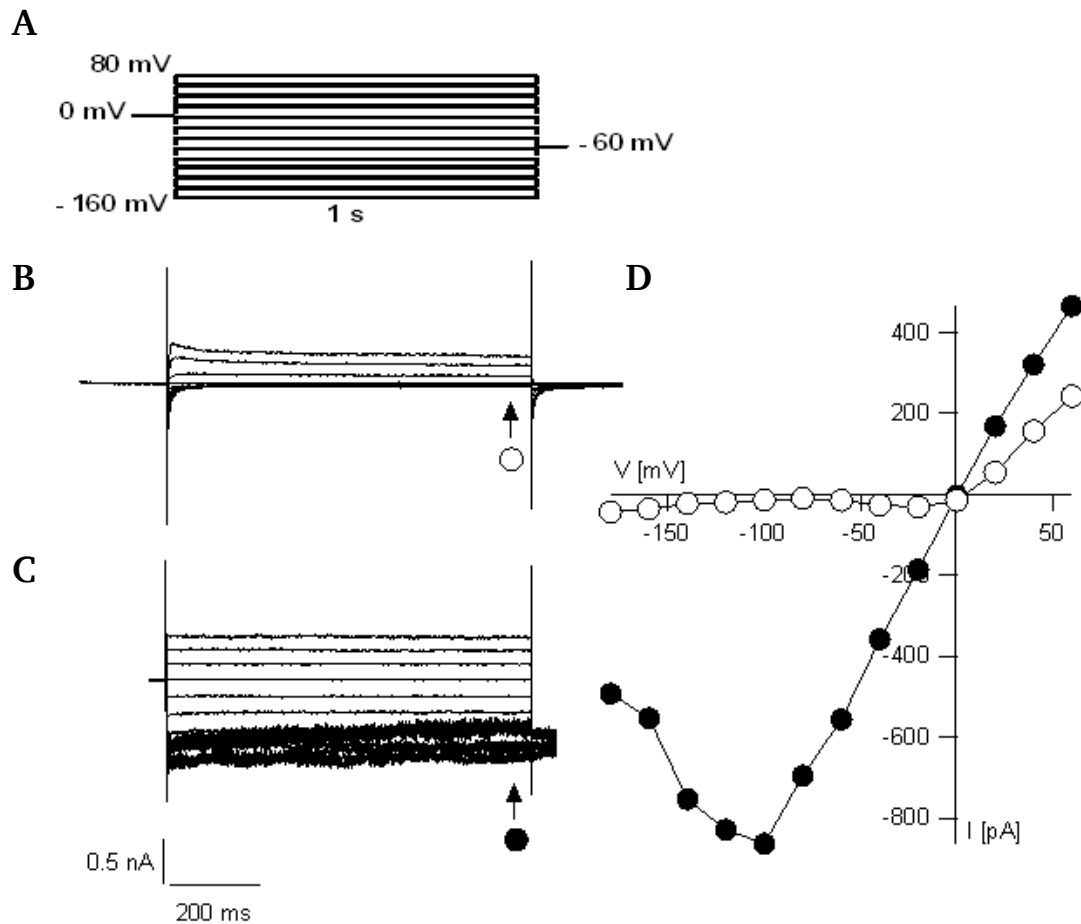
Figure 17: Electrophysiological measurements of HEK293 cells transfected with GFP or with Kcv$_{ATCV-1}$::GFP. Shown are **(B/C)** the current responses to a **(A)** standard pulse protocol and the corresponding **(D)** current-voltage relationships (I/V-curves) of HEK293 cells transfected with **(B)** GFP in 100 mM KCl bath solution and with **(C)** Kcv$_{ATCV-1}$-wt in 100 mM KCl bath solution. Currents were measured in whole cell configuration to standard voltage protocol from holding voltage (0 mV) to test voltages between +60 and -160 mV. The symbols of the I/V-relationships cross-reference with the symbols at the current traces.

To test the relevance of the charged amino acid, we also expressed Kcv$_{ATCV-1}$-K19A in HEK293 cells. In 14 cells, which, judged by the GFP fluorescence, expressed the mutant channel, we were not able to detect any cell in which the conductance was different from that of mock-transfected cells (Figure 18 and Figure 19). The results of these experiments confirm the data from the yeast rescue experiments (Figure 16) in that the amino acid in the position of the lysine cannot be neutralised. This is consistent with the finding that transfection of HEK293

cells with the mutant Kcv_{ATCV-1}-K19R exhibited currents, which were similar to those of the wild type (Figure 18) but with a lower amplitude (Figure 19).
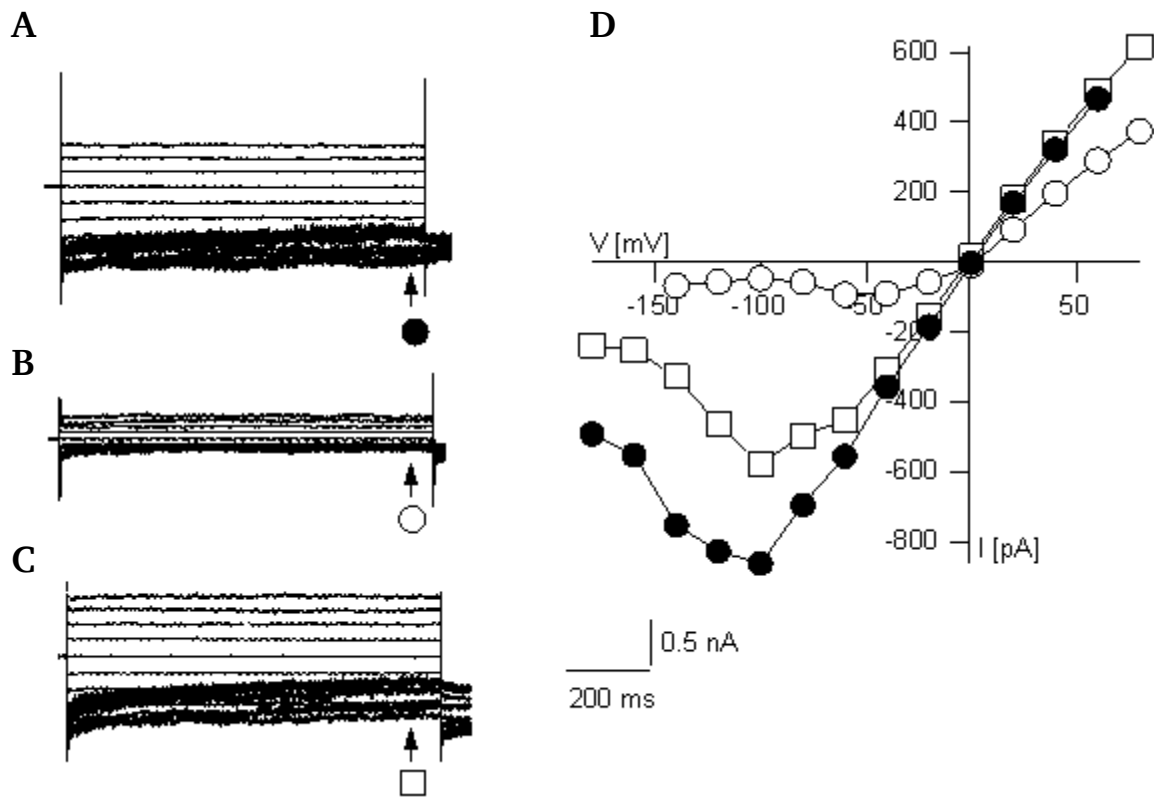
Figure 18: Electrophysiological measurements of HEK293 cells transfected with different Kcv_{ATCV-1}::GFP constructs. Shown are **(A-C)** the current responses to a standard pulse protocol (see Figure 17) and the corresponding **(D)** current-voltage relationships (I/V-curves) of HEK293 cells transfected with **(A)** Kcv_{ATCV-1}-wt, **(B)** Kcv_{ATCV-1}-K19A or **(C)** Kcv_{ATCV-1}-K19R in 100 mM KCl bath solution. Currents were measured in whole cell configuration to standard voltage protocols from holding voltages (0 mV) to test voltages between +60 and -160 mV. The symbols of the I/V-relationships cross-reference with the symbols at the current traces.

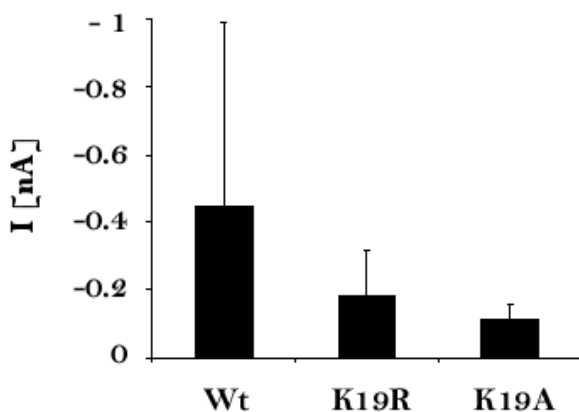**Figure 19: Comparison of the currents at -140 mV of HEK293 cells transfected with different Kcv_{ATCV-1}::GFP constructs.** Shown are the amplitudes of the mean currents with their standard deviation of HEK293 cells, which were transfected with Kcv_{ATCV-1}-wt (Wt, n = 4), Kcv_{ATCV-1}-K19R (K19R, n = 3) or Kcv_{ATCV-1}-K19A (K19A, n = 14) at a test voltage of -140 mV in 100 mM KCl bath solution.

3.5. Discussion

The main finding of the present study is that all Kcv type channels have in the outer transmembrane domain a conserved Lys or Arg at the interface between lipid and water. A positive amino acid in this position is very common in many transmembrane domains and it is thought that their long positive charged side chain is able to "snorkel". In this way, TM helices gain flexibility for the orientation in the membrane. The present data show that the interfacial position of the charged amino acid in a TM helix alone is not sufficient for understanding their impact on structure and function. While two of the tested Kcv type channels have a strict requirement for a positively charged amino acid in this position, the third one does not. This means that at least in Kcv_{PBCV-1} snorkeling is not essential for channel function.

While the pK_a values of Lys and Arg in water are well known, there is an uncertainty about their protonation state in non–aqueous microenvironments. Indeed in the case of membrane proteins, it has been shown that the pK_a of the basic amino acids can be reduced by as much as seven units in a protein environment (Pace *et al.* 2009). The group of Lee *et al.* showed that also a lipid environment can cause a significant decrease of 4.5 units in the pK_a value of these amino acids if they are in the core of the lipid bilayer (see Figure 8B of Li *et al.* 2008a, MacCallum *et al.* 2007, Yoo and Cui 2008).

A finding of this study is that K29 in Kcv_{PBCV-1} can be exchanged with nearly any amino acid without loosing channel activity. This implies that the channel has a very high structural tolerance in this domain with no requirement for a charge. The fact that Lys can be replaced in this channel by the neutral amino acid Ala and that a molecular model of the channel is most stable and active with a deprotonated Lys (Figure 11) suggests that this amino acid may even be deprotonated. Under these circumstances, lysine is not able to snorkel as also seen in simulations of Kcv wildtype from Tayefeh (Tayefeh *et al.* 2009) with protonated or deprotonated lysine at position 29 (Figure 20).
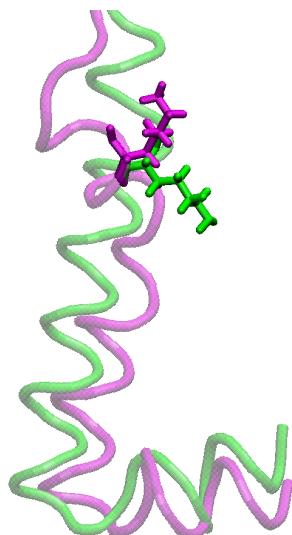
Figure 20: Cartoon of the TMD1 of one subunit of Kcv wildtype. Shown is the first TMD of Kcv wildtype with highlighted lysine at position 29 (Kcv-K29) in its protonated (magenta) or deprotonated (green) form. Only in the protonated state is the lysine able to snorkel.

Such behaviour is strikingly different from Kcv_{ATCV-1} and Kcv_{MT325} for which protonation of the pivotal basic residues is apparently essential. A possible explanation for this phenomenon can be deduced from our earlier modeling studies. It was consistently shown (Tayefeh *et al.* 2009) that protonation of K29 leads to a widening of the intracellular mouth region of Kcv_{PBCV-1}. The computational results furthermore suggest that the mouth diameter has to be restrained within a certain range (Tayefeh *et al.* 2007, 2009). Both too wide and too narrow distances between the C-terminal amino acids, which form the mouth, lead to an inactive channel. The reason for this is the inhibition of a crucial "turnstile" mechanism at the entry to the cavity (the C-termini switch between K^+-coordinated and salt bridge-bound states), which is necessary for ion translocation. On the other hand, the structural homology model for Kcv_{ATCV-1} (Gazzarini *et al.* 2009) based on the deprotonated Kcv_{PBCV-1} structure suggests that the longer (in comparison with Kcv_{PBCV-1}) TMD2s form a C-terminal mouth, which is too narrow for ion translocation. Taking these results together, it is very likely that protonation of Lys is necessary for sufficiently widening the shorter channel, which explains the apparent functional difference.

3.6. Conclusion

All in all the results reveal once more the complexity of protein-lipid-interactions. It is of vital importance to understand these interactions not only in the context of the spatial orientation and the surrounding lipid environment, but also in the context of the secondary structure of a given protein. The same amino acid can have, in a different protein context, a very different

influence on the functional properties and on the stability of a protein. The structural relevance of an individual protein can only be appreciated if all of its interactions are carefully observed.

3.7. References

Abenavoli A, DiFrancesco ML, Schroeder I, Epimashko S, Gazzarrini S, Hansen UP, Thiel G, Moroni A (2009) Fast and slow gating are inherent properties of the pore module of the K$^+$ channel Kcv. *J Gen Physiol.* 134:219-29. doi:10.1085/jgp.200910266

Ashcroft F (2000) Ion Channels and Disease. *Academic Press.*

Doyle DA (2004) Structural changes during ion channel gating. *Trends in Neurosciences* 27:298-302. doi:10.1016/j.tins.2004.04.004

Gazzarrini S, Kang M, Van Etten JL, Tayefeh S, Kast SM, DiFrancesco D, Thiel G, Moroni A (2004) Long-distance interactions within the potassium channel pore are revealed by molecular diversity of viral proteins. *JBC* 279:28443-28449. doi: 10.1074/jbc.M401184200

Gazzarrini S, Kang M, Epimashko S, Van Etten JL, Dainty J, Thiel G, Moroni A (2007) Chlorella virus MT325 encodes water and potassium channels that interact synergistically. *Proc Natl Acad Sci U S A.* 103:5355-60. doi:10.1073/pnas.0600848103

Gazzarrini S, Kang M, Abenavoli A, Romani G, Olivari C, Gaslini D, Ferrara G, van Etten JL, Kreim M, Kast SM, Thiel G, Moroni A (2009) Chlorella virus ATCV-1 encodes a functional potassium channel of 82 amino acids. *Biochem J.* 420:295-303.

Graham FL, Smiley J, Russell WC, Nairn R (1977) Characteristics of a human cell line transformed by DNA from adenovirus type 5. *J. Gen. Virol.* 36, 59-72

Haider S, Grottesi A, Hall BA, Ashcroft FM, Sansom MSP (2005) Conformational Dynamics of the Ligand-Binding Domain of Inward Rectifier K Channels as Revealed by Molecular Dynamics Simulations: Toward an Understanding of Kir Channel Gating. *Biophysical Journal* Volume 88:3310–3320

Hamill, OP, Marty A, Neher E, Sakmann B, Sigworth F (1981) Improved patch-clamp techniques for high-resolution current recording from cells and cell-free membrane patches. *Pflugers Arch.* 391:85–100.

Heginbotham L, Lu Z, Abramson T, MacKinnon R (1994) Mutations in the K$^+$ channel signature sequence. *Biophys J.* 66:1061–1067. PMCID:PMC1275813

Hertel B (2005) Struktur-Funktionsbeziehung in dem minimalen viralen Kalium-Kanal Kcv. Dissertation at the Technischen Universität Darmstadt

Hertel B, Tayefeh S, Mehmel M, Kast SM, Van Etten J, Moroni A, Thiel G (2006) Elongation of outer transmembrane domain alters function of miniature K^+ channel Kcv. *J. Membr. Biol.* 210:21–29. doi:10.1007/s00232-005-7026-4

Hertel B, Tayefeh S, Kloss T, Hewing J, Gebhardt M, Baumeister D, Moroni A, Thiel G, Kast SM (2009) Salt bridges in the miniature viral channel Kcv are important for function. *Eur Biophys J.* doi: 10.1007/s00249-009-0451-z

Hille B (2001) Ion channels of excitable membranes. 3. Aufl., Sinauer Associates Inc.,Sunderland

Ho K, Nichols CG, Lederer JW, Lytton J, Vassilev PM, Kanazirska MV, Hebert SC (1993) Cloning and expression of an inwardly rectifying ATP-regulated potassium channel. *Nature* 362:31 – 38. doi:10.1038/362031a0

Jan LY and Jan YN (1992) Structural elements involved in specific K+ channel functions. *Annu. Rev. Physiol.* 54:537-555

Kang M, Moroni A, Gazzarrini S, DiFrancesco D, Thiel G, Severino M, VanEtten JL (2004) Small potassium ion channel proteins encoded by chlorella viruses. *PNAS* 101:5318-5324

Kuo A, Gulbis JM, Antcliff JF, Rahman T, Lowe ED, Zimmer J, Cuthbertson J, Ashcroft FM, Ezaki T, Doyle DA (2003) Crystal Structure of the Potassium Channel KirBac1.1 in the Closed State. *Science* 300:1922 – 1926 doi:10.1126/science.1085028

Li L, Vorobyov I, MacKerell A.D, Allen TW (2008a) Is arginine charged in a membrane? *Biophys J.* 94:L11–L13. doi:10.1529/biophysj.107.121566.

Li L, Vorobyov I, Allen TW (2008b) Potential of mean force and pKa profile calculation for a lipid membrane-exposed arginine side chain. *J Phys Chem B.* 112:9574-87. doi:10.1021/jp7114912

MacCallum JL, Bennett WFD, Tieleman PD (2007) Partitioning of Amino Acid Side Chains into Lipid Bilayers: Results from Computer Simulations and Comparison to Experiment. *J Gen Physiol.* 129:371–377. doi:10.1085/jgp.200709745.

MacKinnon R (1991) Determination of the subunit stoichiometry of a voltage-activated potassium channel. *Nature* 350:232-235

Miller C (1992) Ion channel structure and function. *Science* 258:240-241

Minor DL, Masseling SJ, Jan YN, Jan LY (1999) Transmembrane Structure of an Inwardly Rectifying Potassium Channel. *Cell* 96:879-891. doi:10.1016/S0092-8674(00)80597-8

Moroni A, Viscomi C, Sangiorgio V, Pagliuca C, Meckel T, Horvath F, Gazzarrini S, Valbuzzi P, Van Etten JL, DiFrancesco D, Thiel G (2002) The short N-terminus is required for functional expression of the virus-encoded miniature K$^+$ channel Kcv. *FEBS Lett.* 530, 65-69

Neher E (1992) Ion channels for communication between and within cells. *EMBO* 11:1673 - 1679

Pace NC, Grimsley RG, Scholtz JM (2009) Protein Ionizable Groups: pK Values and Their Contribution to Protein Stability and Solubility. *JBC* 284:13285–13289. doi: 10.1074/jbc.R800080200

Pagliuca C, Goetze TA, Wagner R, Thiel G, Moroni A, Parcej D (2007) Molecular Properties of Kcv, a Virus Encoded K$^+$ Channel. *Biochemistry* 46:1079–1090. doi:10.1021/bi061530w

Perozo E, Cortes DM, Cuello LG (1999) Structural Rearrangements Underlying K$^+$-Channel Activation Gating. *Science* 285, 73-78. doi:10.1126/science.285.5424.73

Plugge B, Gazzarrini S, Nelson M, Cerana R, Van Etten JL, Derst C, DiFrancesco D, Moroni A, Thiel G (2000) A potassium channel protein encoded by chlorella virus PBCV-1. *Science* 287:1641–1644

Schroeder JI, Hedrich R (1998) Involvement of ion channels and active transport in osmoregulation and signalling of higher plant cells. *Trends in Biochemical Sciences* 14:187-192. doi:10.1016/0968-0004(89)90272-7

Shim WJ, Yang M, Gu LQ (2007) In vitro synthesis, tetramerization and single channel characterization of virus-encoded potassium channel Kcv. *FEBS Lett.* 581:1027-34. doi:10.1016/j.febslet.2007.02.005

Strandberg E, Killian JA (2003) Snorkeling of lysine side chains in transmembrane helices: How easy can it get? *FEBS Lett.* 544:69-73. doi:10.1016/S0014-5793(03)00475-7

Tang W, Ruknudin A, Yang WP, Shaw SY, Knickerbocker A, Kurtz S (1995) Functional Expression of a Vertebrate Inwardly Rectifying K+ Channel in Yeast. *Mol. Biol. of the Cell* 6:1231-1240. PMID:8534918

Tayefeh S, Kloss T, Thiel G, Hertel B, Moroni A, Kast SM (2007) Molecular dynamics simulation study of the cytosolic mouth in Kcv-type potassium channels. *Biochem* 46:4826–4839. doi:10.1021/bi602468r

Tayefeh S, Kloss T, Kreim M, Gebhardt M, Baumeister D, Hertel B, Richter C, Schwalbe H, Moroni A, Thiel G, Kast SM (2009) Model development for the viral potassium channel. *Biophys J* 96:485–498. doi:10.1016/j.bpj.2008.09.050

Ulmschneider, MB, Sansom MS (2001) Amino acid distributions in integral membrane protein structures, *Biochim. Biophys. Acta* 1512:1-14.

Wollmuth PL, Sobolevsky AI (2004) Structure and gating of the glutamate receptor ion channel. *Trends in Neurosciences* 27:321-328. doi:10.1016/j.tins.2004.04.005

Yoo J, Cui Q (2008) Does Arginine remain protonated in the lipid membrane? Insights from microscopic pK_a calculations.
Biophys J. 94:L61–L63. doi:10.1529/biophysj.107.122945.

4.1. Abstract

Ion channels are common in all life forms and play a decisive role for a multitude of biological functions; a dysfunction of ion channels leads in many cases to diseases. In the present study, we analyse the potassium channel Kcv from PBCV-1. Kcv is with only 94 amino acids one of the smallest known potassium channels. Nonetheless, it contains many structural and functional hallmarks of more complex potassium channels; it essentially represents the pore module of them. The combination of small size and robust function makes Kcv a good tool to study structure/function relationships and to achieve an overall better understanding of the structural complexity and functionality of potassium channels. For this reasons, an alanine-scanning mutagenesis of the two transmembrane domains of Kcv was used to identify crucial sites for a proper channel function. The mutants were tested with the help of a yeast complementation assay and in selected cases also with electrophysiological methods. Two structural features, which are essential for channel function, were detected with the help of the scanning. One feature is the anchoring of the first transmembrane domain in the lipid membrane with the help of aromatic residues; the second is an interhelical - -interaction between the two transmembrane domains of Kcv. The functional experiments imply that both features are important for the stabilisation of the protein structure and for the correct positioning of the protein in the lipid membrane. The deletion of one of these features leads to a total loss of channel function, which is probably the result of enhanced protein flexibility and a lack of coordination between the transmembrane domains.

4.2. Introduction

Potassium channels are tetrameric proteins, which mediate K^+ fluxes across membranes. They are common in all life forms from bacteria to higher plants and humans and essential for many biological functions such as the cell-cell-communication, osmoregulatory processes or for the action potential (Hille 2001). Mutations in potassium channels are often linked to diseases like diabetes or epilepsy to name just a few of these so-called channelopathies (George 1995). The existence of potassium channels decreases the energy barrier for the transport of potassium ions across lipid membranes dramatically from 50 kcal*mol^{-1}

(Parsegian 1969) to less than 3 kcal*mol^{-1} (Berneche and Roux 2001). Furthermore, ion channels are profoundly selective, and this selectivity is provided by a specific structure in the channel, the selectivity filter. The latter has the sequence **TxxTxGY/FG**, which is highly conserved through all different types of potassium channels (Heginbotham *et al.* 1994). In addition to the filter domain, also other regions in the modular protein, which are responsible for distinct channel properties, such as ion conductance, gating and subunit assembly, have been revealed by extensive electrophysiological, biochemical and structural studies (Heginbotham *et al.* 1994, Koster *et al.* 1998, Schulteis *et al.* 1998).

Kcv is a viral potassium channel and one of the smallest known potassium channels; a Kcv monomer is with only 94 amino acids minimal indeed, but it reveals, nevertheless, many essential structural and functional hallmarks of more complex K$^+$ channels (Figure 21). Because of the structural simplicity of this functional channel, the Kcv protein offers a good model system (Kang *et al.* 2004) for analysing basic structure/function correlates in K$^+$ channel proteins per se. This is supported by the accessibility of Kcv function by electrophysiological methods; the protein generates currents in different heterologous expression systems like Xenopus oocytes, Human Embryonic Kidney cells (HEK293) and *Saccharomyces cerevesiae*.
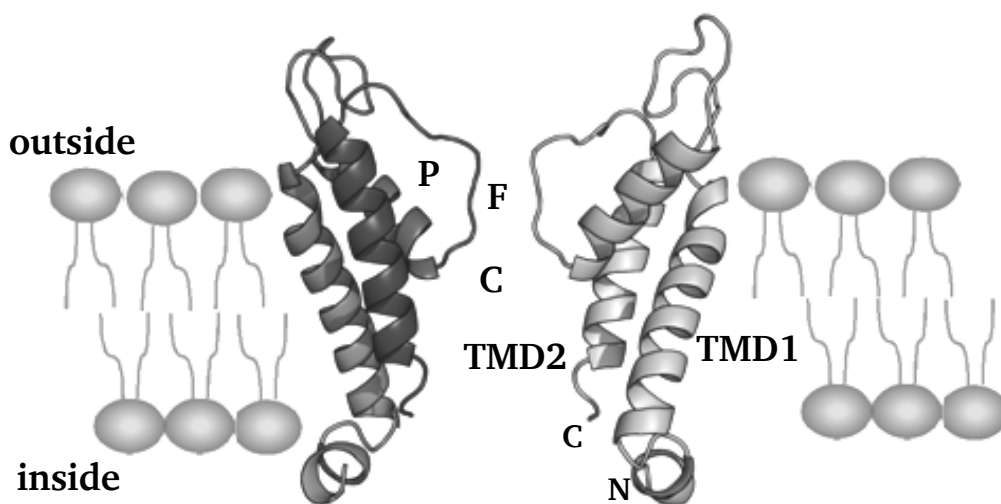

Figure 21: Homology Model of Kcv based on the structure of synthetic KirBac1.1. Shown are two of four subunits as ribbons in the lipid bilayer (gray cartoons) with the transmembrane domains 1 and 2 (TMD1, TMD2) with marked C- and N-terminus, the pore helix (P) and the two main functional areas: the filter region (F) and the cavity (C) (Based on the model of Tayefeh *et al.* 2009)

In spite of its small size, also the Kcv channel is gated and currently at least two different gates are discussed for this channel (Gazzarrini *et al.* 2002 and 2004 Abenavoli *et al.* 2009). Single channel experiments show that extreme negative and positive voltages evoke a fast closing of the channel. This fast gating is explained by a gating feature of the selectivity filter. Furthermore, single channel recordings showed that negative voltages evoke a slow activation of channel activity, suggesting at least one additional gate. There is experimental evidence that the latter gate of Kcv also involves the transmembrane domains (TMD). It was found that mutations in the outer transmembrane domain affected via some unknown long distance interactions the gating of the channel (Baumeister 2010).

Unbiased information on the structural significance of the TMDs and on molecular interactions within the protein, which are important for channel function, can be obtained by an alanine-scan of the relevant domains. In this approach, each amino acid in a primary sequence is individually replaced by the amino acid alanine and the effect of this mutation is tested in a functional assay. In this way, it is possible to eliminate all side chain interactions, except for the C_β atom, without altering the main chain conformation or the insertion of steric effects (Cunningham *et al.* 1989, Holst *et al.* 1998, DiCera 1998). Alanine is a common natural amino acid in all kinds of secondary structures including TMDs (Cunningham *et al.* 1989). For these reasons, alanine is the amino acid of choice in the mutagenesis scan. Hence, the replacement of a residue by alanine should reveal the contribution of the replaced residue to the overall stability and fold of the protein (Clackson and Wells 1995).

In the present study, we use alanine-scanning mutagenesis of the two transmembrane domains of Kcv to uncover structure/function correlates in the miniature potassium channel. A crystal structure of Kcv is not yet available but a homology model of the viral K^+ channel supports the interpretation of the results from the alanine scanning. The latter was elaborated based on the crystal structure of KirBac1.1, a channel, which shares some similarities with Kcv in critical positions (Tayefeh *et al.* 2007, 2009). Extensive MD simulations with the homology model showed that it behaves in a way that is expected for a K^+ channel. This underscores that the homology model of Kcv is a good representation of the real channel structure.

4.3. Material and Methods

4.3.1. Constructs and Mutagenesis

For electrophysiological measurements in HEK293 cells, the Kcv gene without its stop codon was cloned into the BglII and EcoRI site of the pEGFP-N2 vector (Clontech-Takara Bio Europe, Saint-Germain-en-Laye, France) in frame with the downstream enhanced green fluorescent protein (EGFP). For the yeast complementation assay the Kcv gene was cloned into pYES2 (Invitrogen GmbH, Karlsruhe, Germany) into the EcoRI and XhoI site or as a chimera with EGFP into the BamHI and XhoI site of the plasmid (Minor *et al.* 1999). The QuikChange Site-directed Mutagenesis method (Stratagen) was used to insert the point mutations. The inserted mutations were specificly chosen on the primer level or randomised on the primer level by using the wobble base codon NNK (N = AGCT, K = GT), which codes for all possible amino acids The resulting construct sequences were confirmed by DNA sequencing.

4.3.2. *Saccharomyces cerevisiae* Complementation Assay

All selection experiments were done as described in Minor (1999). The yeast strain SGY1528 (Mat *a ade* 2–1 *can* 1–100 *his* 3–11,15 *leu* 2–3,112 *trp* 1–1 *ura* 3–1 *trk* 1::HIS3 *trk* 2::TRP1) was used for all complementation assays (Tang *et al.* 1995) and was kindly provided by Dr. Minor (UCSF, USA). The strain lacks an endogenous potassium uptake system and is, therefore, not able to grow on media that contains less than 10 mM potassium. For the complementation assay, yeast cells were grown in parallel under selective (1mM and 0.5 mM KCl agar plates) and non-selective (100 mM KCl agar plates) conditions for three days at 30 °C.

For the experiments with liquid cultures, 0.5 mM K^+ selective media was used and the optical density was measured at 600 nm (OD_{600}). Therefore, 0.5 mM K^+ selective media was inoculated with a yeast suspension (prepared and washed in the same manner as for the plates) to a final OD_{600} of 0.1 and incubated directly in sterilised 2 ml cuvettes sealed with laboratory film at 30 °C and 230 rpm. After 0 h and 24 h the OD_{600} was measured using a spectrophotometer.

For the disk diffusion assay 20 μl of the 1:100 yeast culture dilution, which was also used for the complementation assay, was plated on 1 mM KCl selective agar plates. In the middle of

the plates was a filter disk placed soaked with 30 μl 10 mM $BaCl_2$ or CsCl. The plates were incubated for three days at 30 °C.

4.3.3. Electrophysiological Measurements

For the electrophysiological measurements, HEK293 cells were transfected with different Kcv constructs cloned in the pEGFP vector. After one day of growth at 37 °C in 5 % CO_2 the transfected cells were dispersed with Accutase® (SIGMA-ALDRICH, Schnelldorf, Germany), disseminated at low density on new 35 mm culture dishes and allowed to settle over night. With the help of an inverted microscope, the patch-clamp measurements were performed on single cells in the whole-cell configuration according to standard protocols (Hamill *et al.* 1981). Currents were recorded with an EPC-9 Patch Clamp amplifier (HEKA, Lambrecht, Germany) and stored on a computer. Data acquisition and analysis was performed with the Pulse software (HEKA, Lambrecht, Germany). The currents were measured at room temperature in different bath solutions containing as a standard 100 mM KCl, 1.8 mM $CaCl_2$, 1 mM $MgCl_2$ and 5 mM HEPES (pH 7.4). In some cases, KCl was replaced by an equimolar concentration of NaCl. For block experiments, barium chloride was added to the 100 mM KCl bath solution to give a final concentration of 10 mM $BaCl_2$. To adjust the osmolarity of the solutions to 300 mOsmol an addition of mannitol was preferred over that of choline chloride (Hertel *et al.* 2009) since the latter inhibits the conductance (Baumeister 2010). For a fast exchange of the solution, the bath chamber was perfused from a perfusion pipette, which was positioned near to the cell analysed; this allowed a fast exchange of the solution in approximately 1 minute. The patch pipettes contained 130 mM D-potassium-gluconic acid, 10 mM NaCl, 5 mM HEPES, 0.1 mM GTP (Na salt), 0.1 μM $CaCl_2$, 2 mM, $MgCl_2$, 5 mM Phosphocreatine, 2 mM ATP (Na salt) (pH 7.4). For the measurements in whole-cell configuration, the holding voltage was 0 mV and the testing voltages were between +60 and -160 mV.

4.3.4. Homology Model Structure Analysis

For analysing the spatial distribution of amino acids in the channel protein, the homology model of Kcv based on the tetrameric form of the KirBac1.1 (PDB-Code: 1P7B) x-ray template structure was used (Tayefeh *et al.* 2009). The open source program PyMOL

(http://www.pymol.org/) was used for studying the 3D structure and the spatial relationship of the amino acid residues and the the ConSurf server (http://consurftest.tau.ac.il/) was used to identification the functionally important regions of Kcv based on the phylogenetic relations between its close sequence homologues (Ashkenazy *et al.* 2010, Landau *et al.* 2005, Glaser *et al.* 2003).

4.4. Results and Discussion

4.4.1. Alanine-scanning Mutagenesis of the two Transmembrane Domains of Kcv

In order to detect functionally important side chains in the amino acid composition of the transmembrane domains of Kcv, the respective amino acids were one by one replaced by the amino acid alanine; the two alanines, which are already present in the wildtype (wt) channel TMDs, were replaced by glycine. All channel mutants were expressed individually in a yeast strain, which lacks a functional K^+ uptake system. These yeasts are only able to survive in medium with a high K^+ concentration. They do not grow on a selective low K^+ medium unless they are expressing a heterologous K^+ uptake system. Figure 22 shows a typical example in which the yeasts were transfected with the empty vector; they only grow on medium with high K^+ but not low K^+ concentration. In contrast yeasts, which express a functional system for K^+ uptake, such as the endogenous K^+ transporter TRK1 (Transport of potassium 1) or the human Kir2.1 channel (Inward rectifier potassium channel 2.1), are able to survive on low K^+ medium (Figure 22). In addition, yeasts, which express the viral K^+ channel Kcv, survive in the selection medium (Figure 22). This means that this yeast rescue system is a suitable test system for evaluating the function of the Kcv channel and its mutants.
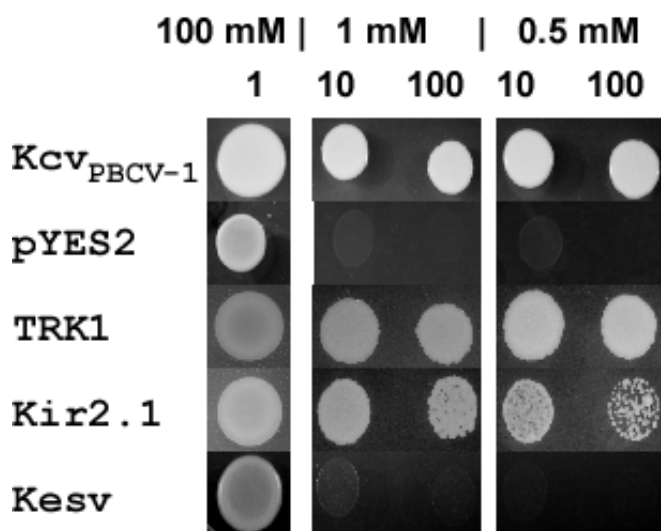
Figure 22: Yeast Complementation Assay of different constructs. Shown is a yeast strain, which lacks a functional K^+ uptake system, which is transformed with different potassium channel constructs or with the empty vector as control. Only yeasts, which express a functional system for K^+ uptake (TRK, Kir2.1 or Kcv) are able to survive on the selective media. Functional channels, which are not sorted to the plasma membrane (Kesv), are not able to rescue the yeast growth. The 100 mM KCl media serve as a control to test if the heterologous expressed proteins are toxic for the yeasts. Hence, all yeasts should grow under this condition.

Figure 23 shows a similar experiment to that of Figure 22. In this case, all the mutants from the scanning mutagenesis of both transmembrane domains are examined for function. Again, all the mutants are able to grow on high K^+ medium meaning that the expression of none of the mutations is deleterious for the cells. Many mutants also grow under the selection conditions. This implies that a large number of amino acid positions in the TMDs tolerate a mutation into alanine without loss of function. The data also highlight several important amino acids, which are crucial for channel function in yeast. The substitutions of nearly all phenylalanines (Phe14, Phe24, Phe30 and Phe31), histidine (His17), isoleucine (Ile20), tyrosine (Tyr28) and proline (Pro32) in the first transmembrane domain show the most dramatic effects; in these cases, the substitution results in a near complete loss of channel function.

The picture is different in the second transmembrane domain. In this domain the scanning reveals that nearly all of the amino acids are not crucial for channel function; yeast growth is mostly unaffected by the replacement with alanine. Only the substitution of histidine (His83) causes a total loss of function while substitution of leucine (Leu94) leads only to a significantly reduced function of growth (for a closer analysis see chapter 4).
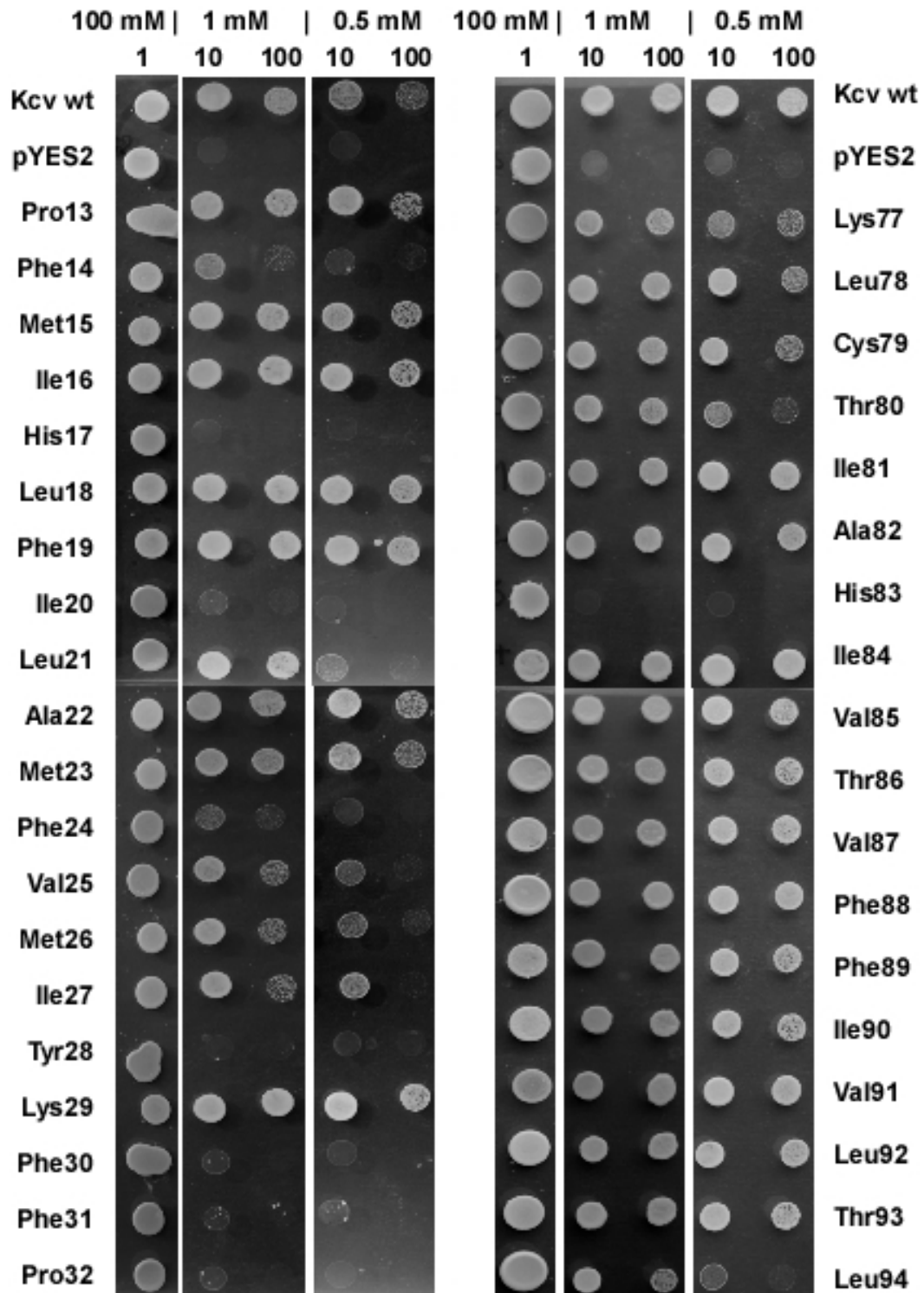
Figure 23: Alanine-scanning mutagenesis of the two transmembrane domains of Kcv. Shown is the yeast complementation assay of the alanine scan of the two TMDs of Kcv, where every position was replaced by alanine or glycine respectively. The assay was done with three different potassium concentrations in the media: 100 mM KCl as control and 1 mM as well as 0.5 mM KCl as selective conditions. The yeast mutants, as well as Kcv-wt and the empty vector as controls, were spotted in different dilutions: 1 (undiluted), 1:10, 1:100 and 1:1000. The test results are partly shown in the figure.

All in all the alanine-scanning mutagenesis allowed us to discover several crucial amino acid side chains in both transmembrane domains, which are essential for channel function. It occurs that the first TMD is more sensitive to mutations while the second TMD is more tolerant to changes.

4.4.2. The First TMD is Essential for Correct Positioning of the Channel

To understand the spatial organisation of the sensitive amino acids in the context of the three-dimensional structure of the channel, we localised their position in the homology model of Kcv (Tayefeh *et al.* 2009). Figure 24 shows the Kcv structure with the respective amino acids highlighted.
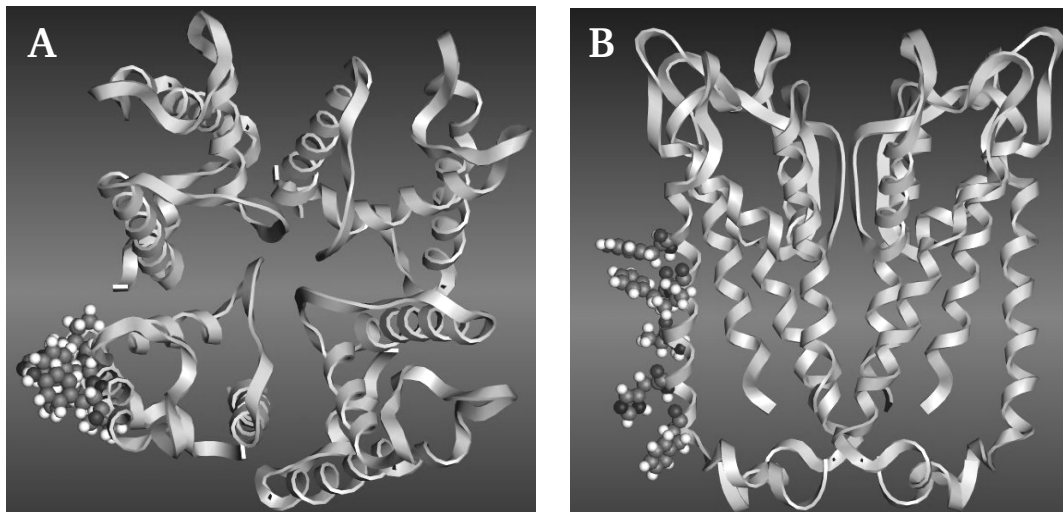
Figure 24: Position of selected amino acid residues of the first transmembrane domain of Kcv. Shown are the four subunits of Kcv as ribbons in **(A)** top view and **(B)** side view with highlighted amino acids of the TMD 1, which were detected by the alanine-scanning mutagenesis, namely Phe31, Tyr28, Phe24, Ile20 and His17. Both views demonstrate that all these residues are positioned on one side of the helix and pointing towards the lipid bilayer (by courtesy of Prof. Stefan M. Kast, TU Dortmund).

With this analysis, it occurs that the relevant amino acids of the first transmembrane domain (TMD1) are nearly all directed with their side chains in the direction of the membrane. Figure 25 illustrates that nearly all of these sensitive amino acids shown in Figure 24 except from Phe31 are also highly conserved within the sequences of all viral potassium channels.
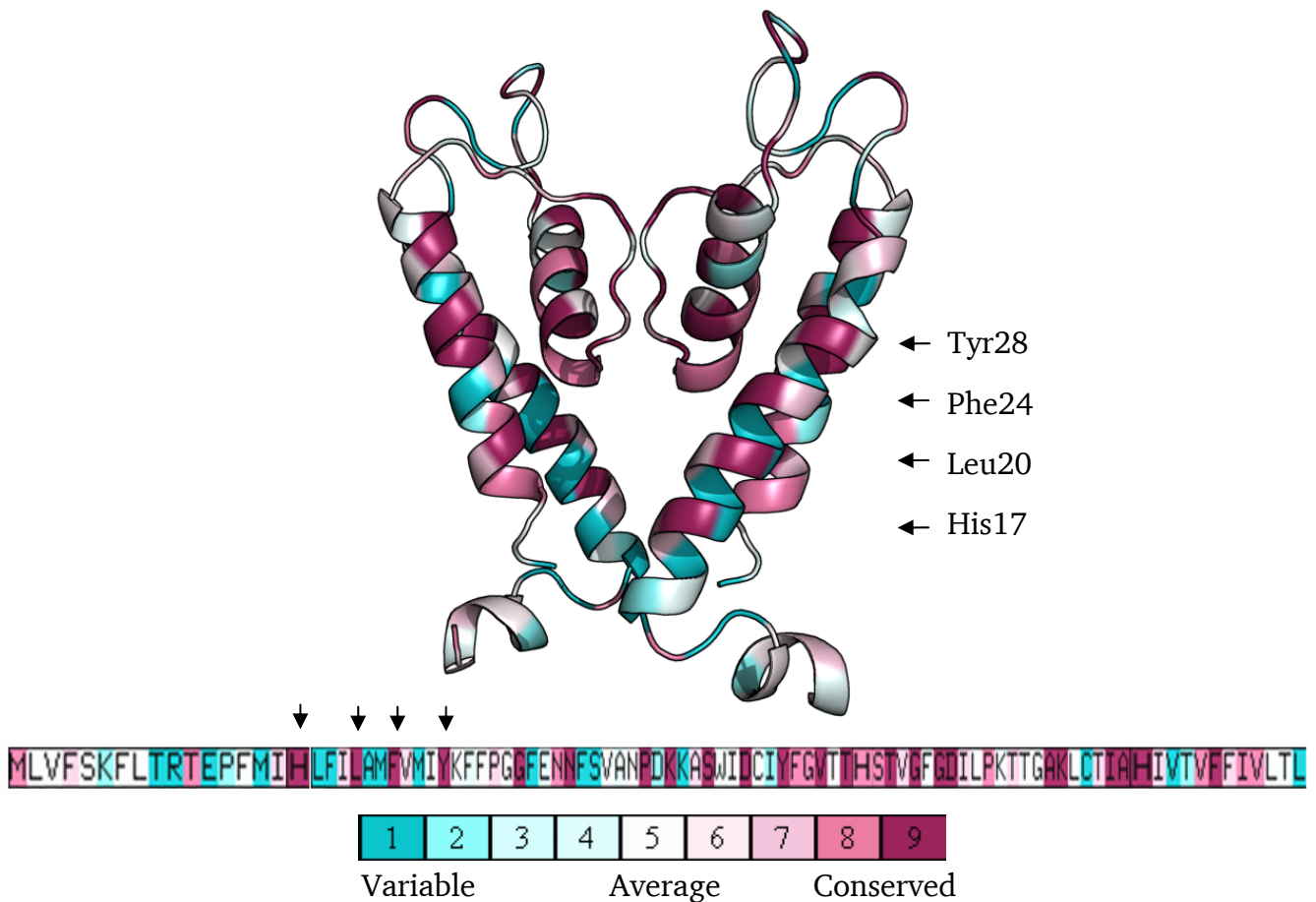
Figure 25: Homology model and sequence of Kcv coloured according to the conservation pattern of the amino acid residues. Shown are two out of four subunits of Kcv as a cartoon in side view and beneath the sequence of Kcv in the same colour code. The different colours indicate the grades of conservation and range from blue = variable residue to purple = highly conserved residues. Four from the five amino acid residues (black arrows), which were detected by the alanine-scanning mutagenesis (see Figure 24) are highly conserved within the viral potassium channels (drawn with http://consurftest.tau.ac.il/).

The conservation and orientation together with the aromatic side chain character of the relevant amino acids suggests that these amino acids are involved in the anchoring of the transmembrane domain in the lipid. The loss of function of these mutants could be explained through the reduced hydrophobicity of the alanine compared to the amino acids in the wt channel. To test the hypothesis two mutants were constructed for position Phe24 and Val25 in which the substituted alanine was replaced by the hydrophobic amino acid leucine. A test of these mutants in the yeast system revealed that the substitution to leucine could not recover channel function (Figure 26); hence, the hydrophobic nature of the amino acid in this position is not the only requirement.
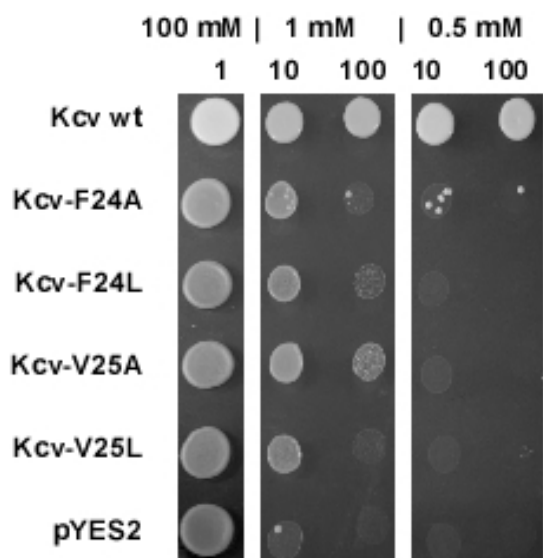
Figure 26: Yeast Complementation Assay of the two positions Phe24 and Val25. Shown is the yeast complementation assay of Kcv wt (positive control), pYES2 (negative control) and of the substitutions of phenylalanine at position 24 (F24) and valine at position 25 (V25) in the first TMD of Kcv against alanine (A) or leucine (L). The complementation assay was done as described in Figure 23. The visible colonies of Kcv-F24A at 0.5 mM KCl are papillae through spontaneous appearing mutations.

Another reason for the loss of function in the mutants could be the absence of aromatic side chains, which might be required for anchoring the TMD1 in the membrane. To test this idea, the amino acids Phe24 and Tyr28 were changed to tryptophan or tyrosine for position 24 or to tryptophan, histidine or phenylalanine for position 28. The results of the yeast complementation assay (Figure 27) imply that an aromatic side chain in these positions is sufficient to assure channel function. All aromatic substitutions were able to rescue more or less channel function in contrast to the exchange to alanine, which totally abolished channel function for both positions (small colonies, so-called papillae, are only due to spontaneous mutations and, therefore, ignorable). The results are not unexpected as, for example, Phe and Tyr are in terms of their structure closely related. The only difference is the presence of a *para*-OH on Tyr (McGaughey *et al.* 1998) and, hence, Tyr is able to takes over the function of Phe and anchor the TMD1 in the membran. Therefore, aromatic amino acids, which are pointing towards the lipid membrane, are a crucial factor for the anchoring of the TMD1 in the membrane and, hence, for a proper channel function.
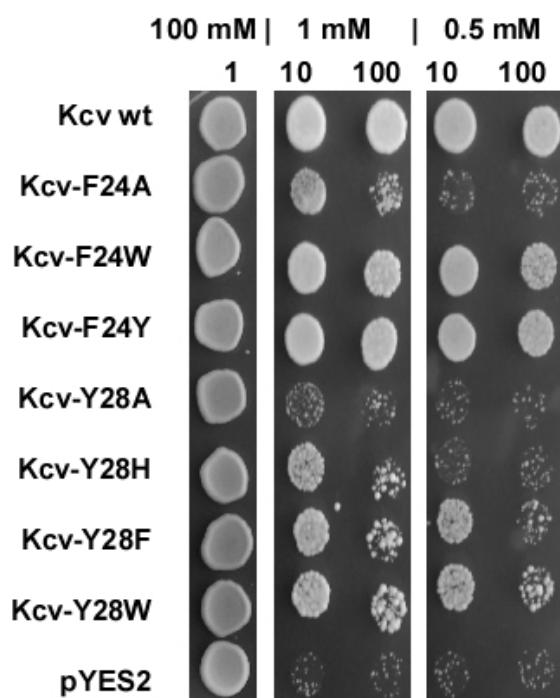
Figure 27: Yeast complementation assay of the two positions Phe24 and Tyr28. Shown is the yeast complementation of the phenylalanine at position 24 (Kcv-F24) and of the tyrosine at position 28 (Kcv-Y28) in the TMD1, which were substituted against alanine (A), histidine (H), phenylalanine (F), tryptophan (W) or tyrosine (Y). The complementation assay was done as described in Figure 23. Small visible colonies as seen for example for pYES2 at 1 mM or 0.5 mM KCl are only papillae through spontaneous appearing mutations. Therefore, the growth of all mutants has to been seen in the context of the background growth of the negative control pYES2.

In addition, another aromatic position, namely the histidine at position 17 (His17), was studied by a randomised mutagenesis study. 12 of the 60 tested yeast colonies transformed with the randomised plasmids showed also growth on 0.5 mM KCl selective plates. Table 3 shows the sequencing results of the growing colonies.

Table 3: Overview of the sequencing results of the randomised mutagenesis study of the histidine at position 17 from Kcv. Listed are the different sequencing results for the position 17 and the number of their occurrence. Tested were the 12 colonies out of 60, which showed growth on selective 0.5 mM KCl media.

Mutation at position His17	Frequency
None or silent mutation	4
Asparagine	4
Tryptophan	3
Serine	1

The obtained mutations were rechecked by a yeast complementation assay and in liquid culture (data not shown). These control experiments revealed that the mutations with asparagine (Kcv-H17N) or with serine (Kcv-H17S) were false positive, i.e. not growing under selective conditions. Only the substitution of histidine to tryptophan was able to rescue

channel function. Therefore, it seems that tryptophan is the only amino acid exchange, which can rescue channel function.

The results of these experiments fit perfectly with the aforementioned results of Figure 27 and underscore the importance of the aromatice side chains for the anchoring of the protein. The results of the experiment show that the exposure and geometric orientation of the side chains towards the lipid bilayer is essential for a proper positioning of the channel in the membrane.

It occurs that nearly all amino acids in the first TMD, which cannot be substituted by alanine have aromatic residues. The only exception is the isoleucine at position 20 in TMD1. Previous studies have already revealed that this position influences the gating of the channel via long distance interactions with the pore (Gazzarrini *et al.* 2004). It was found that the replacement of the isoleucine with valine altered the behaviour of the channel. For example, this mutant is more sensitive against caesium than the wildtype channel in voltage clamp measurements in *Xenopus laevis* oocytes (Gazzarrini *et al.* 2004). In the present study the substitution of Ile20 to alanine leads to a channel, which can only barely rescue yeast growth on selection media. Because of this presumably critical role of Ile20, further mutations were made to test the influence of the position on channel function and behaviour. The following substitutions were chosen: leucine, tryptophan, glycine and valine to test if these mutants have altered properties in the yeast system compared to the measurements in the oocytes.

Figure 28A shows the complementation assay of the different mutants in yeast. The data show that the Kcv-I20V mutant is, as expected from previous experiments, also in yeast functional; it is able to rescue yeast growth on selection media as efficient as the wildtype channel. However, the exchange to Trp or Gly modifies channel function. The substitution of Ile to Trp leads to a mutant, which can still support yeast growth on 1 mM K^+ selective media but not on 0.5 mM KCl. The second mutant Kcv-I20G completely fails to rescue yeast growth under selective conditions.
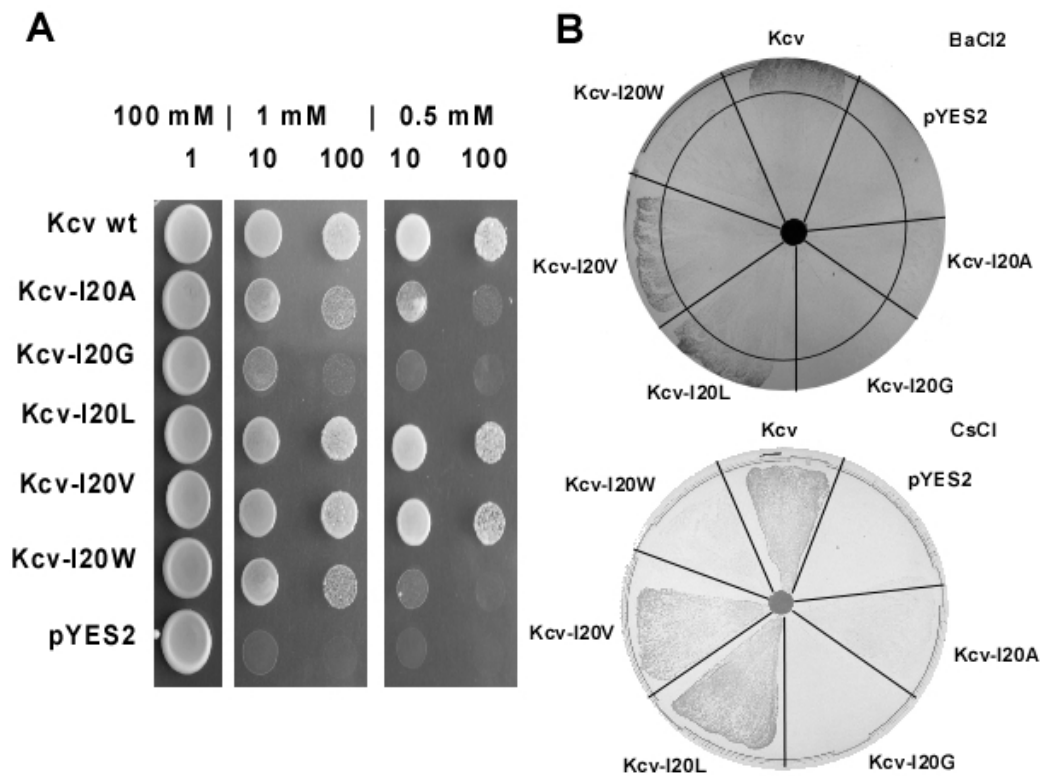
Figure 28: Scanning mutagenesis of the isoleucine at position 20 in the first transmembrane domain of Kcv and testing of ion selectivity of the different mutants. Shown is **(A)** the yeast complementation assay of the different mutants of Kcv, where the isoleucine at position 20 in the TMD1 was replaced by alanine, glycine, leucine, valine or tryptophan. The complementation assay was done as described in Figure 23. The dilution 1:10 was also plated on two 1 mM KCl selective media plates for **(B)** a disk diffusion assay to test the ability of 30 µl of 100 mM barium chlorid (up) or 30 µl of 100 mM caesium chloride (down), which was dropped on a filter disk, to inhibit yeast growth on minimal media. The inner circle on the selective plate with barium chloride indicates the size of the growth inhibition of the yeast whereas no inhibition of growth was recognised with caesium chloride.

In additional experiments, we tested the sensitivity of the channel against barium chloride and caesium chloride with the help of a disk diffusion assay in yeast (Chatelain *et al.* 2009). Figure 28B shows that the functional mutants are sensitive to barium chloride and insensitive to caesium chloride in the same manner as the wt channel. Therefore, the mutation of the isoleucine at position 20 alone does not alter the behaviour of the channel in the yeast system. Hence, it must be concluded, that the sensitivity of Kcv against caesium chloride is depending on the expression system; the channel is caesium sensitive in *Xenopus* oocytes (Gazzarrini *et al.* 2004) but insensitive in HEK293 (Thiel *et al.* 2010) and yeast cells (see Figure 28). Therefore, the results can differ by changing the expression system.

Another important factor, which is highlighted with the help of the homology model, is the interaction of the two TMDs of Kcv. Although the second transmembrane domain (TMD2) seems to be very tolerant to changes, the substitution of His83 leads to a total loss of function. The homology model shows that this residue lies in close contact with another essential amino acid in the TMD1 namely Phe30; also this amino acid does not tolerate a replacement by alanine. A close look at the structure reveals that the two amino acids are structurally interacting by generating a close helix-helix interaction. This kind of mutual interactions between helices are a key factor for stabilising many membrane proteins (Popot and Engelman 1990, Bowie 2005). A detailed look at the structure shows that Phe30 and His83 are interacting over a distance of only 3.3 – 3.4 Å and such a close interaction of aromatic-aromatic side chains is specific and named π-stack (Figure 29). The stack of π-electrons occurs if two or more aromatic molecules are stacked in a parallel manner in a distinct space of about 3.3 Å. London dispersion forces mostly cause these π-π-interactions. Dispersion forces are present between all kinds of molecules and can be stronger or weaker depending on atom or molecule size. Therefore, aromatic stacks can play an important role for correct folding and stability of protein structures like in RNase A, where also a stack of histidine and phenylalanine enhances the stability of the α–helix (Shoemaker *et al.* 1990).
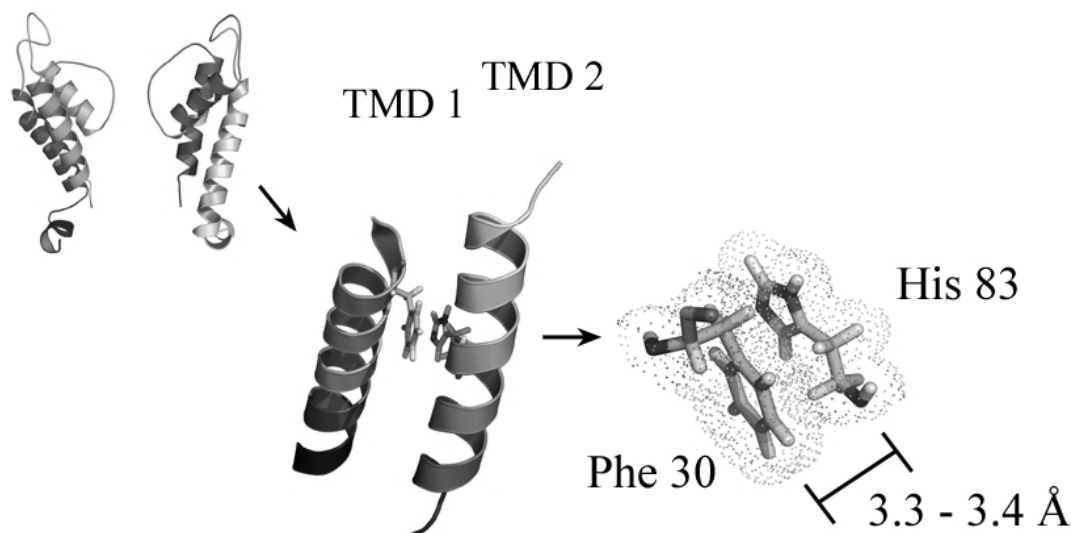
Figure 29: Aromatic-Aromatic Interaction between TMD1 and TMD2 of Kcv. The distance between phenylalanine at position 30 in the TMD1 and histidine at position 83 in the TMD2 are about 3.3 – 3.4 Å. This is the classical spacing for a π-π-interaction (π–stack). Therefore, the two aromatic residues can contribute via this helix-helix interaction to higher protein stability.

To summarise our results, the alanine-scan shows, that there are different crucial positions in both TMDs, which are essential for channel function: Phe14, His17, Ile20, Phe24, Tyr28, Phe30 and Phe31 of the TMD1 and His83 of the TMD2. These findings are supported by the calculation of the b-factors for every amino acid in the protein. The b-factors are a measure for the flexibility of the C -atoms of each amino acid position in the protein and were calculated with the help of the MD simulations of Kcv (Tayefeh *et al.* 2007). High b-factors imply a high flexibility; low values indicate positions that are more rigid.

Figure 30 show the computation of the b-factors for Kcv and reveal a dichotomy of the both TMDs. Both TMDs exhibits at one half high b-factors and are, therefore, flexible whereas the other half of the TMDs are more or less rigid. One important anchor for the TMD1 is the histidine at position 17 and for the TMD2 the histidine at position 83 (Figure 30) and both of them are located in the region of the transition zone between high and low b-factors. These results fit well with our aforementioned results of the alanine-scanning mutagenesis. The replacement of Phe14 reduces the ability of rescuing the yeast growth but not to the same degree as for the amino acids at positions His17, Ile20, Phe24, Tyr28, Phe30 or Phe31 of the TMD1 (Figure 23). Compared to the other six crucial positions in the TMD1 the Phe14 has a relatively high b-factor, which means this position is more flexible than the other positions and this flexibility of the Phe14, or rather the inflexibility of the other positions, is reflected by the sensitivity against amino acid exchanges. The same effect can be seen in the second TMD where His83 is the last amino acid of the TM segment with a low b-factor and, therefore, is the only amino acid, which is highly sensitive against exchanges (Figure 23). So the b-factors support the hypothesis that the total loss of channel function due to an amino acid exchange at these positions in the TMD1 could be explained through a loss of anchoring of the protein in the membrane and, therefore, presumably with an increase in the b-factors at these positions.
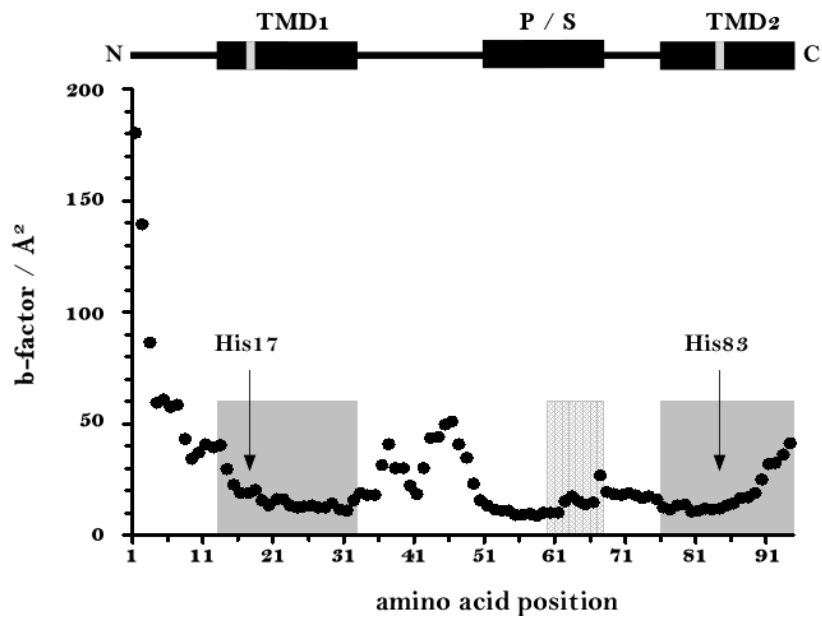
Figure 30: B-factor distribution of Kcv. Shown is the distribution of the b-factors in $\mathring{A}^2$ for the different amino acid positions of the viral potassium channel Kcv. Marked in pattern grey is the signature sequence and in plain grey the two TMDs with highlighted histidines at positions 17 and 83. Above the graph is a sketch of Kcv with the N- and C-terminus (N, C), both TMDs (TMD$_{1/2}$) and the pore region with signature sequence (P/S).

The importance of the histidine at position 17 is also underscored by the results of alanine-insertion experiments (Baumeister 2010). The insertion of an alanine at different positions in the TMD1 leads to non-functional mutants in HEK293 and in yeast cells (Baumeister 2010) when inserted downstream of position 17, i.e. in the rigid part of the TMD. This loss of channel function might be due to the insertion of an alanine at position 17, which leads to a shifted orientation of the downstream crucial histidine. This hypothesis was tested with two mutants where tryptophan was inserted at position 17 and 18. As mentioned before a substitution of histidine to tryptophan (Kcv-H17W) was also in another experiment able to rescue yeast growth. The data in Figure 31 show that the two insertion mutants Kcv-W17 and Kcv-W18 were in the present case not able to restore the growth of the yeasts.
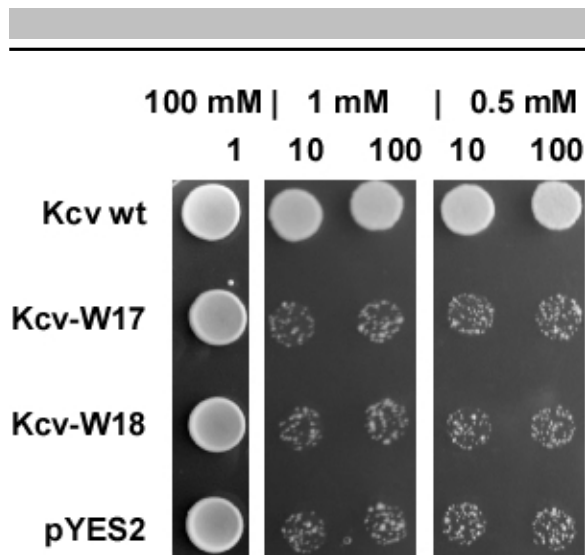
Figure 31: Yeast complementation assay of two insertion mutants of Kcv. Shown is the yeast complementation assay of Kcv wildtype (Kcv wt, positive control), pYES2 (negative control) and of the two insertion mutants, where tryptophan was inserted in the TMD1 at position 17 (Kcv-W17) or at position 18 (Kcv-W18). None of these mutants were able to rescue the yeast growth and only papillae due to spontaneous mutations of the yeasts are visible. The complementation assay was done as described in Figure 23.

These results are not totally unexpected because there are many complex interactions within the protein so that an insertion of a large residue like tryptophan near to a histidine, which also carries a large side chain, can lead to different problems like, for example, steric hindrance.

The same correlation between b-factors and crucial amino acids as described above for the TMD1 is found for TMD2. Also the latter TMD reveals two regions of mobility. While the upstream part of TMD2 is not flexible, the downstream part shows a high degree of flexibility. The histidine at position 83, i.e. the only amino acid, which is highly sensitive against an exchange, is more or less the last amino acid in the TMD2 with a low b-factor (Figure 30). The part downstream of TMD2 is relatively flexible, which means the His83 could be responsible for an anchoring of the upper part of TMD2 to the rigid part of TMD1 through the aformentioned - -interaction between the two TMDs.

In summary, the b-factors of Kcv show a dual distribution within the two TMDs with a rigid part, which is connected to the pore and a highly flexible part directed towards the cytosol. In order to understand whether this architecture of the TMDs is unique or a common building principle in K^+ channels, we analysed the b-factors form the respective pore module of other K^+ channels.

Figure **32** shows that the dual distribution is not only a property of Kcv but can also be found in Kir2.2 (eukaryotic strong inward-rectifier K^+ channel, PDB-Code: 3JYC) and to some extend also in NaK (Na^+/K^+ conducting channel, PDB-Code: 2AHZ). The result of this analysis indicates that the anchoring of the TMDs maybe a structural feature, which is also relevant in

other channels for function. Due to the limited number of high-resolution crystal structures, it is still ambiguous if this distribution is a more general principle or not. Whether this way of anchoring is more important for the small 2TMD motif channels (see Chapter 1) than for the larger 6TMD motif channels, needs to be further investigated.
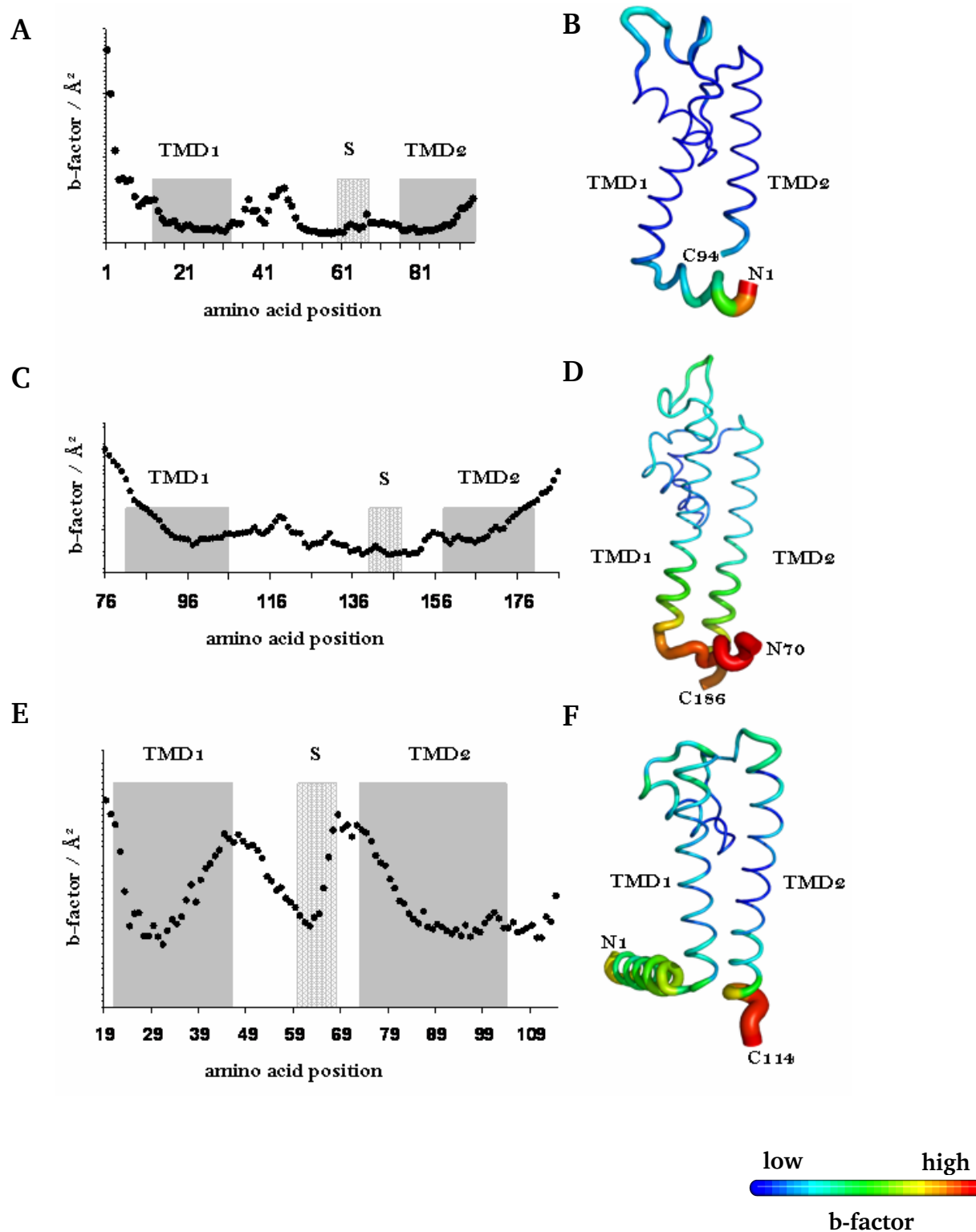
Figure 32: B-factor distributions of Kcv, Kir2.2 and NaK ion channels. Shown are the graphs of the b-factor distributions of the C_α-atoms of the TMD_1-P-TMD_2 motifs from **(A)** Kcv, **(C)** Kir2.2 (PDB-Code: 3JYC) and **(D)** NaK (PDB-Code: 3E86). Highlighted are the two transmembrane domains ($TMD_{1/2}$, plain grey) around the signature sequence (S, patterned grey). The b-factor values depend on the experimental conditions, hence, no values are given, since only the tendency is important for the comparison. **(B, D, F)** illustrates the b-factors as '*b-factor 'putty*'' as implemented in PyMol (www.pymol.org) of one subunit of **(B)** Kcv, **(D)** Kir2.2 and **(F)** NaK. The colour scale ranges from rigid parts with low b-factors coloured in blue to highly flexible parts with high b-factors coloured in red. The thickness of the ribbon increases from low to high b-factors.

Collectively the data show that the combination of alanine-scanning with a three dimensional identification of amino acid positions in the homology model of Kcv, together with information on the dynamics of the protein, is a powerful tool to uncover complex structure/function correlates in this ion channel.

4.4.3. The π-stacks between TMD1 and TMD2 Stabilises the Spatial Structure of the Channel

The data imply, that the aforementioned aromatic-aromatic interaction between Phe30 and His83 is an essential factor for channel function. Examples for the importance of such kind of interactions of aromatic side chains were already found in the case of the acid-sensing ion channels (ASICs) where the π-π-stacking between the extracellular and transmembrane domain is essential for proton gating (Li *et al.* 2008, Yang *et al.* 2009). In addition, the architecture of synthetic formed ion channels relies on this kind of π-π-stacking interactions (Bhosale *et al.* 2006).

The presumed interacting between Phe30 and His83 in Kcv is not a frequently occurring pairing in membrane proteins to make interhelical contact points (Adamian and Liang 2001). An alignment of viral potassium channels in Figure 33 shows that the position His83, however, is highly conserved throughout all viral potassium channels. Even the distantly related potassium channel Kesv from *Ectocarpus siliculosus* Virus (EsV-1) (Delaroque *et al.* 2001) has this position conserved.

Figure 33: Alignment of viral potassium channels of different viruses of the family of Phycodnaviridae. Shown is an alignment of a set of viral potassium channels of different virus groups of the family of Phycodnaviridae. Highlighted in black are the histidines, which correspond to the histidine at the position 83 in Kcv$_{PBCV-1}$ and in grey the semi-conserved positions, which correspond to the phenylalanine at the position 30 in Kcv$_{PBCV-1}$. The vertical-bar above the alignment sketches the secondary structure of Kcv$_{PBCV-1}$. The symbols under the alignment denote the degree of conservation observed in each column:

* - residues identical in all sequences

: - conserved substitutions

. - semi-conserved substitutions.

The position 30 in Kcv is semi-conserved (Figure 33). In Kesv, we find a glutamine in this position i.e. an amino acid, which is uncharged and aliphatic. All other viral ion channels contain in this position a phenylalanine or methionine. Phenylalanine again is an aromatic amino acid with a propensity of π-π-stack interactions. In the case of methionine, it seems possible that the long and extended methyl group is able to stabilise the channel structure through C-H···π-interactions, where methionine is the aliphatic C-H donor and histidine is the aromatic π-acceptor (Brandl *et al.* 2001). To test these assumptions different substitutions of both positions Phe30 and His83 with Ala, Gly, Phe, His, Met or Trp were made. Figure 34 show that only two out of the 14 substitutions are able to rescue yeast growth on selection media. The substitutions, which generate a functional channel, agree with the idea of a π-π-interaction in this site. One of the two positive substitutions of Phe30 is tryptophan i.e. an amino acid with an aromatic side chain. As already expected from the alignments, Phe30 can also be replaced by methionine.
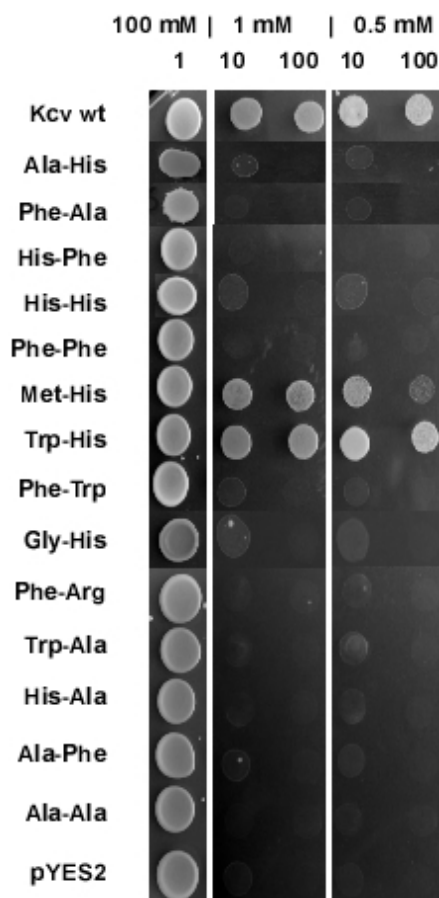
Figure 34: Scanning mutagenesis of the phenylalanine at position 30 in the TMD1 and histidine at position 83 in the TMD2 of Kcv. Shown is the yeast complementation assay of the substitutions of the two positions 30 and 83 in the two TMDs of Kcv, where every position was replaced by different amino acids. The complementation assay was done as described in Figure 23. The labels indicates the substituted amino acids for which Phe30 (first label) and His83 (second label) was exchanged.

Additional data show that also other two mutations namely Kcv-Phe30His and Kcv-Phe30Gly seem to be capable of rescuing yeast growth on selective media. However, in these cases growth could only be detected at high-undiluted yeast concentration on the selective plates (Figure 34) meaning that these channel mutants may have a significantly reduced conductivity and requires K^+ concentrations higher than 1 mM. Therefore, it is possible that at high-undiluted yeast concentrations the local K^+ concentration is raised via the release of the intracellular K^+ of the multitude of dead yeast and that this local increase allows the growth of the two mutant channels Kcv-Phe30His and Kcv-Phe30Gly at high-undiluted yeast concentration on the selective plates.
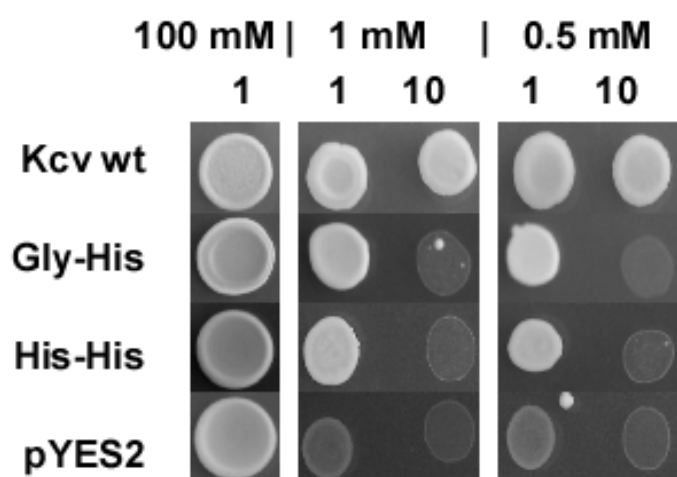
Figure 35: Yeast complementation assay of the phenylalanine at position 30 in the TMD1 of Kcv. Shown are the two substitutions where the Phe30 was replaced by either glycine or histidine together with the positive (Kcv wt) and negative (empty vector) control. The complementation assay was done as described in Figure 23. On the selective plates are the undiluted and the 1:10 diluted samples shown. The labels indicate the substituted amino acids for which Phe30 (first label) was exchanged and the histidine at position 83.

C-H···π-interactions, like the Met-His interaction, can contribute to the stability of proteins with the overall stabilisation energy of about 0.5 to 1.0 $kcal*mol^{-1}$ per interaction and are, therefore, an important factor for folding stability (Brandl *et al.* 2001). Also almost all tryptophan residues in proteins are involved in C-H···π-interactions (Brandl *et al.* 2001). The Trp-His interaction can stabilise a structure by about 1.0 $kcal*mol^{-1}$ (Fernández-Recio *et al.* 1997) and is, therefore, in the same range as the Met-His interaction. Hence, it is not unexpected that the substitution of either methionine or tryptophan can rescue channel function in yeast. This finding highlights the concept of a functional conservation in proteins. This means not a specific amino acid is highly conserved at this position but the characteristics of the amino acid are highly conserved to maintain a functional interaction. In the present case the importance is on the interaction between the two TMDs, which can be brought about either by a π-π-interaction or alternatively also by C-H···π-interactions.

Previous studies on π-π-interactions in proteins revealed that the Trp-His and accordingly the Phe-His interaction is stronger, if the histidine is protonated (Fernández-Recio *et al.* 1997, Armstrong *et al.* 1993). To test, if the histidine at position 83 of Kcv is in a protonated state, a mutant was made in which histidine was replaced by arginine. Arginine was preferred over lysine since arginine is found more frequently to interact with aromatic side chains (Gallivan and Dougherty 1999). With the Kcv-H83R mutant, a positive charge is inserted in this region, which can create a cation-π-interaction between Arg83 and the Phe30 (Gallivan and Dougherty 1999). The yeast complementation assay shows that this mutation is not able to rescue yeast growth on selective media (Figure 34). The results of these experiments suggest that the histidine at position 83 could be in an unprotonated state.

The present data show that the two positions Phe30 and His83 are essential for a proper channel function. The structural importance is given by the formation of intramolecular interactions between the two TMDs. Furthermore, these positions are highly conserved throughout the viral K^+ channels and are susceptible to changes. Moreover, the results emphasise an even higher complexity because there is no reciprocity between the two positions as the mutual exchange of Phe and His leads to a non-functional mutant (Figure 34). Additionally, these results demonstrate that the homology model of Kcv (Tayefeh *et al.* 2009) is a very good reproduction of the real conditions in the protein; delicate interactions such as the π-π-stacking would have not occurred in an inappropriate model. Moreover, as mentioned before, the model of Kcv makes it possible to calculate the b-factors as a measure of flexibility for the amino acids. These b-factors show a good agreement with the results of the alanine-scanning mutagenesis (Figure 30). For example, the b-factors of the interacting amino acid couple Phe30 and His83 is low and, therefore, are these residues rigid and fixed in their positions, which means that this couple can serve for maintaining intramolecular stability. This leads to an overall better understanding of the different mutants.

4.4.4. Electrophysiological Measurements of the π-stack shows Effects on Gating

It was mentioned at the beginning of the previous paragraph that aromatic-aromatic interactions could be important for the gating of ion channels. Therefore, the two functional mutants Kcv-F30W::GFP and Kcv-F30M::GFP, were also studied with electrophysiological

measurements in HEK293 cells to test whether the mutations influence the behaviour of the channel or not.

Figure 36A shows the typical current responses of mock transfected HEK293 cells to a standard pulse protocol. In this case, the cells were transfected with the empty vector pEGFP (control). The control measurements show the characteristic background conductance of HEK293 cells with small K^+ outward currents at positive voltages (K^+ outward rectifier) and marginal inward currents at negative voltages (Figure 36E).
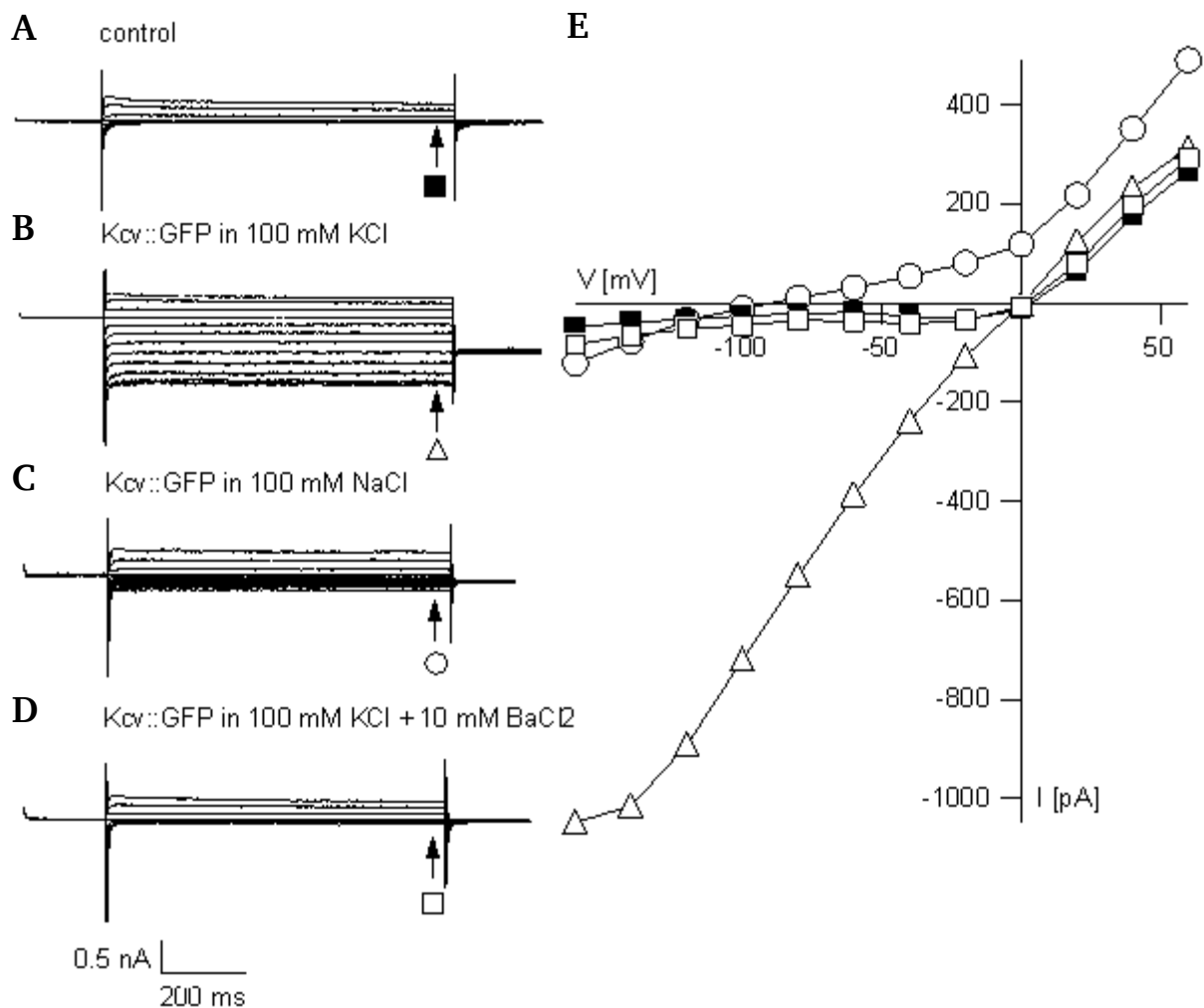
Figure 36: Electrophysiological measurements of HEK293 cells transfected with GFP or with Kcv::GFP. Shown are **(A-D)** the current responses to a standard pulse protocol (see Figure 17) and the corresponding **(E)** current-voltage relationships (I/V-curves) of HEK293 cells transfected with **(A)** GFP in 100 mM KCl bath solution and with **(B)** Kcv wt transfected cells in 100 mM KCl or **(C)** in 100 mM NaCl or **(D)** with 10 mM BaCl2 in the KCl bath solution. Currents were measured in whole cell configuration to standard voltage protocol from holding voltage (0 mV) to test voltages between +60 and -160 mV. The symbols of the I/V-relationships cross-reference with the symbols at the current traces.

To distinguish further on better between functional and non-functional channel mutations, the ratio of cord conductance (-20 mV to -60 mV = G_{neg} versus 0 mV to +60 mV = G_{pos}) of the corresponding current/voltage (I/V) relation curves was calculated as described in Hertel *et al.* 2009. The ratio for mock-transfected HEK293 cells is always less than 1 (0.16 ± 0.27, n = 12). In contrast in HEK293 cells, which are transfected with a chimera of Kcv and GFP (Kcv::GFP / Kcv-wt) this ratio is always greater than 1 (1.38 ± 0.27, n = 21) because Kcv causes large inward (Moroni *et al.* 2002, Hertel *et al.* 2006). Figure 36B shows an example of a measurement of a HEK293 cell expressing Kcv::GFP. The I/V-relation highlights all the features, which are typical for the viral potassium channel. This includes the linear increase in conductance between clamp voltages of 0 mV to -80 mV and a saturation of the inward current at voltages more negative of about -100 mV in HEK293 cells (Moroni *et al.* 2002, Hertel *et al.* 2006). When we use the ratio G_{neg}/G_{pos} with a threshold of one as a parameter to distinguish between cells without and with appreciable Kcv type conductance, we found that 65 % of the HEK293 cells transfected with Kcv::GFP showed a characteristic Kcv channel activity (Figure 37B) (Hertel *et al.* 2009) with currents of -1425 ± 1040 pA (n = 21) at -140 mV. The same analysis using the ratio of G_{neg}/G_{pos} was used in all further studies to differentiate between cells with or without active Kcv type currents.

To test the cation selectivity of Kcv::GFP the potassium chloride in the bath solution was replaced by sodium chloride (Figure 36C). This leads to a strong suppression of the inward currents and furthermore to a negative shift of the reversal potential by -57 ± 32 mV (n = 3); altogether this indicates a strong preference of the channel for potassium over sodium ions. An addition of barium chloride at 10 mM to the bath medium (Figure 36D) resulted in an almost total block of the currents of about 88.8 ± 5.3 % (n = 5). The block was reversible upon removing the blocker.

Figure 37A shows the amplitudes of the mean currents of mock-transfected, with Kcv::GFP and with different mutants transfected HEK293 cells. Figure 37B shows the corresponding percentage of cells, which show Kcv like conductance with a ratio G_{neg}/G_{pos} greater than one. Both sets of data reveal that the substitution of the phenylalanine at position 30 to tryptophan (Kcv-F30W) has no influence on the general channel behaviour. Only the amplitude of the mean current is with -1967 ± 1662 pA at -140 mV slightly larger than that in cells expressing Kcv::GFP. In addition, the portion of cells in which the channel was positively identified, was higher. While 65 % of the cells tested revealed Kcv-wt currents, 86 % of the cells exhibited, according to the aforementioned criteria, a Kcv-F30W::GFP current; the ratio G_{neg}/G_{pos} was

3.13 $\pm$ 1.40, n = 28, Figure 37B). This is 1.3-fold more than the corresponding value of Kcv::GFP. The reversal potential of the mutant current, which was measured after replacing K$^+$ in the bath to Na$^+$ was -59 $\pm$ 44 mV (n = 8). The addition of 10 mM barium chloride to the medium caused a block of the current of about 89 $\pm$ 1.9 % (n = 3). While the mutant seems to express slightly better than the wt channel, the selectivity of the channel mutant for potassium over sodium as well as the sensitivity against barium is like that of the wildtype channel (Figure 37A).

The Kcv-F30M::GFP mutant generates in HEK293 cells no increase in conductance (n = 27, Figure 37A) although this mutation was able to rescue yeast growth (Figure 34). The ratio of G_{neg}/G_{pos} is with 0.12 $\pm$ 0.07 (n = 27) in the range of mock-transfected HEK293 cells.
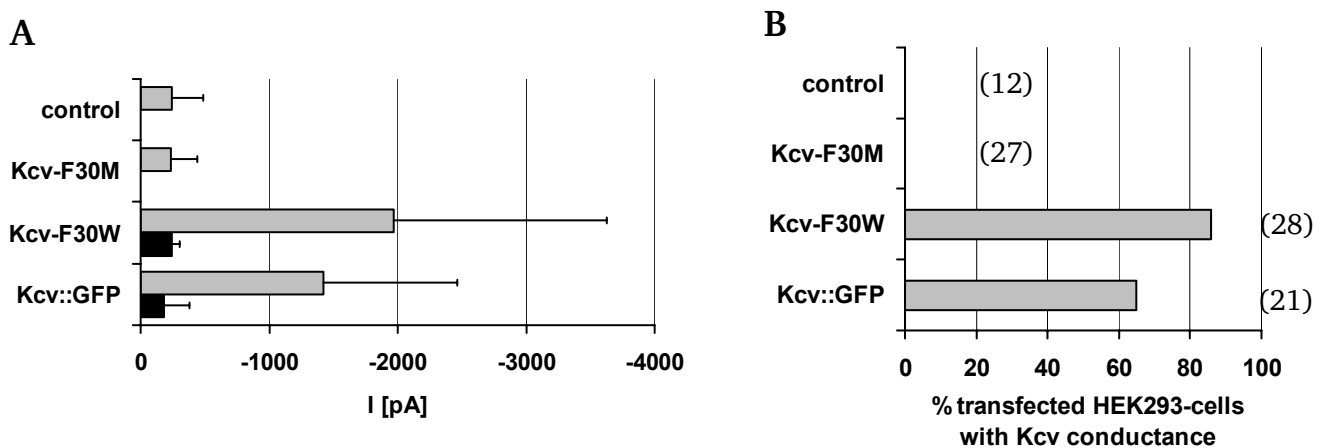
Figure 37: Comparison of mock-transfected and with different Kcv constructs transfected HEK293 cells. Shown are the **(A)** amplitudes of the mean currents with their standard deviation of mock-transfected (control) and with different Kcv constructs (Kcv::GFP and mutants) transfected HEK293 cells at a test voltage of -140 mV in 100 mM KCl bath solution (grey bars) and after the addition of 10 mM BaCl$_2$ to the bath solution (black bars, only for functional mutants shown). **(B)** Percentage of transfected HEK293 cells with Kcv like conductance for the same constructs as in (A). The number of recordings is indicated in brackets.

There are two possible explanations:

1. The currents of the mutated channels are so small that the signal to noise ratio is too low for detection. Therefore, the measurements may look like mock-transfected cells although the channel is active.

2. For the electrophysiological measurements, GFP fusion proteins are used to detect transfected cells. In this case, a GFP protein is fused to every subunit of the channel e.g. the tetramer contains four GFP molecules. GFP is with 238 amino acids 2.5-fold bigger than one subunit of Kcv and this may influence the behaviour of the channel (Baumeister and Hewing, unpublished). In contrast, in the yeast complementation assay no GFP is needed because of the auxotrophic selection of the yeast cells.

To test the hypothesis whether the GFP fusion causes the loss of function in the Kcv-F30M::GFP mutant, the same construct was also tested in yeast cells with a GFP containing variant of pYES2. Figure 38 shows that the GFP has no influence on channel function and the mutated channel is still able to rescue yeast growth on minimal potassium media. Hence, it seems as if the mutation Kcv-F30M either causes in HEK293 cells a significant reduction of the amplitude of currents or strongly affects the percentage of cells with functional channels; also, a combination of both is possible.
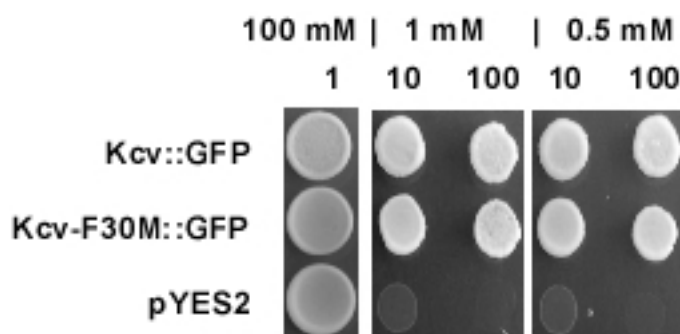
Figure 38: The EGFP-Tag does not prevent the yeast rescue neither for the wildtype channel nor for the exchange mutant Kcv-F30M. Shown is the yeast complementation assay of the substitution of phenylalanine with methionine at position 30 in the first TMD of Kcv, which is fused to EGFP. The complementation assay was done as described in Figure 23.

As a resume, we can conclude that the aromatic-aromatic interactions between Phe30 of TMD1 and His83 of TMD2 are important for the overall stability of the channel via the formation of interhelical π-π-interactions. The mutation of these positions does not influence the selectivity of the channel for K^+ over Na^+ or the sensitivity for Ba^{2+}. However, the mutation seems to increase the fractional expression of the channel e.g. it increases the number of cells, which show after transfection a Kcv like characteristics. This could reflect the difference in energy contribution of the different π-stack mutants to the overall stabilisation energy of the protein.

4.5. Conclusion

Kcv is a miniature K^+ channel of viral origin, which includes many hallmarks of potassium channels. Therefore, it is a good model system to study the very basic structure/function relationships in these types of channels.

This work contributes to the global comprehension of potassium channels with the help of an alanine-scanning mutagenesis of both transmembrane domains of Kcv and with a comparative analysis of these results with the help of the homology model of the channel.

The scanning of the first TMD emphasise the importance of the interaction of this domain with the lipid environment. It is well known that lipids can have a strong influence on channel function and behaviour or on the stabilisation of the protein in the membrane (Barrera *et al.* 2008, Valiyaveetil *et al.* 2002). The results of this work underscore the importance of protein lipid interaction in the outer transmembrane domain for Kcv function. The data are best understood in the context of the homology model. The majority of crucial amino acids in TMD1 are oriented towards the membrane; the aromatic side chain character of these amino acids is most suitable for anchoring TMD1 in the membrane. The distribution of the critical amino acids corresponds well with the b-factors of the Kcv model from MD simulations in the sense that the proposed anchoring of TMD1 by the relevant amino acids correlates with a low mobility of TMD1 and the adjacent turret. An exception in this scenario is Phe14, which is located in a mobile part of TMD1. However, worth noting is that the mutant Kcv-F14A only reduced the complementation efficiency of the channel; the mutations to alanine in the immobile part of Kcv on the other hand abolish channel function but can be preserved by the substitution of aromatic residues.

The b-factors of TMD2 are a mirror image of those from TMD1; the former is rigid at the N-terminus and mobile at the C-terminus. The present data imply that this behaviour is controlled by an interaction between the two TMDs. The alanine-scan shows that with the exception of His83 none of the amino acid side chains in TMD2 are crucial for function. This implies that the TMD2 is not actively anchored in the membrane. The stabilisation of TMD2 is rather brought about by an intramolecular interaction via a π-stack between the phenylalanine in the rigid part of the first and the histidine of the second TMD. This idea

again corresponds well with the distribution of the b-factors in TMD2, which start to increase downstream of His83. Anchoring of TMD1 and coupling to TMD2 seems connected because the disruption of either one or the other leads to a breakdown of conductivity.

All in all the results reveal a complex network of interactions within a K^+ channel monomer, which are essential for proper function. These interactions are not limited to the protein itself, but also to the interactive interactions between protein and lipid environment. Additional, a clustering of two subunits of different channel proteins is supposable.

4.6. References

Adamian L and Liang J (2001) Helix-Helix Packing and Interfacial Pairwise Interactions of Residues in Membrane Proteins. *J. Mol. Biol.* 311:891-907. doi:10.1006/jmbi.2001.4908

Armstrong KM, Fairman R, Baldwin RL (1993) The (i,i+4) Phe-His Interaction Studied in an Alanine-based α-Helix. *J. Mol. Biol.* 1:284-291. doi:10.1006/jmbi.1993.1142

Ashkenazy H, Erez E, Martz E, Pupko T, Ben-Tal N (2010) ConSurf 2010: calculating evolutionary conservation in sequence and structure of proteins and nucleic acids. *Nucl. Acids Res.* 2010; doi:10.1093/nar/gkq399

Balss J, Papatheodorou P, Mehmel M, Baumeister D, Hertel B, Delaroque N, Chatelain FC, Minor DL, Van Etten JL, Rassow J, Moroni A, Thiel G (2008) Transmembrane domain length of viral K^+ channels is a signal for mitochondria targeting. *PNAS* 105:12313-12318. doi:10.1073/pnas.0805709105

Barrera FN, Renart ML, Poveda JA, de Kruijff B, Killian JA, González-Ros JM (2008) Protein Self-Assembly and Lipid Binding in the Folding of the Potassium Channel KcsA. *Biochemistry* 47:2123–2133. doi:10.1021/bi700778c

Baumeister D (2010) Struktur-Funktions-Beziehung Viraler Kaliumkanäle - Einfluss der Transmembrandomänen/helices auf die Funktion von Kaliumkanälen. *Dissertation at the Technischen Universität Darmstadt*

Bernèche S and Roux B (2001) Energetics of ion conduction through the K^+ channel. *Nature* 414:73-77. doi:10.1038/35102067

Bhosale S, Sisson AL, Sakai N, Matile S (2006) Synthetic functional π-stack architecture in lipid bilayers. *Org. Biomol. Chem.* 4:3031-3039. doi:10.1039/b606487f

Bowie JU (2005) Solving the membrane protein folding problem. *Nature* 438:581-589. doi:10.1038/nature04395

Brandl M, Weiss MS, Jabs A, Sühnel J, Hilgenfeld R (2001) C-H··· π-interactions in proteins. *J. Mol. Biol.* 1:357-377. doi:10.1006/jmbi.2000.4473

Chatelain FC, Gazzarrini S, Fujiwara Y, Arrigoni C, Domigan C, Ferrara G, Pantoja C, Thiel G, Moroni A, Minor DL (2009) Selection of Inhibitor-Resistant Viral Potassium Channels Identifies a Selectivity Filter Site that Affects Barium and Amantadine Block. *PLoS One* 4:e7496. doi:10.1371/journal.pone.0007496

Clackson T and Wells JA (1995) A Hot Spot of Binding Energy in a Hormone-Receptor Interface. *Science* 267:383-386. doi: 10.1126/science.7529940

Cunningham BC, Wells JA (1989) High-Resolution Epitope Mapping of hGH-Receptor Interaction by Alanine-Scanning Mutagenesis. *Science* 244:1081-1085. doi: 10.1126/science.2471267

Delaroque N, Müller DG, Bothe G, Pohl T, Knippers R, Boland W (2001) The complete DNA sequence of the Ectocarpus siliculosus virus EsV-1 genome. *Virology* 287:112-132

DiCera E (1998) Site-Specific Thermodynamics: Understanding Cooperativity in Molecular Recognition. *Cem. Rev.* 98:1565-1591. doi: 10.1021/cr960135g

Domene C, Vemparala S, Klein ML, Vénien-Bryan C, Doyle DA (2006) Role of Aromatic Localization in the Gating Process of a Potassium Channel. *Biophys J.* 90:L01–L03. doi:10.1529/biophysj.105.072116

Fernández-Recio J, Vázquez A, Civera C, Sevilla P, Sancho J (1997) The Tryptophan/Histidine interaction in α-helices. *J. Mol. Biol.* 1:184-197. doi:10.1006/jmbi.1996.0831

Gallivan JP and Dougherty DA (1999) Cation-π-interactions in structural biology. *PNAS* 96:9459-9464. PMID:10449714

Gazzarrini S, Van Etten JL, DiFrancesco D, Thiel G, Moroni A (2002) Voltage-Dependence of Virus-encoded Miniature K^+ Channel Kcv. *J. Membrane Biol.* 187:15-25. doi:10.1007/s00232-001-0147-5

Gazzarrini S, Kang M, Van Etten JL, Tayefeh S, Kast SM, DiFrancesco D, Thiel G, Moroni A (2004) Long-distance interactions within the potassium channel pore are revealed by molecular diversity of viral proteins. *JBC* 279:28443-28449. doi: 10.1074/jbc.M401184200

George, A. L. (1995) Molecular genetics of ion channel diseases. *Kidney International* 48:1180-1190. doi:10.1038/ki.1995.401

Glaser F, Pupko T, Paz I, Bell RE, Bechor D, Martz E, Ben-Tal N (2003) ConSurf: Identification of Functional Regions in Proteins by Surface-Mapping of Phylogenetic Information. *Bioinformatics* 19:163-164.

Hamill OP, Marty A, Neher E, Sakmann B, Sigworth FJ (1981) Improved patch-clamp techniques for high-resolution current recording from cells and cell-free membrane patches. *Pflugers Arch* 391:85–100. doi:10.1007/BF00656997

Heginbotham L, Lu Z, Abramson T, MacKinnon R (1994) Mutations in the K^+ channel signature sequence. *Biophys J.* 66:1061–1067. PMCID:PMC1275813

Hertel B, Tayefeh S, Mehmel M, Kast SM, Van Etten J, Moroni A, Thiel G (2006) Elongation of outer transmembrane domain alters function of miniature K^+ channel Kcv. *J Membr Biol* 210:21–29. doi:10.1007/s00232-005-7026-4

Hertel B, Tayefeh S, Kloss T, Hewing J, Gebhardt M, Baumeister D, Moroni A, Thiel G, Kast SM (2009) Salt bridges in the miniature viral channel Kcv are important for function. *Eur Biophys J.* doi: 10.1007/s00249-009-0451-z

Hessa T, Kim H, Bihlmaier K, Lundin C, Boekel J, Andersson H, Nilsson I, White SH, von Heijne G (2005) Recognition of transmembrane helices by the endoplasmic reticulum translocon. *Nature* 433:377-381. doi:10.1038/nature03216

Hille B (2001) Ion channels of excitable membranes. 3. Edition, Sinauer Associates Inc., Sunderland

Holst B, Zoffmann S, Elling CE, Hjorth SA Schwartz TW (1998) Steric Hindrance Mutagenesis versus Alanine Scan in Mapping of Ligand Binding Sites in the Tachykinin NK1 Receptor. *Mol. Pharmacology* 53:166–175. PMID:9443945

Hodgkin AL, Huxley AF (1952) A quantitative description of membrane current and its application to conduction and excitation in nerve. *J. Physiol.* 117:500-544

Jiang Y, Lee A, Chen J, Cadene M, Chait BT, MacKinnon R (2002) Crystal structure and mechanism of a calcium-gated potassium channel. *Nature* 417:515-522. doi:10.1038/417515a

Kang M, Moroni A, Gazzarrini S, DiFrancesco D, Thiel G, Severino M, VanEtten JL (2004) Small potassium ion channel proteins encoded by chlorella viruses. *PNAS* 101:5318-5324. doi: 10.1073/pnas.0307824100

Killian JA (2003) Synthetic peptides as models for intrinsic membrane proteins. *FEBS Lett.* 555:134-138. doi:10.1016/S0014-5793(03)01154-2

Killian JA, von Heijne G (2000) How proteins adopt to a membrane-water interface. *Trends Biochem. Sci.* 25:429-434. doi:10.1016/S0968-0004(00)01626-1

Koster JC, Bentle KA, Nichols CG, Ho K (1998) Assembly of ROMK1 (Kir 1.1a) inward rectifier K^+ channel subunits involves multiple interaction sites. *Biophys J.* 74:1821–1829. PMCID:PMC1299526

Kuo A, Domene C, Johnson LN, Doyle DA, Vénien-Bryan C (2005) Two different conformational states of the KirBac3.1 potassium channel revealed by electron crystallography. *Structure* 13:1463–1472. doi:10.1016/j.str.2005.07.011

Landau M, Mayrose I, Rosenberg Y, Glaser F, Martz E, Pupko T, Ben-Tal N (2005) ConSurf 2005: the projection of evolutionary conservation scores of residues on protein structures. *Nucl. Acids Res.* 33:W299-W302. doi:10.1093/nar/gki370

Li T, Yang Y, Canessa CM (2008) Interaction of the Aromatics Tyr-72/Trp-288 in the Interface of the Extracellular and Transmembrane Domains Is Essential for Proton Gating of Acid-sensing Ion Channels. *J. Biol. Chem.* 284:4689-4694. doi:10.1074/jbc.M805302200

Liang J, Adamian L, Jackups RJ (2005) The membrane–water interface region of membrane proteins: structural bias and the anti-snorkeling effect. *TRENDS in Biochemical Sciences* 30:355-357. doi:10.1016/j.tibs.2005.05.003

McGaughey GB, Gagné M, Rappé AK (1998) π-Stacking Interactions: ALIVE AND WELL IN PROTEINS. *J. Biol. Chem.* 273:15458-15463. doi: 10.1074/jbc.273.25.15458

Minor DL, Masseling SJ, Jan YN, Jan LY (1999) Transmembrane Structure of an Inwardly Rectifying Potassium Channel. *Cell* 96:879-891. doi:10.1016/S0092-8674(00)80597-8

Moroni A, Viscomic C, Sangiorgioc V, Pagliucaa C, Meckel T, Horvathe F, Gazzarrinia S, Valbuzzia P, Van Etten JL, DiFrancescob D, Thiel G (2002) The short N-terminus is required for functional expression of the virus-encoded miniature K$^+$ channel Kcv. *FEBS Letters* 530:65-69. doi:10.1016/S0014-5793(02)03397-5

Parsegian A (1969) Energy of an ion crossing a low dielectric membrane: solutions to four relevant electrostatic problems. *Nature* 221:844-846. doi:10.1038/221844a0

Perozo E, Cortes DM, Cuello LG (1999) Structural Rearrangements Underlying K$^+$-Channel Activation Gating. *Science* 285:73-78. doi:10.1126/science.285.5424.73

Planque MRR, Killian JA (2003) Protein/lipid interactions studied with designed transmembrane peptides: role of hydrophobic matching and interfacial anchoring. *Molecular Membrane Biology* 20:271-284. doi:10.1080/09687680310001605352

Plugge B, Gazzarrini S, Nelson M, Cerana R, Van Etten JL, Derst C, DiFrancesco D, Moroni A, Thiel G (2000) A Potassium Channel Protein Encoded by Chlorella Virus PBCV-1. *Science* 287:1641 - 1644. doi:10.1126/science.287.5458.1641

Popot JL and Engelman DM (1990) Membrane protein folding and oligomerization: the two-stage model. *Biochemistry* 29:4031–4037. doi:10.1021/bi00469a001

Schulteis CT, Nagaya N, Papazian DM (1998) Subunit Folding and Assembly Steps Are Interspersed during Shaker Potassium Channel Biogenesis. *J. Biol. Chem.* 273:26210-26217. doi:10.1074/jbc.273.40.26210

Shoemaker KR, Fairman R, Schultz DA, Robertson AD, York EJ, Stewart JM, Baldwin RL (1990) Side-chain interactions in the C-peptide helix: Phe8 ⋯His12$^+$. *Biopolymers* 29:1-11. doi:10.1002/bip.360290104

Strandberg E, Killian JA (2003) Snorkeling of lysine side chains in transmembrane helices: how easy can it get? *FEBS Letters* 544:69-73. doi:10.1016/S0014-5793(03)00475-7

Tang W, Ruknudin A, Yang WP, Shaw SY, Knickerbocker A, Kurtz S (1995) Functional Expression of a Vertebrate Inwardly Rectifying K$^+$ Channel in Yeast. *Mol. Biol. of the Cell* 6:1231-1240. PMID:8534918

Tayefeh S, Kloss T, Thiel G, Hertel B, Moroni A, Kast SM (2007) Molecular dynamics simulation study of the cytosolic mouth in Kcv-type potassium channels. *Biochem* 46:4826–4839. doi:10.1021/bi602468r

Tayefeh S, Kloss T, Kreim M, Gebhardt M, Baumeister D, Hertel B, Richter C, Schwalbe H, Moroni A, Thiel G, Kast SM (2009) Model development for the viral potassium channel. *Biophys J* 96:485–498. doi:10.1016/j.bpj.2008.09.050

Thiel G, Baumeister D, Schroeder I, Kast SM, Van Etten JL, Moroni A (2010) Minimal art: Or why small viral K$^+$ channels are good tools for understanding basic structure and function relations. *Biochimica et Biophysica Acta (BBA) – Biomembranes Article in Press.* doi:10.1016/j.bbamem.2010.04.008

Valiyaveetil FI, Zhou Y, MacKinnon R (2002) Lipids in the Structure, Folding, and Function of the KcsA K$^+$ Channel. *Biochemistry* 41:10771-10777. doi:10.1021/bi026215y

Yang H, Yu Y, Li WG, Yu F, Cao H, Xu TL, Jiang H (2009) Inherent Dynamics of the Acid Sensing Ion Channel 1 Correlates with the Gating Mechanism. *PLoS Biol.* 7(7): e1000151. doi:10.1371/journal.pbio.1000151

Yau WM, Wimley WC, Gawrisch K, White SH (1998) The preference of tryptophan for membrane interfaces. *Biochemistry* 37:14713-14718. doi:0.1021/bi980809c

5.1. Abstract

Molecular dynamic (MD) simulations and related computational methods are powerful tools to understand and predict structure/function correlates in channel proteins. Here we combine computational and experimental methods in order to analyse the influence of single point mutations in the miniature viral potassium channel Kcv. Kcv is with only 94 amino acids one of the smallest known potassium channels; it exhibits most of the functional and structural hallmarks of potassium channels and is, therefore, a good model system to investigate basic structure/function relations in K$^+$ channels. There is no crystal structure available yet but a homology based MD model of the Kcv channel has proved to explain and predict many experimental findings. Using this model, we were able here to examine the influenc of mutations of the C-terminal amino acid, which affect function, on the level of the protein structure. The model calculations show that point mutations of the last amino acid influence the cumulated potassium ion concentration profiles in the mutants; the most pronounced difference occurs in the K$^+$ concentration in the channel cavity. The computed pattern of K$^+$ concentration changes as a function of the amino acid in position 94 of Kcv and corresponds well with a functional test of Kcv mutants in a yeast recue system. The most important result is that the channel does not tolerate an elevation of the K$^+$ concentration in the cavity.

5.2. Introduction

Ion channels are of crucial importance for a multitude of biological functions like the control of the electrical excitability of neurons and muscles (Catterall 1984), cell-cell-communication (Neher 1992) or osmoregulation (Schroeder *et al.* 1989). Therefore, ion channels are common in all forms of life from bacteria up to higher plants and humans.

One important subfamily of these proteins are the potassium ion channels, which, as the name implies, are highly selective for potassium ions (K$^+$). Characteristically K$^+$ channels conduct K$^+$ 10 to 1000 times better than sodium ions (Na$^+$) (Hille 2001).

K$^+$ channels are tetrameric proteins, meaning that they are clusters of four subunits (MacKinnon 1991). The K$^+$ conducting pore, which is formed in the centre of the tetramer, contains the selectivity filter with the signature sequence **TxxTxGY/FG** (Miller 1992, Jan and

Jan 1992). The latter is highly conserved throughout all K$^+$ channels. Therefore, it can be used as recognition feature for potassium conduction proteins (Heginbotham *et al.* 1994).

One of the smallest known K$^+$ channels is the viral potassium channel Kcv (K$^+$ channel **C**hlorella **V**irus) from the virus PBCV-1 (*Paramecium bursaria* **C**hlorella **V**irus Type **1**), which infects endosymbiontic living chlorellae (Plugge *et al.* 2000, Van Etten *et al.* 2002). Despite of the small monomer size of only 94 amino acids Kcv exhibits, nonetheless, many essential hallmarks of more complex potassium channels. Like the pore unit of all other K$^+$ channels Kcv is built of two transmembrane domains (TMD), which are connected by a pore loop (P Loop) including the signature sequence **TxxTxGFG** (Figure 39). Because the entire Kcv channel is in terms of structure not more than the pore module of complex potassium channels, it presents a simple model system to study the most basic structure/function relationships in K$^+$ channels (Kang *et al.* 2004).
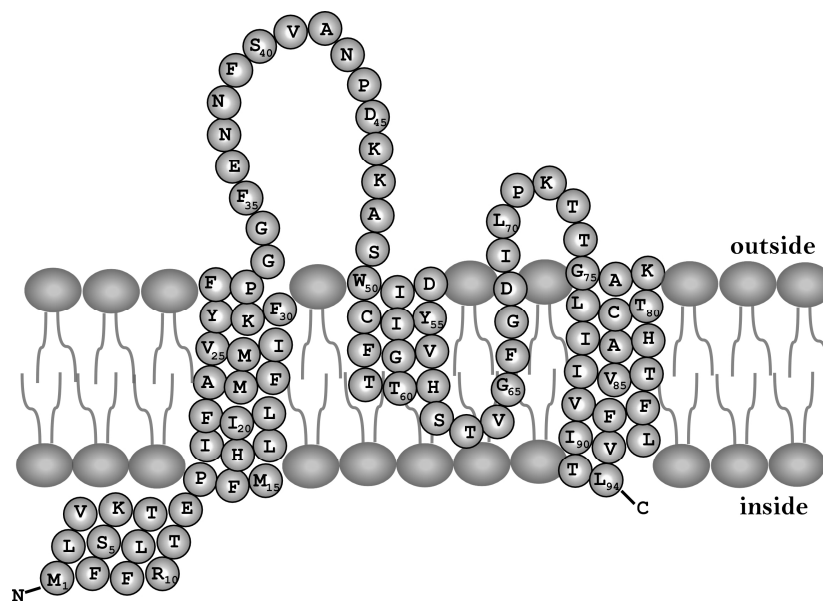
Figure 39: Schematic model of the viral potassium channel Kcv. The minimalist viral potassium channel Kcv exhibits only 94 amino acids (grey balls) and consists of two transmembrane domains connected by the pore loop with the signature sequence **TxxTxGFG**. The cytosolic N-terminus (N) is only 12 amino acids long; a cytosolic C-terminus is missing.

The electrical properties of Kcv are well characterised in different heterologous expression systems like *Xenopus* oocytes (Plugge *et al.* 2000) or Human Embryonic Kidney cells (HEK293) (Moroni *et al.* 2002). It was also shown that growth assays of yeast mutants of *Saccharomyces cervesiae* (Tang *et al.* 1995) are suitable for testing Kcv activity (Figure 22). The combination

of functional testing and insight into the simple structure of the Kcv channel are now paving the way to understand structure correlates of this simple channel protein.

One peculiar feature of Kcv is that it exhibits an only 12 amino acid long cytosolic N-terminus and no cytosolic C-terminus. The canonical bundle crossing of the second transmembrane domains (TMD2), which is important for gating in other K^+ channels (Cuello *et al.* 1998, Heginbotham *et al.* 1999, Meuser *et al.* 1999), is, therefore, absent in Kcv. Single channel recordings of Kcv activity, however, show that this channel still exhibits typical gating fluctuations (Abenavoli *et al.* 2009) even in the absence of a canonical bundle crossing (Gazzarrini *et al.* 2002 and 2004). An analysis of two different gating modes in Kcv suggests that one gate is directly associated with the selectivity filter. This gate explains the behaviour of the channel to close fast in the sub-millisecond range at extreme negative or positive voltages (Abenavoli *et al.* 2009). The exact position of the second slower gate is still ambiguous. Single channel recordings show that negative voltages cause a slow voltage dependent activation of channel activity implying the presence of at least one additional gate This second gate probably involves the C-terminus of Kcv, which builds the mouth of the channel, i.e. the entrance site for K^+ from the cytosol to the cavity of the channel (Hertel *et al.* 2009, Tayefeh *et al.* 2007). Several experimental and computational studies have revealed that the C-terminal negative charged carboxyl groups of the four subunits bind a K^+ ion and inhibit in this way the permeation of further K^+ ions. The opening of this gate like structure is probably due to the formation of salt bridges between the N- and C-terminus of the channel. Computational studies revealed that a disruption of the salt bridge patterns between the C- and N-terminus eliminates an opening of this gate. The K^+ ion remains in these mutants bound to the negative C-terminus and prevents the entry of other K^+ ions into the cavity. Extensive mutational studies revealed that a minimal length of the N-terminus is required for a correct forming of the salt bridges (Moroni *et al.* 2002, Hertel *et al.* 2009) and, hence, for channel function. Furthermore, the analysis of the termini showed that two features are crucial for the building of the salt bridges: **i.** charged amino acids in the N-terminus and **ii.** a free carboxyl group at the C-terminus. This carboxyl group is provided by the terminal leucine at position 94 (Leu94). In a chimera in which Kcv is fused at the C-terminus with EGFP the first negative charged amino acid in the linker region between the channel and the fused EGFP takes the role of the salt bridge partner (Hertel *et al.* 2009).

An alanine-scanning mutagenesis of both TMDs, combined with yeast growth assays (see chapter 3) revealed that a free carboxyl group at the C-terminus alone is not sufficient for a proper channel function. It occurred that the exchange of Leu94 for alanine (Ala) resulted in a reduced ability of this channel mutant to rescue the growth of K^+ uptake deficent yeast mutants. The result of this experiment implies that a free carboxyl group at the C-terminus is not alone influencing channel activity; the hydrophobic mouth of Kcv seems to interact in some other manner with the gate.

In the present work, we further examine the hypothesis of salt bridge independent interactions of the C-terminus of Kcv on channel function. For this purpose, we calculated on the basis of the simulation model of Kcv the K^+ profiles of different channel mutants in which the terminal Leu94 was exchanges against all possible amino acids. The computed results were compared with experiments in which we monitored the efficency of selected Kcv mutants to complement yeast growth on selective media. The data imply a direct correlation between functionality of the channel and K^+ concentration in the cavity of Kcv due to a C-terminal mediated charge transfer between C-terminus and cavity.

5.3. Material and Methods

5.3.1. Constructs and Mutagenesis

For the yeast complementation assay, the Kcv gene was cloned into the EcoRI and XhoI site of a modified version (Minor *et al.* 1999) of the plasmid pYES2 (Invitrogen GmbH, Karlsruhe, Germany). For electrophysiological measurements in HEK293 cells (human embryonic kidney cells), the Kcv gene without its stop codon was cloned into the BglII and EcoRI site of the pEGFP-N2 vector (Clontech-Takara Bio Europe, Saint-Germain-en-Laye, France) in frame with the downstream enhanced green fluorescent protein (EGFP). The resulting fusion protein allows to identify transfected HEK293 cells. The different point mutations were inserted via the QuikChange Site-directed Mutagenesis method (Stratagen) and the resulting constructs were checked by DNA sequencing.

5.3.2. Saccharomyces cerevisiae Complementation Assay

All complementation assays were done as described in Minor *et al.* 1999 with the yeast strain SGY1528 (Mat *a ade* 2–1 *can* 1–100 *his* 3–11,15 *leu* 2–3,112 *trp* 1–1 *ura* 3–1 *trk* 1::HIS3 *trk* 2::TRP1) (Tang et al. 1995), which was kindly provided by Dr. Minor (UCSF, USA). This mutant yeast strain is deficient in the two potassium uptake systems TRK1 and TRK2. Hence, this strain is not able to grow on low potassium concentrations unless the yeasts express a functional potassium uptake system heterologously. For the yeast complementation assay on plates, the yeasts were grown in parallel under selective (0.5 mM KCl and 1mM KCl) and non-selective (100 mM KCl) conditions for three days at 30 °C. For measurements in which yeast growth was monitored by optical density, 2 ml of selective liquid media containing 0.5 mM KCl were inoculated with yeasts to give an optical density of 0.1 at 600 nm (OD_{600}). The cuvettes were sealed with laboratory film and incubated at 30 °C and 230 rpm. After 0h, 6h, 24h, 48h and 72h the OD_{600} was measured with a spectrophotometer.

5.3.3. Electrophysiological Measurements

For the electrophysiological measurements, HEK293 cells were transfected with the Kcv::GFP fusion protein as described previously (see chapter3, page 45). After one day of growth in 35 mm culture dishes at 37 °C with ambient 5 % CO_2, the transfected cells were dispersed with Accutase® (SIGMA-ALDRICH, Schnelldorf, Germany), sowed at low density on new 35 mm culture dishes and allowed to settle over night. The patch-clamp measurements were performed on isolated single cells in the whole-cell configuration according to standard protocols (Hamill *et al.* 1981). Currents were recorded with an EPC-9 Patch Clamp amplifier (HEKA, Lambrecht, Germany). Data acquisition and analysis was performed with the Pulse software (HEKA, Lambrecht, Germany). For the measurements in whole-cell configuration, the holding voltage was 0 mV and the testing voltages were between +60 and -160 mV. The currents were measured at room temperature in different bath solutions containing as a standard 100 mM KCl, 1.8 mM $CaCl_2$, 1 mM $MgCl_2$ and 5 mM HEPES/KOH (pH 7.4). For a closer examination of the influence of the different mutations on channel properties like selectivity and blockage of the channel the composition of the standard bath solutions was changed in two ways: either 100 mM KCl was replaced by 100 mM NaCl or 10 mM $BaCl_2$ was

added on top to the 100 mM KCl bath solution. In all cases, the osmolarity was kept constant at 300 mOsmol by adding mannitol.

The patch pipettes contained 130 mM D-potassium-gluconic acid, 10 mM NaCl, 5 mM HEPES, 0.1 mM GTP (Na salt), 0.1 μM $CaCl_2$, 2 mM, $MgCl_2$, 5 mM Phosphocreatine and 2 mM ATP (Na salt) (pH 7.4). A fast exchange of the solution of the bath chamber was guaranteed by a perfusion pipette, which was positioned near to the cell of interest. This perfusion allowed a fast exchange of the whole chamber solution in approximately 1 minute.

5.3.4. Homology Model Structure Analysis and Calculations

The open source program PyMOL (http://www.pymol.org/) was used for studying the 3D structure and the spatial relationship of different point mutations in the channel protein.

The model of Kcv is based on the tetrameric form of the KirBac1.1 (PDB-Code: 1P7B) x-ray template structure (Tayefeh *et al.* 2009). Based on the Kcv model all Kcv-Leu94X modells were generated with MODELLER (Marti-Renom *et al.* 2000). To assign the force field parameters and for adding missing protons the academic version of CHARMM V31b1 were used (Brooks *et al.* 1983). The pore diameters of the different Kcv-Leu94X structures were calculated by HOLE (Smart *et al.* 1996). For the calculations of the spatial distributions of potassium ions in the Kcv channel and its mutants the 3D-RISM integral equation theory with a partial series expansion of order 3 (PSE-3 closure) (Kast and Kloss 2008) were applied to the the different channel structures. Prof. Dr. Stefan Kast (TU Dortmund University) performed all calculations of the Kcv channel and its mutants.

5.4. Results and Discussion

5.4.1. A Terminal Free Carboxyl Group Alone is not Sufficient for Proper Channel Function

Previous alanine-scanning mutagenesis studies of the two TMDs of Kcv revealed several important sites in both TMDs, which are crucial for a proper channel function. Interestingly the second TMD only bears two sites, which are sensitive to substitutions by alanine (Ala). Using yeast complementation as a functional assay it occures that histidine at position 83, which was discussed in the previous chapter (see chapter 3), and leucine at the terminal position 94 (Leu94) are critical sites. Figure 40 shows the typical results of a yeast complementation assay. For these experiments a yeast strain was used, which lacks an endogenous K^+ transport system. These yeast mutants are only able to survive on media with high K^+ concentrations (100 mM KCl = control plate). On a selection medium with low K^+ (1 mM or 0.5 mM KCl) they can only grow if they express a heterologous potassium uptake system like Kcv (Figure 22).
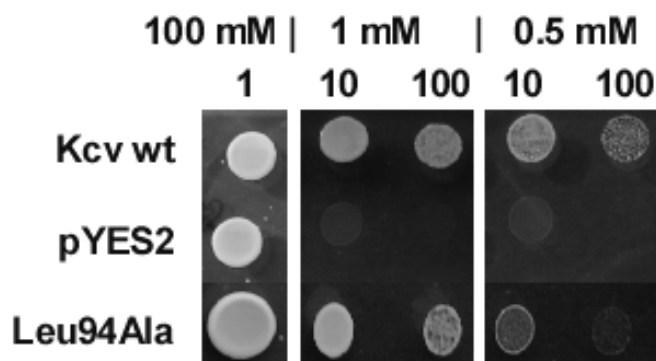
Figure 40: Yeast complementation assay of the last amino acid of Kcv. Shown is a yeast complementation assay in which the mutant yeast expresses Kcv wt as positive control, the empty vector pYES2 as negative control and the alanine exchange mutant Kcv-Leu94Ala. The yeast comple-mentation assay was done as described in Figure 23.

A related study (Hertel *et al.* 2009), which was concentrated with the salt bridge pattern between positively charged amino acid residues of the N-terminus and the C-terminus, revealed that a free carboxyl group at the C-terminal end is of crucial importance for the formation of the salt bridges (Figure 41) and, therefore, for channel function.
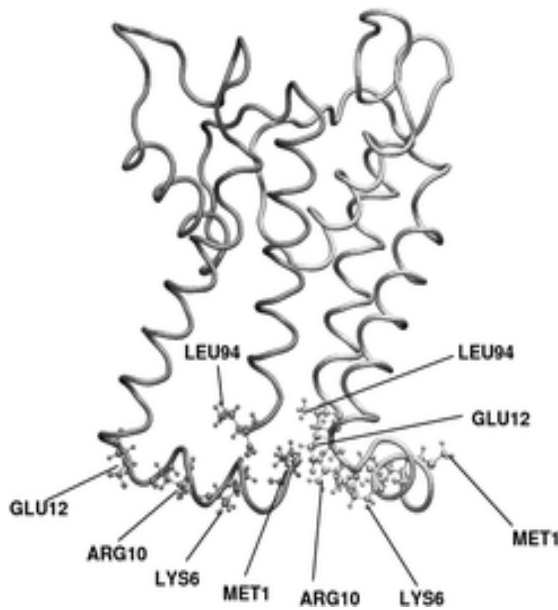
Figure 41: Salt bridge pattern between two subunits of Kcv wt. Shown is the salt bridge pattern between the C- and N-termini of one or two subunits of Kcv. The protein backbone of the average structure of Kcv is shown as a cartoon and the salt bridge partners as ball and stick model (according to Hertel *et al.* 2010).

In the alanine-scanning mutagenesis of the second TMD, Leu94 was replaced by alanine (Kcv-Leu94Ala, Figure 40). This means in terms of structure that the amino acid side chain is reduced to a methyl group but the negative carboxyl group is still present. So the formation of the salt bridges should not be affected.

The functional test of the Kcv-Leu94Ala mutant suggests that a free carboxyl group is not the only important factor for channel function because the mutation leads to a reduced channel function. The data in Figure 40 show that the Kcv-Leu94Ala mutant grows much less on selective medium than the wt channel.

Because of the apparent importance of Leu94, we analysed the spatial distribution of the C-terminus in more detail using the model of Kcv (Tayefeh *et al.* 2009). Figure 42 shows that the three last amino acid residues of Kcv, namely leucine at position 92, 94 and threonine at position 93 form a distinct ring-like structure, which we may call here a hydrophobic mouth.
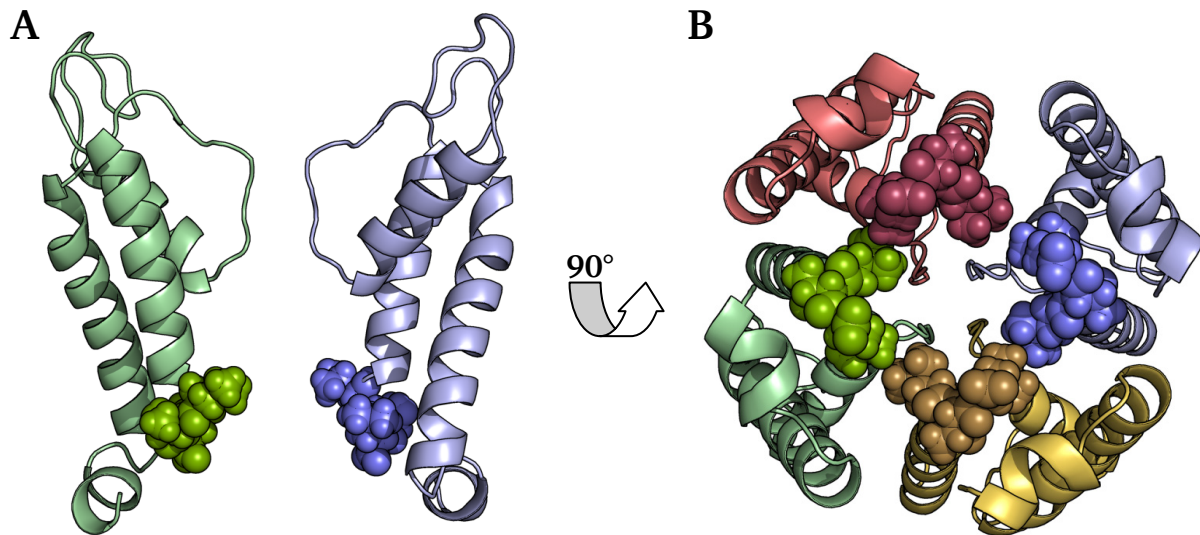
Figure 42: The C-terminal hydrophobic mouth of Kcv. Shown are **(A)** two subunits of Kcv wt in side view and **(B)** all four subunits of Kcv wt in bottom view. The protein backbone is drawn as a cartoon and the last three amino acids of the C-terminus (leucine 92, threonine 93 and leucine 94) are shown as spheres. The bottom view clearly shows the annular hydrophobic mouth at the entrance to the cavity.

The results of the functional data and the structural considerations imply that the amino acids of the C-terminus influence channel function not only through the formation of salt bridges between TMD1 and TMD2, but apparently also via other yet unknown structural features.

5.4.2. Computational Predictions of the Internal K$^+$ Concentration

To test this assumption the K$^+$ concentration ([K$^+$]) profiles of all possible Leu94 exchange mutants were calculated by Prof. Stefan Kast (TU Dortmund, Germany) using the 3D-RISM integral equation theory with a partial series expansion of order 3 (PSE-3 closure) (Kast and Kloss 2008).

Figure 43 shows the z coordinates that were used for the calculations of the different profiles. Furthermore, Figure 43 shows the allocation of the inner channel volume in six distinct sections. These sections are the accessible volumes from the HOLE analysis (Tayefeh *et al.* 2009) in which K$^+$ ions can accumulate.

Figure 44A shows as an example the calculated [K$^+$] profile for the Kcv wt channel; it illustrates very well the different concentrations of K$^+$ ions along the channel axis. All K$^+$ concentration profiles display the x-axis of the z coordinates in Ångström (Å) (Figure 43). The y-axis shows the potassium concentration ($c_K{}^+$) relative to the concentration of in the bulk solution (c_{bulk}).

For a better interpretation of these K$^+$ concentration profiles, we calculated also the corresponding cumulated [K$^+$] profiles, which provide direct information about the K$^+$ concentrations in the different chambers of the channel (Figure 43). Therefore, the integrals from the [K$^+$] profile c(z) over the channel volume ($V_{channel}$) of the different mutants are plotted. The x-axis displays in this case $K_{c(K+)} * V_{channel}$ with $K_{c(K+)} = c_{(K+)}/c_{bulk}$ in Å^3. Notably the channel volumes of the different mutants are quasi identical. Figure 44B shows exemplary the cumulated [K$^+$] profile for Kcv wt. The difference of the [K$^+$] between two steps in the curve, e.g. beginning and end of each inner volume, represents the accumulation or depletion of K$^+$ ions in this region. For example, the difference of the values between -17.7 Ångström (Å) and 2.7 Å of the cumulated [K$^+$] profile is a measure for the [K$^+$] in the cavity ([K$^+$]$_{cav}$) (volume section 2 of Figure 43). Therefore, the curve of Figure 44B shows the same hexamerous classification as the channel itself (Figure 43). For a detailed description of the calculations, see Kast *et al.* submitted.
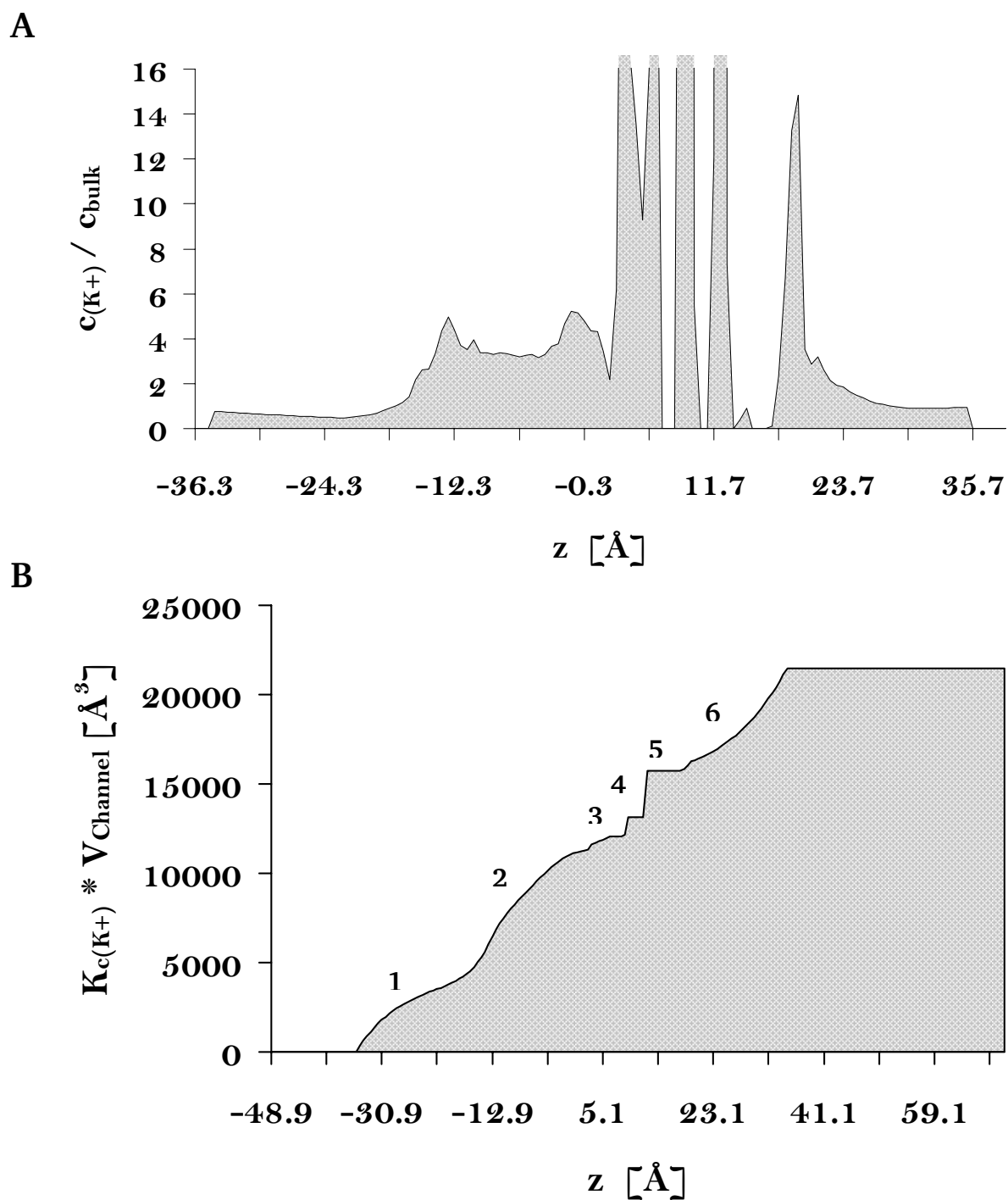
Figure 44: K⁺ concentration profile and the cumulated K⁺ concentration profile for Kcv wt. (A) The K$^+$ concentration profile of Kcv wt shows [K$^+$] along the channel axis z in Ångström (Å). The y-axis is cut off at $c_{(K+)}/c_{bulk}$ = 16. **(B)** The corresponding cumulated profile displays the integral of [K$^+$] profile over the channel volume in Å^3. In this case $K_{c(K+)} = c_{(K+)}/c_{bulk.}$ The numbers 1 to 6 designate the [K$^+$] steps in the channel (according to Figure 43).

Figure 45 now shows the cumulated profiles of all possible mutants including also the "mutation" Kcv-L94L for a better comparability of the results. It is obvious that the different curves are clustered in three groups (i-iii) according to their charge state:

i. negatively charged amino acids

ii. uncharged amino acids

iii. positively charged amino acids
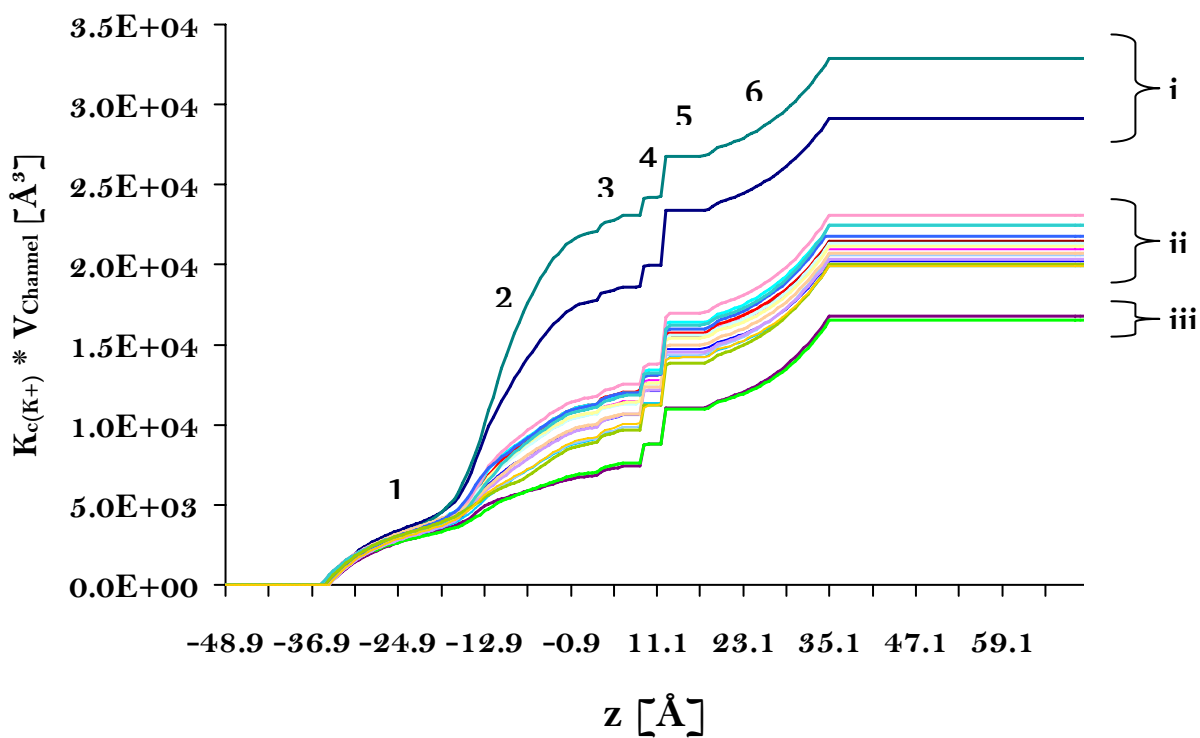
Figure 45: Cumulated K$^+$ concentration profiles of the different Kcv-Leu94 mutants. The cumulated [K$^+$] profiles of the different Kcv-Leu94 mutants display the integral of the [K$^+$] profile over the channel volume in Å^3. In this case $K_{c(K+)} = c_{(K+)}/c_{bulk}$; The value $V_{Channel}$ of all mutants is nearly identical to that of the wildtype channel and does not influence the calculation. The different profiles are separated in three groups: **i.** negatively charged amino acids (D, E), **ii.** uncharged amino acids **iii.** positively charged amino acids (R, K). The numbers 1 to 6 designate the [K$^+$] steps in the different channel mutations (according to Figure 43). The different mutants are not labelled in detail.

Based on the calculations in Figure 45 seven different mutants were chosen according to the three different groups and tested experimentally for their functionality. Leu 94 in Kcv wt was mutated to the following amino acids:

i: aspartic acid (Asp, D)

ii: alanine (Ala, A), histidine (His, H), proline (Pro, P), tryptophan (Trp, W) and tyrosine (Tyr, Y).

iii: arginine (Arg, R)

For group ii five different substitutions were selected in order to test the full range of different amino acid flavours. The substitutions together with the character of the amino acid side chains is summarised in Table 4.

Table 4: **Overview of the different mutations for the leucine at position 94 in the second TMD of Kcv.** Shown are the different mutations of Leu94, which were tested experimentally together with the properties of the substituted amino acids.

Mutation of Leu94 to:	Amino acid characteristics
Alanine (Ala, A)	Tiny, Hydrophobic
Arginine (Arg, R)	Positive charge, Hydrophilic
Aspartic Acid (Asp, D)	Negative charge, Hydrophilic
Histidine (His, H)	Aromatic, Hydrophilic
Proline (Pro, P)	Cyclic, Hydrophobic
Tryptophan (Trp, W)	Aromatic, Hydrophobic
Tyrosine (Tyr, Y)	Aromatic, Hydrophobic

The activity of Kcv wildtype (Kcv wt) and its mutants were assayed with the aforementioned yeast complementation assay. For a better quantitative comparison of the performance of the different Kcv mutants, we monitored yeast growth in 0.5 mM KCl media in liquid culture. Figure 46 shows the results for the Kcv-L94 mutants listed in Table 4.
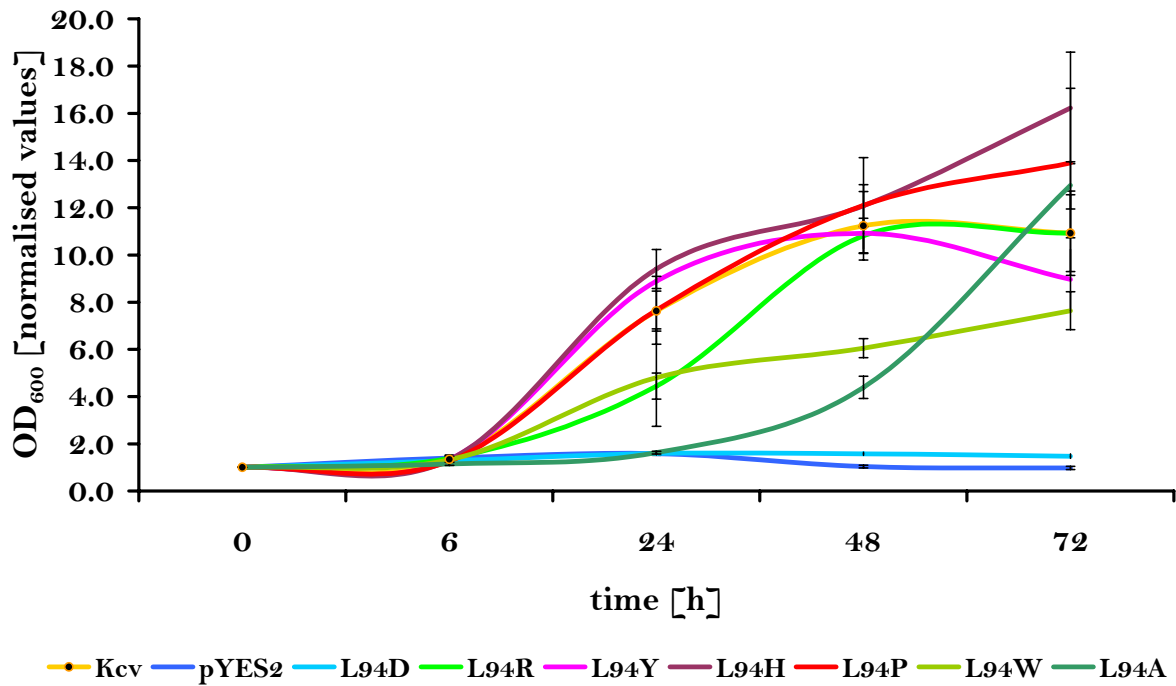
Figure 46: Growth assays of the experimentally tested Kcv-L94 mutants in 0.5 mM K$^+$ selective medium. The plot shows the optical densities measured at 600 nm (OD$_{600}$) of yeast growth medium. Potassium uptake deficient yeasts were transfeted with Kcv wt, different Kcv mutants or vector only and grown in 0.5 mM KCl selective media. Data are mean +/- standard deviations (SD) of n > 4 independent experiments The OD$_{600}$ values are normalised to the OD at the start of the inocculation.

Kcv wt exhibits a normal sigmoidal growth curve in yeasts with a maximum after 48 hours (h), followed by a declining growth rate due to autoinhibitory effects and apoptosis. Therefore, for all further analysis the optical density after 48 hours was used for comparison of the different growth rates of the transformed yeasts.

The experiments show that all of the selected mutations are able to rescue yeast growth on selective media with the exception of asparagine (L94D). Yeasts transformed with Kcv-L94D show no growth in the selective media beyond that of the negative control. The substitutions of Leu94 to histidine (L94H) or proline (L94P) leads to growth rates, which are only after 48 h slightly higher than in the wildtype. The substitution to arginine (L94R) and tyrosine (L94Y) result in channels, which complement the yeast mutants at least during the onset of the growth phase in a similar way as the wildtype; deviation from the control growth only starts late during the experiment. The exchange of Leu94 to tryptophan (L94W) and alanine (L94A) significantly reduces the growth rate of the yeast mutants and both mutants show significant reduced cell numbers after 48 h of growth. The L94A mutants in contrast show only after some lack time an accelerated growth and reach a wildtype like density only after 72 h.

The yeast complementation assay has the disadvantage that it only provides indirect information on channel function. The assay contains no information on the biophysical properties of the different channel mutants. A higher growth rate of the yeast is not necessarily due to a higher conductance or open probability of the mutated channel protein. The optimal range of the yeast growth depends, for example, also on an optimal internal potassium concentration in the cells. Hence channels with a high conductance or open probability, may in principle result in an increase of the intracellular K^+ concentration and in turn generate the same slow growth rate as channels with a low conductivity.

For further studies, the experimental results of the yeast complementation assay were analysed in the context of the cumulated profiles of the calculated $[K^+]$. Therefore, the differences of the $[K^+]$ at each of the six steps (Figure 43 / Figure 45) were calculated and normalised with respect to the wildtype. The resulting Table 5 gives an overview of the mutants and shows the corresponding accumulation or depletion of K^+ in each chamber (Figure 43) in comparison to the wildtype.

Table 5: Depletion and accumulation of K⁺ in the different channel mutants. Shown is the calculated depletion and accumulation of K⁺ at six different steps (see Figure 45) along the conductance pathway of Kcv-L94 channel mutants. The functionality of the eight tested constructs in yeasts is given in the last row (n.s. = not specified). All values are normalised to the values of the wildtype and coloured from blue to magenta according to the expected depletion or accumulation of K⁺.

Step	1	2	3	4	5	6	
z [Å] range	−33.9 −17.70	−17.7 2.70	2.7 8.70	8.7 11.70	11.7 18.30	18.3 35.10	Function in Yeast
L94A	0.06	−0.07	−0.15	0.29	0.11	−0.08	Yes
L94D	0.18	0.81	0.03	0.31	0.31	0.00	No
L94L	0.00	0.00	0.00	0.00	0.00	0.00	Yes
L94H	0.05	−0.03	−0.13	0.41	0.14	0.05	Yes
L94R	−0.08	−0.54	−0.32	0.35	−0.11	0.00	Yes
L94C	0.05	−0.07	−0.10	0.15	0.13	0.03	n.s.
L94E	0.23	1.40	0.21	0.18	−0.02	0.05	n.s.
L94F	−0.01	−0.15	−0.14	0.45	0.02	−0.05	n.s.
L94G	−0.19	−0.25	−0.07	0.49	0.11	−0.02	n.s.
L94I	−0.03	−0.07	−0.05	0.15	0.14	0.00	n.s.
L94K	−0.19	−0.50	−0.28	0.13	−0.15	−0.04	n.s.
L94M	0.03	−0.05	−0.15	0.17	0.06	0.00	n.s.
L94N	0.05	−0.29	−0.01	0.29	0.20	0.08	n.s.
L94P	−0.09	0.07	−0.03	0.25	0.22	0.06	Yes
L94Q	−0.01	−0.15	−0.07	0.50	−0.07	0.01	n.s.
L94S	0.04	−0.20	−0.21	0.64	0.02	0.00	n.s.
L94T	0.04	−0.03	−0.09	0.12	0.09	0.00	n.s.
L94V	−0.11	−0.01	−0.06	0.34	0.18	0.08	n.s.
L94W	−0.03	−0.33	−0.06	0.52	0.02	0.07	Yes
L94Y	0.00	−0.25	0.04	0.20	0.12	−0.01	Yes

< −0.4	> −0.4 − −0.2	> −0.2 − 0.0	> 0.0 − 0.2	> 0.2 − 0.4	> 0.4	> 1
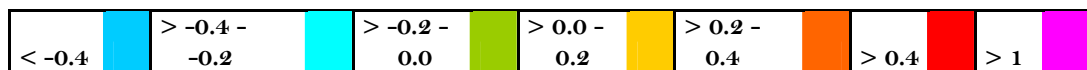
The calculations of Table 5 together with the experimental data give a first impression on possible correlations between $[K^+]$ in the different channel volumes and functionality of the channel. The approach furthermore enables us to search for patterns in the distribution of the $[K^+]$ along the conducting patway of the channel, which could be crucial for a proper channel function.

The unexpected and interesting finding is that the mutations at the C-terminus have no direct influence on the $[K^+]$ at the C-terminus itself (step 1) because no significant changes occur in this area. Indeed, the K^+ concentration in the cavity ($[K^+]_{cav}$) (step 2 and partly step 3) seems to be the crucial factor, which determines the functionality of the channel; changes of $[K^+]$ in this part of the channel correlates well with the functionality of the channels in the complementation assay. Notably, a depletion of K^+ at step 2 (for example in Kcv-L94A, L94W or L94R) goes together with a reduced growth rate of the yeast mutants, which express these mutant channels. A drastic accumulation of K^+ on the other hand (e.g. Kcv-L94D) abolishes the growth of yeasts, which express the respective channel mutant.

It is important to note that the depletion or accumulation of K^+ at step 2 can only give a first evidence for the functionality of the channel; it cannot yet explain in detail the different behaviours of the functional channels. There are many more intra- and intermolecular interactions, which influence channel function or modulate the behaviour of the channel like, for example, the salt bridge pattern between the N- and C-terminus of Kcv (Hertel *et al.* 2009)

During the evaluation of the cumulated $[K^+]$ profiles shown in Figure 45 three different amino acid groups were exposed according to the flavour of the amino acids, namely: positively charged, negatively charged and uncharged amino acids. The calculation results shown in Table 5 reveal, furthermore, an even more complex correlation between C-terminus and $[K^+]_{cav}$; that means not only positively charged but also uncharged amino acids, like serine or asparagine, lead to a depletion of K^+ in the cavity.

The depletion or accumulation of K^+ in the cavity implies that this parameter affects channel function. In this context, we wanted to analyse the physicochemical flavour of the amino acids, which determines the K^+ concentration in this compartment. It has already been mentioned that charge residues are not sufficient to explain the estimated K^+ concentration differences at step 2 between the different mutants. Another possible parameter is the difference in the molecular weights of the amino acids.

Figure 47 shows the comparison of the accumulation or depletion of K^+ in the cavity (Table 5, step 2) as a function of the the molecular masses of the substituted amino acids. The plot

exhibits no correlation between molecular mass and the calculated changes in $[K^+]_{cav}$. Hence, the mechanism by which the amino acid flavour of the C-terminus influences the $[K^+]$ in the cavity remains unexplained.
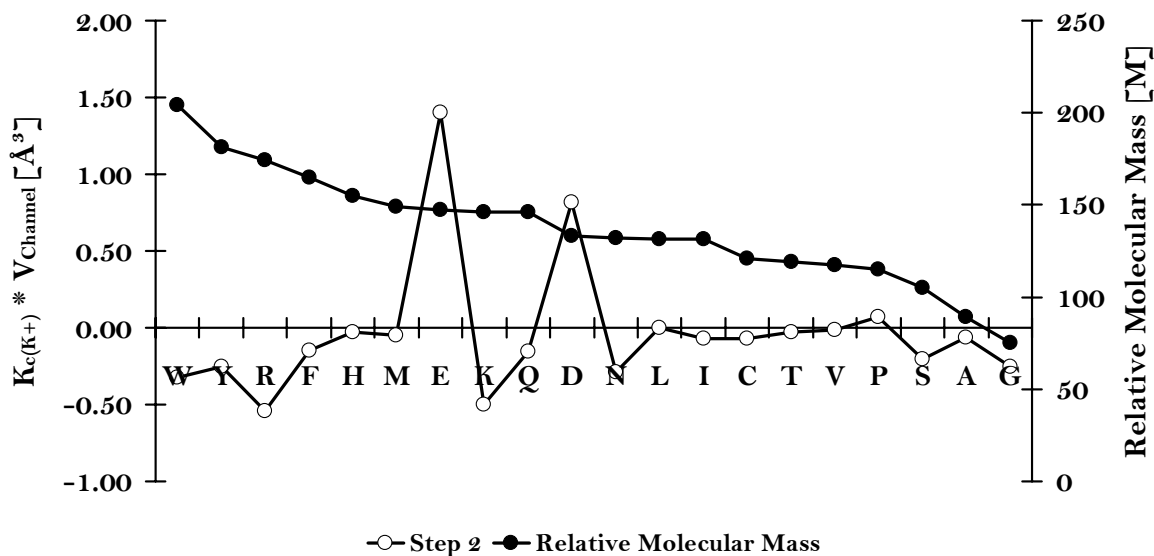
Figure 47: Comparison of the changes in K⁺ concentration in the cavity as a function of the molecular mass of the substituted amino acids. The plot shows the calculated accumulation or depletion of K⁺ in the cavity of Kcv and the molecular mass of the amino acids, which were substituted for the leucine at position 94.

5.4.3. Internal K⁺ Concentration Correlates with the Functionality of Channel Mutants

The calculations of structure related differences in the concentration of K^+ in the channel pathway are in a good agreement with the functional data on various channel mutants.

To further test the robustness of these model predictions, several mutations based on the theoretical predictions were created; the mutants were then tested experimentally for function. Table 6 summarises the different mutants and gives an overview of the expected functionality of these constructs.

Table 6: Overview of a subset of tested Leu94 mutants. The table shows four mutations of Leu94 with the corresponding properties of the amino acids and the expected functionality in yeast. The predictions of mutant channel function in yeasts are based on the calculations of the depletion and accumulation of K$^+$ in the channel mutants (for details see Table 5).

Mutation of Leu94 to:	Amino acid characteristics	Expected functionality
Glutamic Acid (Glu, E)	Negatively charged, Hydrophilic	None functional like Kcv-L94D
Glycine (Gly, G)	Hydrophilic	Less functional
Lysine (Lys, K)	Positively charged, Hydrophilic	Less functional likes Kcv-L94R
Serine (Ser, S)	Hydrophilic	Less functional

Figure 48 shows the yeast complementation assay of the respective mutants. Nearly all predictions from the theoretical consideration coincided with the results of the growth assay. The drastic accumulation of K$^+$ in the cavity of Kcv-L94E should result in a non-functional mutant. This is consitant with the gowth assay of yeast expressing Kcv-L94D; this mutant reveals after 48h no growth (Figure 46). The increasing cell number after 72 h is probably due to spontaneous mutations of the yeasts.

The predicted accumulation of K$^+$ in the cavities of Kcv-L94G and Kcv-L94S is considered to reduce the functionality of the channels. As expected from the prediction the growth of yeast mutants, which express these mutants, is greatly reduced. This is consistent with other mutants like Kcv-L94W, which show also reduced growth of the yeast mutants (Figure 46) and an accumulation of K$^+$ in the cavity (Table 5).

The only deviation between prediction and experimental result is found in the context of mutant Kcv-L94K. This mutant was expected to show a reduced growth rate in yeasts comparable with the mutant Kcv-L94R (Figure 46). The experiment however shows that Kcv-L94K grows even better than the wildtype (Figure 48) even though the calculations of Table 5 show a reduced [K$^+$]$_{cav.}$. From the perspective of the predictions, Kcv-L94K should function like Kcv-L94R.
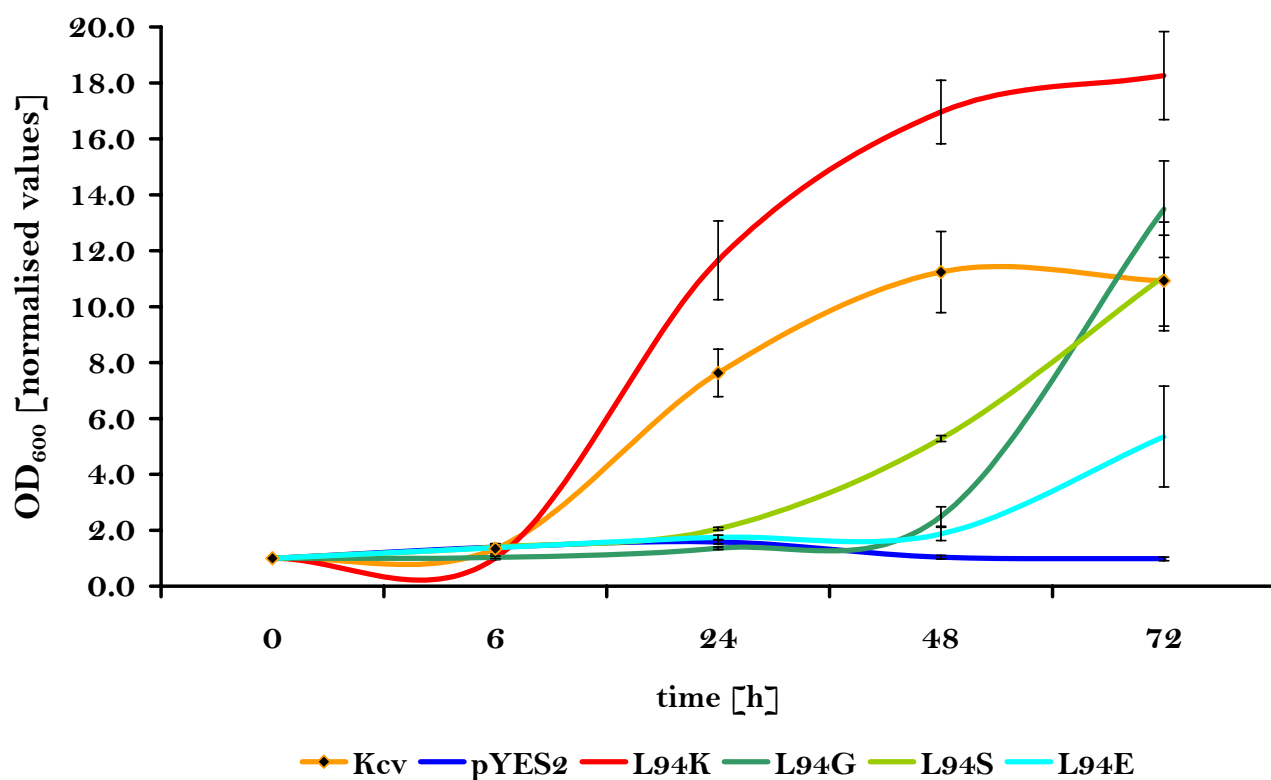
Figure 48: Growth assay of the experimentally tested Kcv-L94 mutants in 0.5 mM K⁺ selective medium. The data show the optical densities measured at 600 nm (OD_{600}) in 0.5 mM KCl selective media of the four Kcv-L94 mutants ($n \geq 4$) and of Kcv wt and pYES2 as positive and negative controls. The OD_{600} values are normalised to the density at the start of the experiment.

5.4.4. Influence of C-terminal Charges

The good functionality of Kcv-L94K implies that this mutant may have a higher $[K^+]_{cav}$ than predicted. This could be achived if the lysine in this position is not protonated. Table 5 shows that in particular the protonation of lysine is responsible for the significant reduction of K^+ in the cavity. This would not be the first case in which a lysine has been found in a non-canonical deprotonated stage. Previous studies of a lysine of Kcv at position 29 at the end of the first TMD (Capter 2) showed that this lysine as well has to be deprotonated for a functional channel simulation (Tayefeh *et al.* 2009). Also in other proteins it was reported that the pK_a value of amino acids can shift more than 4 units within the hydrophobic environment of the membrane (Li *et al.* 2008a, MacCallum *et al.* 2007, Yoo and Cui 2008). Hence a lysine at the end of the transmembrane domain of Kcv could well be in a deprotonated state because of the membrane environment.

To examine whether a deprotonated Lys at position 94 could explain the experimental results of Kcv-L94K, the cumulated $[K^+]$ profile was also calculated for the respective deprotonated Kcv-L94K mutant (Kcv-L94K$_{deprot}$). Figure 49 shows the cumulated $[K^+]$ profiles for the mutants Kcv-L94K$_{deprot}$, Kcv-L94K$_{prot}$ and the wildtype channel.
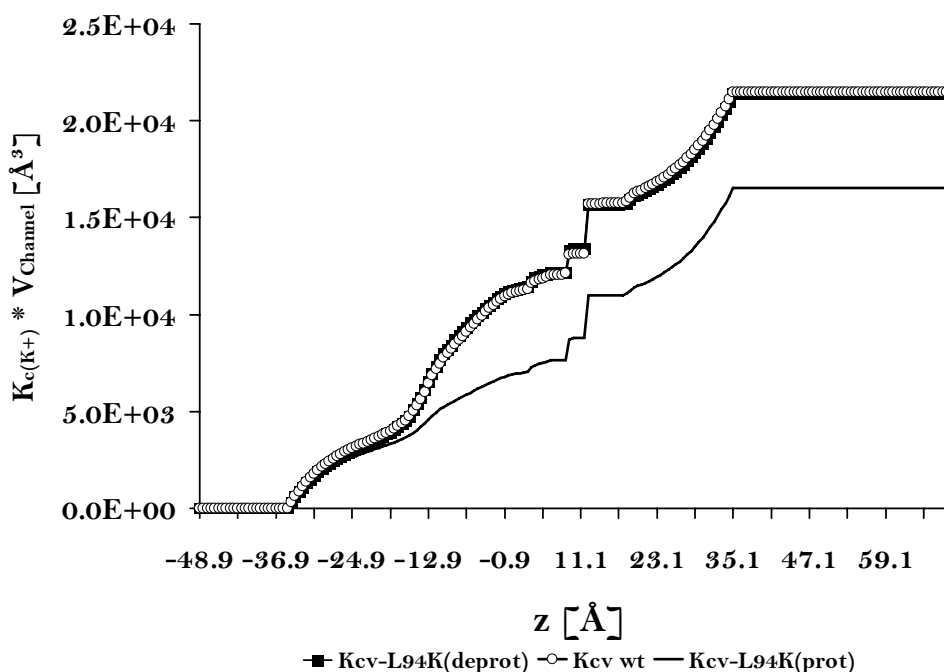
Figure 49: Cumulated K$^+$ concentration profiles of Kcv wt, Kcv-L94K$_{prot}$ and Kcv-L94K$_{deprot}$. The cumulated profiles of the three different constructs Kcv wt, Kcv-L94K$_{prot}$ and Kcv-L94K$_{deprot}$ reveal that a deprotonated lysine at position 94 does not influence the K$^+$ concentration in the channel. In contrast, the K$^+$ concentration in the protonated state is drastically reduced. The cumulated K$^+$ concentration profiles display the integral of the K$^+$ concentration profiles over the channel volume in Å^3. In this case $K_{c(K+)} = c_{(K+)} / c_{bulk}$; The value $V_{Channel}$ of all mutants is nearly identical to that of the wildtype channel and does not influence the calculation.

Figure 49 shows that the concentration profile of Kcv-L94K$_{deprot}$ is nearly identical to the profile of the wildtype channel. The calculations in Table 7 furthermore confirm that the cumulated K$^+$ concentration profile for Kcv-L94K with a deprotonated lysine at position 94 equals the wildtype channel; other than the protonated version of Kcv-L94K, it does not show a depletion of K$^+$ in the cavity.

Table 7: Depletion and accumulation of K$^+$ in the channel mutant Kcv-L94K with protonated and deprotonated lysine. The data show the calculated depletion and accumulation of K$^+$ at six different steps (see Figure 45) of Kcv-L94K in its protonated or deprotonated form. All values are normalised to the values of the wildtype and coloured from blue to magenta according to the occurring depletion or accumulation of K$^+$.

Step	z [Å]	range	L94K$_{prot}$	L94K$_{deprot}$
1	–33.9	–17.70	–0.19	0.00
2	–17.7	2.70	–0.50	0.02
3	2.7	8.70	–0.28	–0.10
4	8.7	11.70	0.13	0.21
5	11.7	18.30	–0.15	–0.12
6	18.3	35.10	–0.04	0.00

< -0.4		> -0.4 – -0.2		> -0.2 – 0.0		> 0.0 – 0.2		> 0.2 – 0.4		> 0.4		> 1	
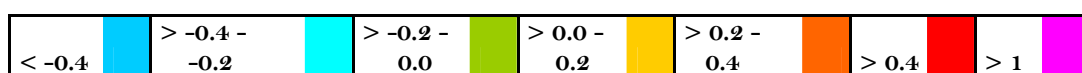
The good agrrement between theoretical calculations and experimental data support the idea that the lysine in the mutant Kcv-L94K is in its deprotonated state and, hence, can therefore form a functional channel. The problem with this interpretation is that the terminal amino acid of Kcv is not buried within the membrane but faces the hydrophilic environment of the cavity. However, it has been shown that the pK$_a$ of the basic amino acids can be reduced by as much as seven units in a protein environment (Pace *et al.* 2009). Therefore, the circumstances, which lead to a deprotonation of the lysine, are still unknown and further analysis is necessary.

The present results show that the insertion of an additional charge at the C-terminus of the TMD2 drastically reduces or even abolish channel function. Hence, we hypothesise that the insertion of a complementary charged residue might balance the additional net charge and may recover channel function. Therefore, a double mutant Kcv-L94D-95R was created. In this mutant, an additional positive charge (arigine at position 95) was introduced on the background of the non-functional mutant Kcv-L94D. The function of the mutant was tested experimentally; a calculation of the impact of this mutation on the [K$^+$] in the channel pathway was for technical reasons not possible.

The complementation assay of Kcv-L94D-95R is shown in Figure 50. As assumed, the double mutant is able to recover function of the non-functional Kcv-L94D mutant. Moreover, the growth rate of the transformed yeasts is significantly higher than in the wildtype. Therefore,

the insertion of a complementary charge can balance the additional inserted net charge and, hence, rescue channel function.
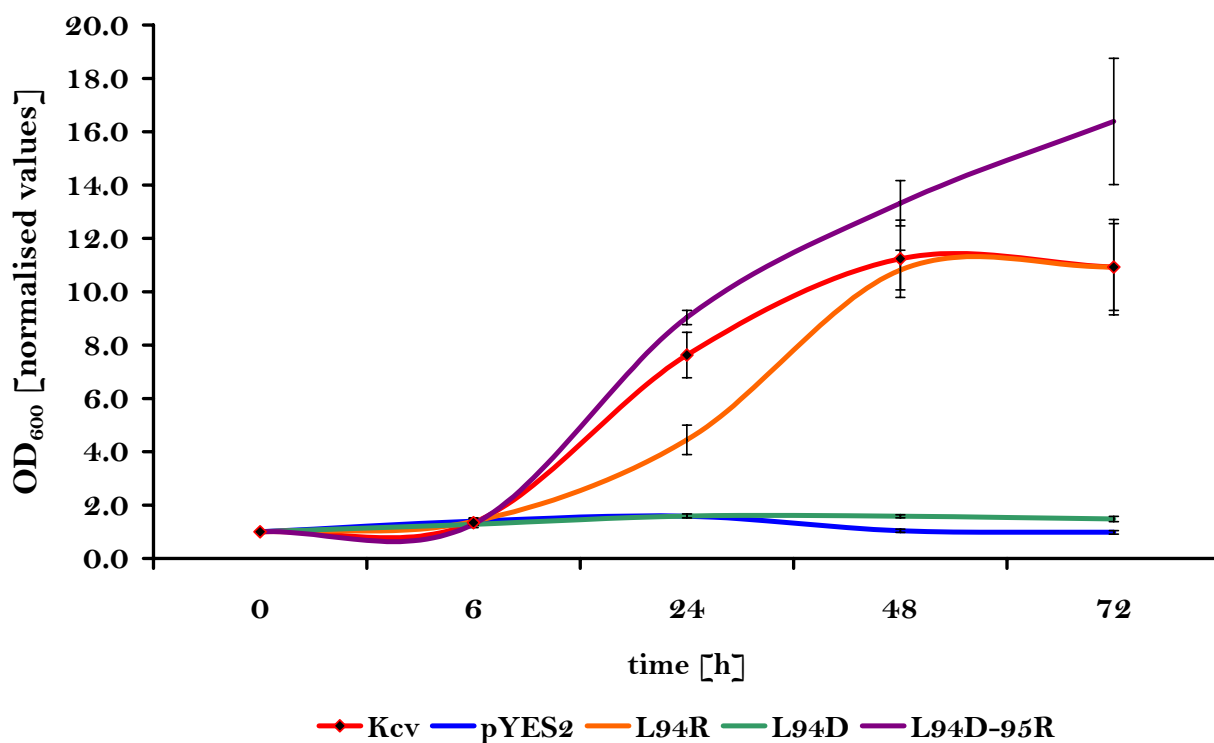
Figure 50: Growth assay of the the double mutant Kcv-L94D-95R. Shown are the optical densities measured at 600 nm (OD_{600}) in 0.5 mM KCl selective media of the different Kcv-L94 mutants ($n \geq 4$) and of Kcv wt and pYES2 as positive and negative controls. The OD_{600} values are normalised to the density at the start of the experiment.

5.4.5. Electrophysiological Measurements

To uncover the effect of the mutants on channel kinetic, two mutants namely Kcv-L94H and Kcv-L94Y were also analysed electrophysiologically.

Both channel mutants are able to generate functional channels in HEK293 cells. They show the same kinetics as the wildtyp (Figure 36). Due to the low signal-to-noise ratio of the configuration and the expected small differences between the different functional channels, further analysis of the mutants was not carried out.

5.5. Conclusion

The viral potassium channel Kcv reveals many critical hallmarks of complex potassium channels; the miniature K^+ channel essentially represents the pore module of all potassium channels and is, therefore, a good model system to study the most basic structure/function relationships in K^+ channels.

It has been shown that the formation of salt bridges between positively charged amino acids in the N-terminus and the free carboxyl group of the terminal amino acid of the C-terminus is an important factor for channel function (Moroni *et al.* 2002, Hertel *et al.* 2009); disruption of each of the interaction partners leads to the loss of channel function. An alanine-scanning mutagenesis study (see chapter 3) revealed many important residues in both TMDs for channel function. One of these important residues is the C-terminal leucine at the end of the second TMD. Substitution of this leucine against alanine causes a reduced ability to rescue yeast growth in selective media with low potassium concentrations (Figure 40). These results imply that the formation of the salt bridges is not the only critical factor for channel function. Because the exchange from leucine to alanine maintains the free carboxyl group at the C-terminus, the formation of salt bridges should not be affected.

To uncover the influence of the C-terminal amino acid on channel function, a combined approach of experimental and computational studies was designed. Therefore, the K^+ concentration profiles (Figure 44) and the corresponding cumulated profiles (Figure 45) were calculated for all possible amino acid substitutions. The calculations reveal that the internal K^+ concentration in the cavity of the channel is dependent on the C-terminal amino acid substitution.

Additionally, a set of amino acid substitutions were also experimentally tested for functionallity. The results reveal a good agreement between the internal K^+ concentration in the cavity and the functionallity of the channel expressed in yeast. Accumulation of K^+ in the cavity abolish channel function completely, depletion leads to a significant reduced functionallity. Therefore, an optimal concentration of K^+ in the cavity is one important factor for channel function but not the only channel behaviour modulating factor.

Former studies of Furini *et al.* (2007) in contrast revealed for the bacterial potassium channel KcsA a linear correlation of K^+ concentration in the cavity and channel current (see Figure 7 of Furini *et al.* 2007). Based on the electrodiffusion theory (Poisson-Nernst-Plank theory) they hypothesised that this correlation is may a general mechanism for potassium channels (Furini *et al.* 2007). Notabley the group of Furini *et al.* only used a computational method without experimental verification.

In contrast, the present data cannot verify this hypotesis of Furini *et al.* (2007). Our results reveal a much more complex correlation between internal K^+ concentration and channel function. Neither mutations, which causes too low nor such, which causes too high K^+ concentrations in the cavity are able to complement successfully the deletion yeast strain. Therefore, our model of an optimal internal K^+ concentration seems to be a better representation of the reality because the computational data are in good agreement with experimental results.

5.6. References

Abenavoli A, DiFrancesco ML, Schroeder I, Epimashko S, Gazzarrini S, Hansen UP, Thiel G, Moroni A (2009) Fast and slow gating are inherent properties of the pore module of the K$^+$ channel Kcv. *J Gen Physiol.* 134(3):219-29. doi:10.1085/jgp.200910266

Baumeister D (2010) Struktur-Funktions-Beziehung Viraler Kaliumkanäle - Einfluss der Transmembrandomänen/helices auf die Funktion von Kaliumkanälen. *in Press.*

Brooks BR, Bruccoleri RE, Olafson BD, States DJ, Swaminathan S, Karplus M (1983). CHARMM: a program for macromolecular energy, minimization, and dynamics calculations. *J. Comput. Chem.* 187–217. doi:10.1002/jcc.540040211

Catterall WA (1984) The molecular basis of neuronal excitability. Science 223:653-661

Cuello, L.G., J.G. Romero, D.M. Cortes, and E. Perozo (1998) pH-dependent gating in the Streptomyces lividans K$^+$ channel. *Biochemistry* 37:3229–3236.

Furini S, Zerbetto F, Cavalcanti S (2007) Role of the Intracellular Cavity in Potassium Channel Conductivity. *J. Phys. Chem. B* 111(50):13993-14000. doi: 10.1021/jp0747813

Gazzarrini S, Van Etten JL, DiFrancesco D, Thiel G, Moroni A (2002) Voltage-Dependence of Virus-encoded Miniature K$^+$ Channel Kcv. *J. Membrane Biol.* 187:15-25. doi:10.1007/s00232-001-0147-5

Gazzarrini S, Kang M, Van Etten JL, Tayefeh S, Kast SM, DiFrancesco D, Thiel G, Moroni A (2004) Long-distance interactions within the potassium channel pore are revealed by molecular diversity of viral proteins. *JBC* 279:28443-28449. doi: 10.1074/jbc.M401184200

Heginbotham L, Lu Z, Abramson T, MacKinnon R (1994) Mutations in the K$^+$ channel signature sequence. *Biophys J.* 66:1061–1067. PMCID:PMC1275813

Heginbotham, L, LeMasurier M, Kolmakova-Partensky L, Miller C (1999) Single *Streptomyces lividans* K$^+$ channels: functional asymmetries and sidedness of proton activation. *J. Gen. Physiol.* 114:551–560.

Hertel B, Tayefeh S, Kloss T, Hewing J, Gebhardt M, Baumeister D, Moroni A, Thiel G, Kast SM (2009) Salt bridges in the miniature viral channel Kcv are important for function. *Eur Biophys J.* doi: 10.1007/s00249-009-0451-z

Jan LY and Jan YN (1992) Structural elements involved in specific K$^+$ channel functions. *Annu. Rev. Physiol.* 54:537-555

Kang M, Moroni A, Gazzarrini S, DiFrancesco D, Thiel G, Severino M, VanEtten JL (2004) Small potassium ion channel proteins encoded by chlorella viruses. *PNAS* 101:5318-5324

Kast SM, Kloss T (2008) Closed-form expressions of the chemical potential for integral equation closures with certain bridge functions. *THE JOURNAL OF CHEMICAL PHYSICS* 129. doi: 10.1063/1.3041709

Kast SM, Kloss T, Tayefeh S, Thiel G. Role of Filter Conformation and Ion Competition for K$^+$ Channel Selectivity, *J. Am. Chem. Soc. Submitted*

Li T, Yang Y, Canessa CM (2008) Interaction of the Aromatics Tyr-72/Trp-288 in the Interface of the Extracellular and Transmembrane Domains Is Essential for Proton Gating of Acid-sensing Ion Channels. *J. Biol. Chem.* 284:4689-4694. doi:10.1074/jbc.M805302200

MacCallum JL, Bennett WFD, Tieleman PD (2007) Partitioning of Amino Acid Side Chains into Lipid Bilayers: Results from Computer Simulations and Comparison to Experiment. *J Gen Physiol.* 129(5):371–377. doi:10.1085/jgp.200709745.

MacKinnon R (1991) Determination of the subunit stoichiometry of a voltage-activated potassium channel. Nature 350:232-235

Marti-Renom MA, Stuart A, Fiser A, Sánchez R, Melo F, Sali A (2000). Comparative protein structure modeling of genes and genomes. *Annu. Rev. Biophys. Biomol. Struct.* 29:291–325.

Meuser, D., H. Splitt, R. Wagner, and H. Schrempf (1999) Exploring the open pore of the potassium channel from *Streptomyces lividans*. *FEBS Lett.* 462:447–452.

Miller C (1992) Ion channel structure and function. *Science* 258:240-241

Moroni A, Viscomic C, Sangiorgioc V, Pagliucaa C, Meckel T, Horvathe F, Gazzarrinia S, Valbuzzia P, Van Etten JL, DiFrancescob D, Thiel G (2002) The short N-terminus is required for functional expression of the virus-encoded miniature K$^+$ channel Kcv. *FEBS Letters* 530:65-69. doi:10.1016/S0014-5793(02)03397-5

Neher E (1992) Ion channels for communication between and within cells. *EMBO* 11(5):1673 - 1679

Pace NC, Grimsley RG, Scholtz JM (2009) Protein Ionizable Groups: pK Values and Their Contribution to Protein Stability and Solubility. *JBC* 284:13285–13289.

Planque MRR, Killian JA (2003) Protein/lipid interactions studied with designed transmembrane peptides: role of hydrophobic matching and interfacial anchoring. *Molecular Membrane Biology* 20:271-284. doi:10.1080/09687680310001605352

Plugge B, Gazzarrini S, Nelson M, Cerana R, Van Etten JL, Derst C, DiFrancesco D, Moroni A, Thiel G (2000) A Potassium Channel Protein Encoded by Chlorella Virus PBCV-1. *Science* 287:1641 - 1644. doi:10.1126/science.287.5458.1641

Schroeder JI, Hedrich R (1998) Involvement of ion channels and active transport in osmoregulation and signalling of higher plant cells. *Trends in Biochemical Sciences* 14(5):187-192. doi:10.1016/0968-0004(89)90272-7

Smart OS, Neduvelil JG, Wang X, Wallace BA, Sansom MSP (1996). HOLE: a program for the analysis of the pore dimensions of ion channel structural models. J. Mol. Graph. 14:354–360. doi:10.1016/S0263-7855(97)00009-X

Tang W, Ruknudin A, Yang WP, Shaw SY, Knickerbocker A, Kurtz S (1995) Functional Expression of a Vertebrate Inwardly Rectifying K^+ Channel in Yeast. *Mol. Biol. of the Cell* 6:1231-1240. PMID:8534918

Tayefeh S, Kloss T, Kreim M, Gebhardt M, Baumeister D, Hertel B, Richter C, Schwalbe H, Moroni A, Thiel G, Kast SM (2009) Model development for the viral potassium channel. *Biophys J* 96:485–498. doi:10.1016/j.bpj.2008.09.050

Van Etten JL, Graves MV, Müller DG, Boland W, Delaroque N (2002) Phycodnaviridae – large DNA algal viruses. *Arch. Virol.* 147:1479-1516

Yoo J, Cui Q (2008) Does Arginine remain protonated in the lipid membrane? Insights from microscopic pKa calculations. *Biophys J.* 94(8):L61–L63. doi:10.1529/biophysj.107.122945.

6. Chapter 5 – Excursus: Further analysis of the 3D model of Kcv

Until now, there is no crystal structure of the viral potassium channel Kcv available. However, the aforementioned studies show that an optimised homology model of Kcv, which is based on the tetrameric form of the KirBac1.1 (PDB-Code: 1P7B) x-ray template structure (Tayefeh *et al.* 2009) serves as a good basis for analysing possible intramolecular interactions in the protein structure.

Here I further analyse this model of Kcv with implications on channel functions.

In chapter 3, investigations of the b-factors, which are an indirect measure of protein flexibility, show that the simulated structure of Kcv reveals similarities in the b-factor distribution to more complex channels, namely Kir2.2 and NaK (Figure 32). The three channels share the same segmented flexibility in their TM segments with flexible parts pointing towards the cytoplasmatic side and a rigid part pointing towards the extracellular side (Figure 32). Furthermore, with the help of the model of Kcv it is possible to identify also structural analogies to other potassium channels.

A closer look on the localisation of the aromatic residues in Kcv for example (Figure 51 C and D) reveals a tripartite distribution of these residues consisting of an external [E] and internal [I] interfacial region plus a band [B] located in the centre (Figure 51 C). Such aromatic belts on both sides of TMDs are presumptively important for the anchoring of the protein in the lipid bilayer (compare chapter 1, Figure 8) (Planque and Killian 2003). The same tripartite localisation can be found in the bacterial potassium channel KirBac1.1, but only in the open state model (Figure 51A). In the closed state (Figure 51B) the crystal structure reveals that the localisation of the aromatic residues is evenly distributed along the whole length of the TMDs (Domene *et al.* 2006) due to an altered orientation of the phenylalanines of the central band [B] of the TMDs (Figure 51B). These structural changes occur due to conformational changes, which the protein undergoes in its TM regions during gating. They are most relevant for the interaction of the protein with the lipid environment (Domene *et al.* 2006).
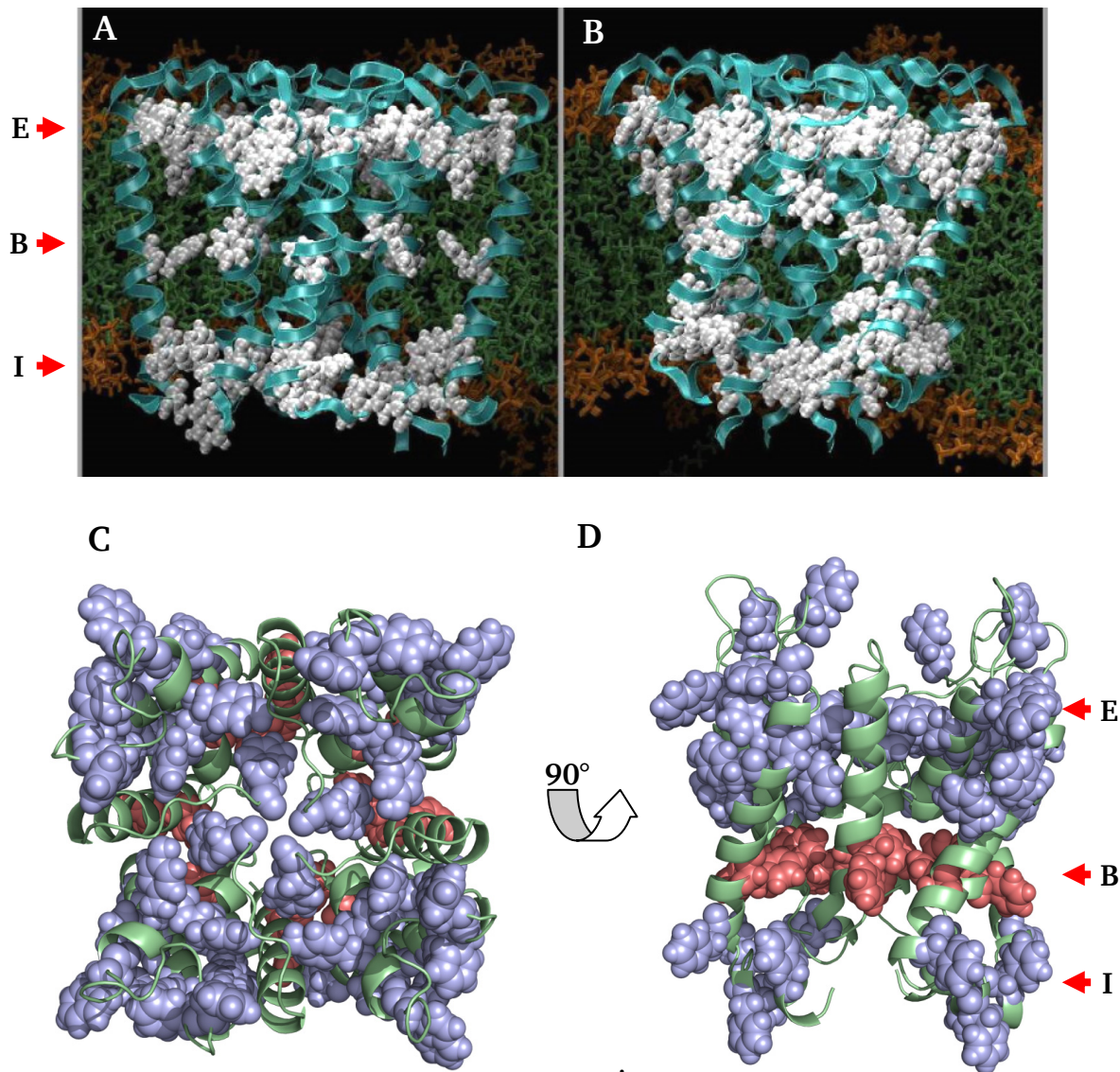
Figure 51: Illustration of the localisation of the aromatic residues at the water-lipid-interface of KirBac1.1 and Kcv. (A) The images show a model of KirBac1.1 in the open state. The cartoon of the protein backbone is drawn in cyan and the aromatic residues (Phe, Trp and Tyr) are shown in space-filling format in grey. The red arrows indicate the position of the aromatic residues, which show a tripartite distribution in the open state model (external [E] and internal [I] interfacial regions plus a band [B] located at the central cavity section). **(B)** In the closed state, the location of the aromatic residues is evenly distributed along the length of the transmembrane helices (according to Domene *et al.* 2006). **(C)** Top view and **(D)** side view of the Kcv homology model. The protein backbone is drawn in pale green and the aromatic residues (Phe, Trp and Tyr) are shown in space-filling format in violet (upper [E] and lower [I] belt) or red (central belt [B]). The red arrows indicate that the position of the aromatic residues is similar to the tripartite distribution in the open state model of KirBac1.1.

The central aromatic belt of Kcv, like the central band of KirBac1.1, is built only by phenylalanines. In the case of Kcv this are the phenylalanines at position 19 (TMD1), 88 and 89 (TMD2). Because of the comparable distribution of the aromatic residues of Kcv and KirBac1.1, it is possible that the phenylalanines in the central band of Kcv are also involved in gating just like in KirBac1.1 (Domene *et al.* 2006). This hypothesis can only be tested, if a crystal structure of Kcv in open and closed state becomes available, which allows to check, whether the distribution of these residues differ between the open and closed states. Different existing functional and non-functional simulation models of Kcv wt (Tayefeh *et al.* 2009), however, may already provide first hints on the involvement of these aromatic residues in Kcv on gating. In this context, we have to keep in mind that a non-functional model is not necessarily comparable with a closed state model because the loss of function can have different reasons.

Figure 52 shows the structure of one functional and three non-functional simulation models of Kcv wildtype (Tayefeh *et al.* 2009) with highlighted aromatic residues, namely Phe, Trp and Tyr.

helical – protonated (non-functional)

helical – deprotonated (functional)

NMR – protonated (non-functional)

NMR – deprotonated (non-functional)
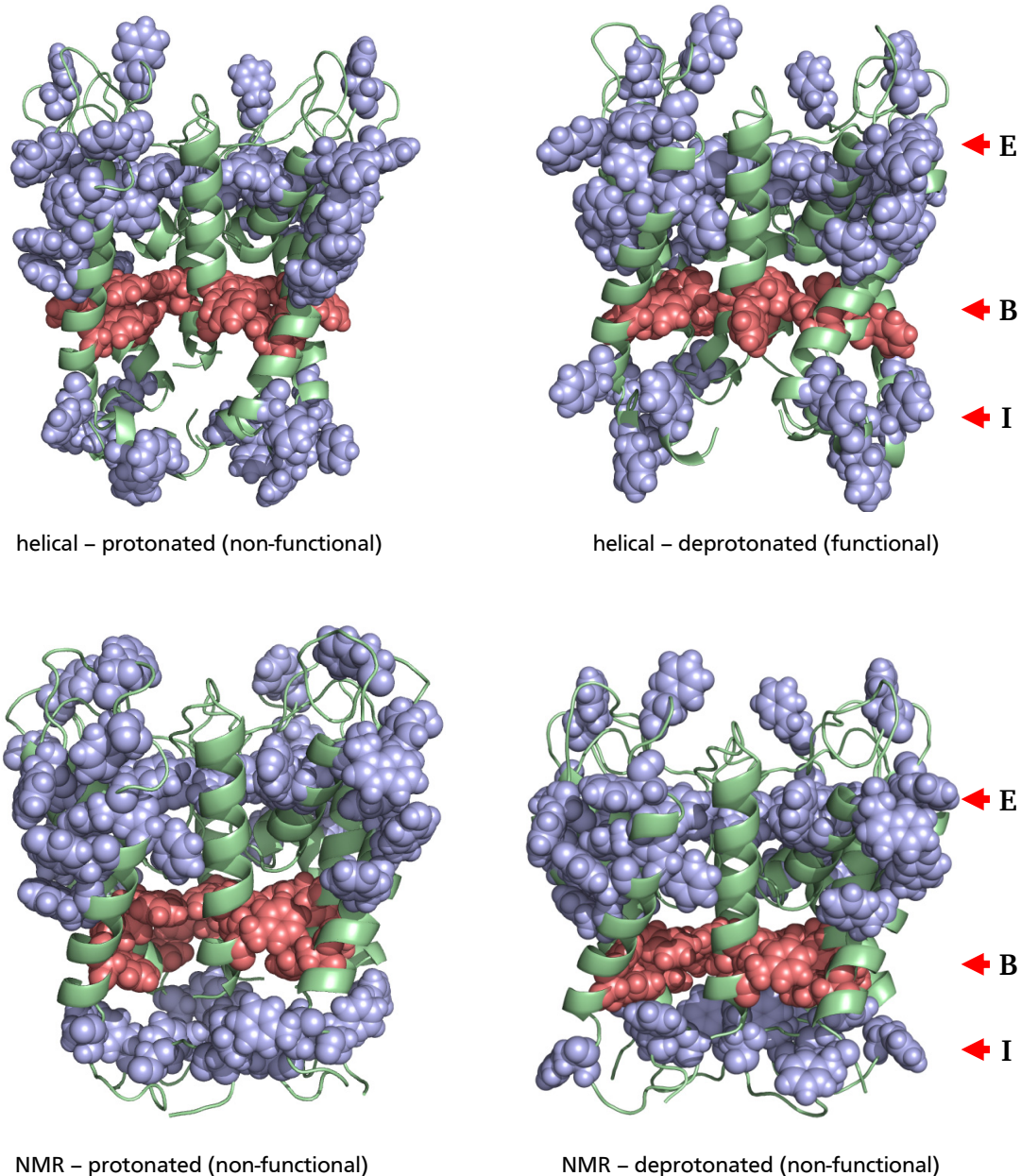
Figure 52: Four different simulation models of Kcv with highlighted aromatic amino acids. Shown are four different functional and non-functional simulation models of Kcv (Tayefeh *et al.* 2009) in side view. The protein backbones are drawn in pale green and the aromatic residues (Phe, Trp and Tyr) are shown in space-filling format in violet (upper and lower belt) or red (central belt). It is obvious that the loss of function of the non-functional simulation models is independent from the tripartite distribution of the aromatic residues, because the tripartite distribution is preserved in all four models. The red arrows indicate the position of the aromatic residues, which show a tripartite distribution with external [E] and internal [I] interfacial regions plus a band [B] located at the central cavity section.

In all four models, a tripartite distribution of the aromatic residues is more or less visible. This could be a first hint that gating in Kcv is independent from the spatial distribution of the phenylalanines in the middle band. However, for a precise statement, crystal structures in the closed and open state are necessary.

Taking all results together it appears that Kcv shares many structural and functional properties with other more complex ion channels, like the basic assembly principle, the b-factor distribution, gating properties, high selectivity and sensitivity against potassium channel blockers, to name just a few. This may show that viral ion channels are potential candidates for the ancestors of potassium channels.

6.1. References

Domene C, Vemparala S, Klein ML, Vénien-Bryan C, Doyle DA (2006) Role of Aromatic Localization in the Gating Process of a Potassium Channel. *Biophys J.* 90(1):L01–L03. doi:10.1529/biophysj.105.072116

Tayefeh S, Kloss T, Kreim M, Gebhardt M, Baumeister D, Hertel B, Richter C, Schwalbe H, Moroni A, Thiel G, Kast SM (2009) Model development for the viral potassium channel. *Biophys J.* 96:485–498. doi:10.1016/j.bpj.2008.09.050

7. Summary

The viral potassium channel Kcv from *Paramecium bursaria* chlorella virus 1 (PBCV-1) is with only 94 amino acids minimal in size. Indeed, Kcv is one of the smallest potassium channels known so far, but still exhibits almost structural and functional hallmarks of complex potassium ion channels. Here we analyse the importance of the two transmembrane domains (TMD) for channel function. Using an alanine-scanning approach in combination with yeast complementation and electrophysiological recordings, we identified crucial important sites in both TMDs, which are important for channel function. Many of the key amino acids are located in the outer transmembrane domain and are essential for the correct positioning of the protein in the lipid membrane.

(i) Snorkeling effects in Kcv_{PBCV-1} are nonessential for a proper channel function

A lysine near the water/lipid interface in a TM segment is able to snorkel. This snorkeling can increase the hydrophobic length of TM segments and helps to span the lipid membrane. Computational studies of Kcv_{PBCV-1} have shown that the lysine at position 29 in the TMD1 has to be deprotonated for proper channel function. Extensive mutational studies of the lysine at position 29 in Kcv_{PBCV-1} have shown that all amino acid exchanges, with exception of proline, are allowed at this position. This means that Kcv_{PBCV-1} indeed tolerates a neutral amino acid in this position without loosing function. However, when the equivalent lysine, which is highly conserved in viral channels, is substituted by alanine in the related channels Kcv_{MT325} or Kcv_{ATCV-1}, these channels loose their function. The latter two channels do not have the cytosolic N-terminal domain, which is essential in Kcv_{PBCV-1}. We therefore propose that the snorkeling effect is becoming essential in the structural context of the Kcv channels without cytosolic N-terminus, and that this feature is not crucial for the functionality of Kcv_{PBCV-1}.

(ii) Aromatic amino acids in the TMD1 are crucial for the anchoring of the protein in the lipid membrane

TMD1 contains several aromatic amino acids. According to the structural model of Kcv, these aromatic side chains are facing towards the lipid membrane and anchor the channel in the membrane. The anchoring is also reflected in the distribution of the b-factors of Kcv, which

are a measure for the flexibility or rigidity of the amino acids. The N-terminus of Kcv and the first half of the TMD1 exhibit high b-factors and are flexible; the rest of the TMD1, starting from His17, is rigid with low b-factors. The alanine exchange experiments underscore the functional importance of this anchoring. An exchange of the aromatic residues in TMD1 beginning with His17 greatly reduces or abolishes channel function. These negative effects on channel function can be explained by a decreased anchoring of the protein in the membrane.

(iii) The π-stack between the two TMDs stabilises the spatial structure of the channel

Alanine-scanning mutagenesis together with information on the three dimensional structure of Kcv identified intramolecular interactions between the TMD1 (Phe30) and the TMD2 (His83). A π-π-interaction between aromatic rings in TMD1 and TMD2 generates a tight connection (π-stack) between the two TMDs and coordinates them into the correct position. A mutation of one of the π-stack-partners leads nearly in all cases to the loss of the channel function. Only substitutions in one partner amino acid (Phe30), which also allow π-stacking interactions (Try, Met), are still able to maintain channel function. The results of these experiments imply that the intramolecular contact between the TMDs is essential for function. The position of the π-stack in the channel model suggests, that the rigid part of TMD1 allows the stabilising of the upper part of TMD2 via this connection.

(iv) The C-terminal amino acid influences the potassium concentration in the cavity

Mutations of the last C-terminal amino acid of the TMD2 in Kcv_{PBCV-1} affect the activity of the channel. Computational data of the potassium concentration profiles of the different mutants predict that these mutations influence the internal potassium concentration of the channel. These changes do not occur, as expected, directly at the mouth of the channel but in the cavity. A theoretically predicted depletion or accumulation of potassium in the cavity, as a result of a mutation of the terminal amino acid, generates channels, which show in the experiments either a lower or no activity. Therefore, small changes in the amino acid sequence could cause drastic effects in the global K^+ concentration distribution in the channel and, therewith, influences channel function. The good agreement between theory and experiment suggests that an optimal K^+ concentration is essential for a proper channel function; a too high or too low K^+ concentration leads to reduced or no channel function. Furthermore, the

results reveal the quality of the homology model of Kcv, which enables us to find long-term interactions between the C-terminus and the cavity, an interaction, which is independent on the salt bridges at the cytosolic entrance of the channel.

8. Zusammenfassung

Der virale Ionenkanal Kcv aus dem *Paramecium bursaria* Chlorella Virus 1 (PBCV-1) ist mit nur 94 Aminosäuren sehr klein. In der Tat handelt es sich bei Kcv um einen der kleinsten bekannten Kaliumkanäle, der aber nichtsdestotrotz alle stukturellen und funktionellen Merkmale komplexer Kaliumkanäle besitzt. In dieser Arbeit wurde der Einfluss der beiden Transmembrandomänen (TMD) auf die Kanalfunktion untersucht. Durch die Kombination eines Alanin-Scans mit Hefekomplementationstests und elektrophysiologischen Messmethoden war es möglich, Positionen in beiden TMDs zu identifiziren, die für die Kanalfunktion essentiell sind. Viele dieser Schlüsselaminosäuren befinden sich dabei in der äußeren TMD und sind von grundlegender Bedeutung für die richtige Positionierung des Proteins in der Membran.

(i) *"Snorkeling"* Effekte sind für die Funktionalität von Kcv$_{PBCV-1}$ nicht essentiell

Ein Lysin in der Nähe der Wasser/Lipid Grenzschicht ist in der Lage zu „*snorkeln*". Dieser „*snorkeling*" Effekt kann die hydrophobe Länge eines TM Segments erhöhen und damit die Inserierung in die Membran erleichtern. Computergestütze Analysen von Kcv$_{PBCV-1}$ haben gezeigt, dass das Lysin an Position 29 in der ersten TMD von Kcv$_{PBCV-1}$ im deprotonierten Zustand vorliegen muss, um eine funktionelle Kanalsimulation zu erzeugen. Ausführlich Mutationsstudien dieser Position in Kcv$_{PBCV-1}$ zeigten aber, dass alle Aminosäureaustausche, mit der Ausnahme von Prolin, zu einem funktionellen Kanal führen. Das bedeutet, das Kcv$_{PBCV-1}$ auch ungeladene Aminosäuren an dieser Position toleriert, ohne dass dadurch die Kanalfunktion beeinträchtigt wird. Vergleichbare Positionen des Lysins sind innerhalb der viralen Kaliumkanäle hochkonserviert.Wird nun aber das Lysin in den verwandten Kanälen Kcv$_{MT325}$ oder Kcv$_{ATCV-1}$ gegen Alanin ausgetauscht, führt dies zum Verlust der Funktionalität dieser Kanäle. Die beiden Kanäle Kcv$_{MT325}$ und Kcv$_{ATCV-1}$ besitzen nicht die für Kcv$_{PBCV-1}$ essentielle cytosolische N-terminale Domäne. Daher ist es möglich, dass „*snorkeling*" Effekte zwar für die Funktionalität von Kcv Kanäle ohne cytosolischen N-Terminus von entscheidener Bedeutung sind, nicht aber für Kcv$_{PBCV-1}$.

(ii) Aromatische Aminosäuren der TMD1 sind wichtig für die Verankerung
des Proteins in der Lipidmembran

Die erste TMD von Kcv ist reich an aromatischen Aminosäuren. Das Strukturmodell von Kcv verdeutlicht, dass die Seitenketten dieser aromatischen Aminosäuren zur Membran hin orientiert sind und dadurch den Kanal in der Membran verankern. Diese Verankerung spiegelt sich auch in der Verteilung der b-Faktoren wieder, welche ein Maß für die Flexibilität bzw. Starrheit einer Aminosäure sind. Der N-Terminus von Kcv und die erste Hälfte der TMD1 besitzen hohe b-Faktoren und sind demnach flexibel, der Rest der TMD1, beginnend mit His17, ist starr und besitzt niedrige b-Faktoren. Alanin-Substitutionsexperimente bestätigen dabei, dass die Verankerung entscheidend ist für die Funktionalität. Ein Austausch der aromatischen Aminosäuren der TMD1 führt, ab dem His17, zu einer stark verringerten Kanalfunktion bzw. zu einem völligen Verlust der Funktionalität. Dieser negative Effekt auf die Funktionalität kann durch die verminderte Verankerung des Proteins in der Membran erklärt werden.

(iii) Der π-stack zwischen den beiden TMD stabilisiert die räumliche Struktur
des Kanals

Mit der Hilfe des Alanin-Scans und des dreidimensionalen Modells von Kcv war es möglich, intramolekulare Interaktionen zwischen der ersten (Phe30) und zweiten TMD (His83) zu identifizieren. Diese π-π-Wechselwirkungen (π-stack) zwischen den aromatischen Ringen der TMD1 und TMD2 führen zu einer festen Verbindung zwischen den beiden Domänen und halten sie somit in der richigen Position. Durch die Mutation eines der beiden Wechselwirkungspartner kommt es in nahezu allen Fällen zu einem Verlust der Kanalfunktion. Die einzige Ausnahme dabei bildet die Substitution des Phe30 zu Aminosäuren, die ebenfalls in der Lage sind einen π-stack auszubilden (Tyr, Met) und somit die Kanalfunktion erhalten können. Die Ergebnisse verdeutlichen die Bedeutung der intramolekularen Interaktionen zwischen den beiden TMD für die Kanalfunktion. Die Positionierung des π-stacks im Kanalmodell läßt vermuten, dass mittels dieser Wechselwirkungen der starre Teil der TMD1 eine Stabilisierung des oberen Abschnittes der TMD2 bedingt.

(iv) Die C-terminale Aminosäure beeinflußt die Kaliumkonzentration in der Cavität

Mutationen der letzten Aminosäure des C-Terminus der TMD2 von Kcv_{PBCV-1} beeinflussen die Kanalaktivität. Berechnungen von Kalium-Konzentrationsprofilen verschiedener Kanalmutanten ergaben, dass diese Mutationen die interne Kaliumkonzentration des Kanals beeinflussen. Diese Konzentrationsveränderungen treten dabei nicht, wie erwartet, direkt am Eingang des Kanals auf, sondern in der Cavität. Dabei stimmen die theoretisch getroffenen Vorhersagen über eine An- oder Abreicherung von Kalium in der Cavität, durch die Mutation der C-terminalen Aminosäure, mit der experimentell beobachteten reduzierten Kanalaktivität bzw. dem völligen Verlust der Funktionalität überein. Somit verursachen kleine Veränderungen der Aminosäuresequenz weitreichende Veränderungen in der globalen Konzentrationsverteilung der Kaliumionen im Kanal und beeinflussen damit dessen Funktion. Die gute Übereinstimmung zwischen Theorie und Experiment legt die Vermutung nahe, dass eine optimale Kaliumkonzentration die Vorraussetzung für die richtige Funktion des Kanals ist. Zu hohe oder zu niedrige Konzentrationen dagegen können die Funktionalität herabsetzen oder gar ganz verhindern. Des Weiteren spiegeln die Ergebnisse die Qualität des Homologiemodells von Kcv wider welches es ermöglicht, weitreichende Interaktionen zwischen dem C-Terminus und der Cavität aufzudecken, die scheinbar unabhängig von dem Vorhandensein der Salzbrücken an der cytosolischen Eingangsseite des Kanals sind.

9. Danksagung

Zum Abschluss dieser Arbeit möchte ich mich bei all denjenigen bedanken, die auf die ein oder andere Art und Weise zum Gelingen dieser Arbeit beigetragen haben. Dabei gilt mein Dank vor allem:

Prof. Dr. Gerhard Thiel, für die Betreuung dieser sehr spannenden und interessanten Arbeit. Für die stetige Hilfe und Unterstützung bei allen schwierigen Fragestellungen. Für die angenehme Arbeitsatmosphäre, die dafür gesorgt hat, dass man sich jeden Tag aufs Neue wieder gerne an die Arbeit gemacht hat, um die kleinen und großen wissenschaftlichen Probleme zu lösen.

Prof. Dr. Adam Bertl, für alle freundlichen Ratschläge und guten Hinweise, wenn die Hefen mal wieder nicht so wollten, wie ich es gerne gehabt hätte und für die Übernahme des Koreferats.

Prof. Dr. Stefan Kast, für die immer geduldige Beantwortung all meiner Fragenemails. Für die Unterstützung und Hilfestellung, um nicht den Überblick bei all den integrierenden, modellierenden,

und simulierenden Fragestellungen zu verlieren.

Dr. Brigitte Hertel, für Ihre freundlichen und hilfsbereite Art nicht nur bei wissenschaftlichen Problemen.

Meinen Zimmergenossen, mit denen ich viele lustige Arbeitstag verbringen durfte: **Timo Greiner**, der einem jederzeit hilfsbereit mit Rat und Tat zur Seite stand sowie **Alice Kress, Charlotte von Chappuis, Bastian Roth** und **Timo Wulfmeyer**, denn ohne sie wäre es nur halb so lustig gewesen.

Der gesamten **AG Thiel / Homann** für die wunderschöne Zeit mit all den netten Gesprächen, lustigen Pizza-, Poker- und Grillrunden und natürlich auch für die spannenden Kicker-Tuniere, die einen den Frust missglückter Experimente schnell vergessen ließen.

Besonderer Dank gilt meinen Eltern **Angelika** und **Manfred Gebhardt** und meiner Schwester **Sandra Wallat**, die immer an mich geglaubt haben und mir die Freiheit gegeben haben, meine Träume zu verwirklichen.

Weiterer Dank gilt meinem Verlobten **Ilias Trachanas**, für all die Liebe, Freundschaft und Unterstützung während der gesamten Zeit.

Name	Manuela Gebhardt
Date of birth	29.01.1982
Place of birth	Berlin

Education

1988 to 1994 11th basic primary school Pankow, Berlin

1995 to 2001 Friedrich-List-Gymnasium Pankow, Berlin

Academic Experience

10/2001 – 07/2006 study of biology at the TU-Darmstadt

2006/2007 diploma thesis at the TU-Darmstadt, Institute of Botany in the Membrane Biophysics Group of Prof. Dr. Gerhard Thiel

Title: "Structure-function-relationship of the minimal viral potassium channel Kcv – Influence of the positive charge of the lysine at position 29 in the first transmembrane domain on the activity of the channel"

Since 10/2007 Ph.D. at the TU-Darmstadt, Institute of Botany in the Membrane biophysics group of Prof. Dr. Gerhard Thiel

Papers

Model development for the viral Kcv potassium channel

Tayefeh *et al.*, Biophys J. 2009 Jan; 96(2):485-98

Salt bridges in the miniature viral channel Kcv are important for function

Hertel *et al.*, European Biophysics Journal 2009 April

Talks and Posters

2007 Hamburg - Botanikertagung: Jahrestagung der Deutschen Botanischen Gesellschaft:

Title: "The amino acid Lys can be in a deprotonated state within the protein/lipid context of a K^+-channel"

2008 Heidelberg - Symposium on Viral Membrane Proteins:

Title: "The Role of Transmembrane Domains in Kcv Function"

11. Affidavit

Herewith I declare, that I prepared the Doctoral thesis

 "Structure/Function Analysis of the Viral Potassium Channel Kcv - Mutagenesis studies of the two transmembrane domains"

on my own and with no other sources and aids than quoted. This thesis has not been submitted to any other examination authoriy in its current or an altered form, and it has not been published

Darmstadt, 08.10.2010

_____

Dipl.-Biol. Manuela Gebhardt

12. Eidesstattliche Erklärung

Ich erkläre hiermit an Eides statt, dass ich die vorliegende Dissertation selbstständig und nur mit den angegebenen Hilfsmitteln angefertigt habe.

Ich habe bisher noch keinen Promotionsversuch unternommen.

Darmstadt, den 08.10. 2010

_____

Dipl.-Biol. Manuela Gebhardt

Experiments, data analysis and writing of the present thesis with exception of the following items, were all done by myself. The homology model of Kcv$_{PBCV-1}$ (PDB- Code: 1P7B) and the related MD simulations in Figs. 10, 11, 20 and 43 were done by Dr. Sascha Tayefeh (Tayefeh et al. 2009).

- Sequences of unpublished viral potassium channels in Figs 15 and 33 we provided by Timo Greiner (TU-Darmstadt, Germany) and Dr. Ming Kang (University of Lincoln, Nebraska).

- The K$^+$ concentration profiles/cumulated K$^+$ concentration profiles in Figs 24, 44, 45 and 49 and in Tables 5 and 7 of all possible Leu94 exchange mutants were calculated by Prof. Dr. Stefan Kast (TU-Dortmund, Germany).

Table 8: Overview over 109 amino acid parameters, which were tested for a correlation between the amino acid parameters and the assay data of the different Lys29 substitutions (see Figure 14).

Amino Acid Parameters	Reference	Correlation coefficient
Molar fraction (%) of 2001 buried residues	*Nature* 277:491-492(1979)	0.53
Conformational preference for parallel beta strand.	*Nature* 282:109-111(1979)	0.51
Proportion of residues 95% buried (in 12 proteins)	*J. Mol. Biol.* 105:1-14(1976)	0.50
Membrane buried helix parameter.	*Biochim. Biophys. Acta* 869:197-214(1986)	0.49
Hydropathicity	*J. Mol. Biol.* 157:105-132(1982)	0.47
Average surrounding hydrophobicity.	*Nature* 275:673-674(1978)	0.46
surrounding hydrophobicity;	*Molecular Simulation* Vol. 34, No. 9, August 2008, 1–48	0.45
total nonbonded energy	*Molecular Simulation* Vol. 34, No. 9, August 2008, 1–48	0.45
Hydration potential (kcal/mole) at 25 °C	*Biochemistry* 20:849-855(1981)	0.44
Normalized consensus hydrophobicity scale.	*J. Mol. Biol.* 179:125-142(1984)	0.44
buriedness	*Molecular Simulation* Vol. 34, No. 9, August 2008, 1–48	0.43
power to be at the N-terminal a-helix;	*Molecular Simulation* Vol. 34, No. 9, August 2008, 1–48	0.42
Conformational preference for total beta strand (antiparallel+parallel).	*Nature* 282:109-111(1979)	0.41

Normalized frequency for beta-sheet.	*Biochemistry* 17:4277-4285(1978)	0.39
average number of surrounding residues	*Molecular Simulation* Vol. 34, No. 9, August 2008, 1–48	0.39
Hydrophobicity scale (Contribution of hydrophobic interactions to the stability of the globular conformation of proteins).	*J. Am. Chem. Soc.* 84:4240-4274(1962)	0.39
average long-range contacts;	*Molecular Simulation* Vol. 34, No. 9, August 2008, 1–48	0.39
Transmembrane tendency	*Protein Sci.* 15:1987-2001(2006)	0.38
Free energy of transfer from inside to outside of a globular protein.	*Nature* 277:491-492(1979)	0.38
combined surrounding hydrophobicity (globular and membrane	*Molecular Simulation* Vol. 34, No. 9, August 2008, 1–48	0.38
Conformational parameter for beta-sheet.	*Protein Engineering* 1:289-294(1987)	0.38
short- and medium-range nonbonded energy;	*Molecular Simulation* Vol. 34, No. 9, August 2008, 1–48	0.35
solvent-accessible reduction ratio;	*Molecular Simulation* Vol. 34, No. 9, August 2008, 1–48	0.34
Conformational parameter for alpha helix (computed from 29 proteins).	*Adv. Enzym.* 47:45-148(1978)	0.34
Mean fractional area loss (f) [average area buried/standard state area].	*Science* 229:834-838(1985)	0.34
Gibbs free energy change of hydration for native protein;	*Molecular Simulation* Vol. 34, No. 9, August 2008, 1–48	0.34
B-structure tendencies;	*Molecular Simulation* Vol. 34, No. 9, August 2008, 1–48	0.32
normalized consensus hydrophobicity;	*Molecular Simulation* Vol. 34, No. 9, August 2008, 1–48	0.32

Amino acid composition (%) in the UniProtKB/Swiss-Prot data bank	Release notes for UniProtKB/Swiss-Prot release 56.0 - July 2008	0.31
Conformational preference for antiparallel beta strand.	*Nature* 282:109-111(1979)	0.30
Hydrophobicity scale (contact energy derived from 3D data)	*Macromolecules* 18:534-552(1985)	0.29
Mobilities of amino acids on chromatography paper (RF)	*Int. J. Biochem.* 2:537-544(1971)	0.29
Conformational parameter for alpha helix.	*Protein Engineering* 1:289-294(1987)	0.29
long-range nonbonded	*Molecular Simulation* Vol. 34, No. 9, August 2008, 1–48	0.28
Hydrophobicity of physiological L-alpha amino acids	*Anal. Biochem.* 193:72-82(1991)	0.28
Hydrophobicity scale (pi-r)	*J. Mol. Biol.* 200:513-522(1988)	0.27
Overall amino acid composition (%).	*Proteins: Structure, Function and Genetics* 4:99-122(1988)	0.27
Optimized matching hydrophobicity (OMH)	*J. Mol. Biol.* 171:479-488(1983)	0.26
Hydrophobicity indices at ph 3.4 determined by HPLC	*Peptide Research* 3:75-80(1990)	0.25
Hydrophobicity (delta G1/2 cal)	*Proteins: Structure, Function and Genetics* 2:130-152(1987)	0.23
Hydrophobicity indices at ph 7.5 determined by HPLC.	*Peptide Research* 3:75-80(1990)	0.23
Hydrophobicity scale (pi-r).	*Eur. J. Med. Chem.* 18:369-375(1983)	0.23
a-helical tendencies;	*Molecular Simulation* Vol. 34, No. 9, August 2008, 1–48	0.23
Gibbs free energy change of hydration for unfolding protein;	*Molecular Simulation* Vol. 34, No. 9, August 2008, 1–48	0.22
Gibbs free energy change of hydration for denatured protein;	*Molecular Simulation* Vol. 34, No. 9, August 2008, 1–48	0.22

Conformational parameter for beta-sheet (computed from 29 proteins).	*Adv. Enzym.* 47:45-148(1978)	0.21
Normalized frequency for alpha helix.	*Biochemistry* 17:4277-4285(1978)	0.20
unfolding enthalpy change of hydration;	*Molecular Simulation* Vol. 34, No. 9, August 2008, 1–48	0.17
unfolding enthalpy change	*Molecular Simulation* Vol. 34, No. 9, August 2008, 1–48	0.15
Hydrophobic constants derived from HPLC peptide retention times	*Biochem. J.* 199:31-41(1981)	0.15
unfolding hydration heat capacity change;	*Molecular Simulation* Vol. 34, No. 9, August 2008, 1–48	0.15
power to be at the middle of a-helix;	*Molecular Simulation* Vol. 34, No. 9, August 2008, 1–48	0.13
chromatographic index;	*Molecular Simulation* Vol. 34, No. 9, August 2008, 1–48	0.13
equilibrium constant with reference to the ionization property of COOH group;	*Molecular Simulation* Vol. 34, No. 9, August 2008, 1–48	0.12
average medium- -range contacts;	*Molecular Simulation* Vol. 34, No. 9, August 2008, 1–48	0.12
Estimated hydrophobic effect for residue burial	*Molecular Simulation* Vol. 34, No. 9, August 2008, 1–48	0.11
Estimated hydrophobic effect for side chain burial c	*Molecular Simulation* Vol. 34, No. 9, August 2008, 1–48	0.11
solvent-accessible surface area for unfolding;	*Molecular Simulation* Vol. 34, No. 9, August 2008, 1–48	0.09
Residue non-polar surface area b	*Molecular Simulation* Vol. 34, No. 9, August 2008, 1–48	0.06
Number of codon(s)	Most textbooks	0.04
Relative mutability of amino acids (Ala=100).	In "*Atlas of Protein Sequence and Structure*", Vol.5, Suppl.3 (1978)	0.03

unfolding Gibbs free energy change	*Molecular Simulation* Vol. 34, No. 9, August 2008, 1–48	0.02
Retention coefficient in TFA	*Anal. Biochem.* 124:201-208(1982)	0.02
thermodynamic transfer hydrophobicity;	*Molecular Simulation* Vol. 34, No. 9, August 2008, 1–48	0.02
Molar fraction (%) of 3220 accessible residues.	*Nature* 277:491-492(1979)	0.01
unfolding entropy change of hydration;	*Molecular Simulation* Vol. 34, No. 9, August 2008, 1–48	0.00
Retention coefficient in HPLC, pH 2.1	*Proc. Natl. Acad. Sci.* USA 77:1632-1636(1980)	-0.01
unfolding enthalpy changes of chain;	*Molecular Simulation* Vol. 34, No. 9, August 2008, 1–48	-0.01
Retention coefficient in HPLC, pH 7.4.	*Proc. Natl. Acad. Sci.* USA 77:1632-1636(1980)	-0.02
Average area buried on transfer from standard state to folded protein.	*Science* 229:834-838(1985)	-0.03
isoelectric point;	*Molecular Simulation* Vol. 34, No. 9, August 2008, 1–48	-0.04
refractive index;	*Molecular Simulation* Vol. 34, No. 9, August 2008, 1–48	-0.05
bulkiness;	*Molecular Simulation* Vol. 34, No. 9, August 2008, 1–48	-0.06
Bulkiness	*J. Theor. Biol.* 21:170-201(1968)	-0.07
Retention coefficient in HFBA.	*Anal. Biochem.* 124:201-208(1982)	-0.09
compressibility	*Molecular Simulation* Vol. 34, No. 9, August 2008, 1–48	-0.10
helical contact area	*Molecular Simulation* Vol. 34, No. 9, August 2008, 1–48	-0.12
Refractivity.	*J. Theor. Biol.* 50:167-184(1975)	-0.13
unfolding entropy changes of chain;	*Molecular Simulation* Vol. 34, No. 9, August 2008, 1–48	-0.15
Antigenicity value X 10.	*FEBS Lett.* 188:215-218(1985)	-0.16

Polarity.	*J. Theor. Biol.* 21:170-201(1968)	-0.16
partial specific volume;	*Molecular Simulation* Vol. 34, No. 9, August 2008, 1–48	-0.17
Average flexibility index	*Int. J. Pept. Protein. Res.* 32:242-255(1988)	-0.17
solvent-accessible surface area for denatured,	*Molecular Simulation* Vol. 34, No. 9, August 2008, 1–48	-0.18
Hydrophilicity scale derived from HPLC peptide retention times.	*Biochemistry* 25:5425-5431(1986)	-0.19
Hydrophobicity (free energy of transfer to surface in kcal/mole)	*Arch. Biochem. Biophys.* 161:665-670(1974)	-0.20
unfolding entropy change	*Molecular Simulation* Vol. 34, No. 9, August 2008, 1–48	-0.20
Atomic weight ratio of hetero elements in end group to C in side chain	*Science* 185:862-864(1974)	-0.20
unfolding Gibbs free energy changes of chain;	*Molecular Simulation* Vol. 34, No. 9, August 2008, 1–48	-0.20
Hydrophilicity.	*Proc. Natl. Acad. Sci.* U.S.A. 78:3824-3828(1981)	-0.21
flexibility (number of side-chain dihedral angles).	*Molecular Simulation* Vol. 34, No. 9, August 2008, 1–48	-0.23
Recognition factors	*Can. J. Chem.* 60:2606-2610(1982)	-0.23
mean r.m.s. fluctuational displacement;	*Molecular Simulation* Vol. 34, No. 9, August 2008, 1–48	-0.23
volume (number of nonhydrogen side-chain atoms)	*Molecular Simulation* Vol. 34, No. 9, August 2008, 1–48	-0.27
Molecular weight	Most textbooks	-0.28
molecular weight;	*Molecular Simulation* Vol. 34, No. 9, August 2008, 1–48	-0.28
polarity	*Molecular Simulation* Vol. 34, No. 9, August 2008, 1–48	-0.28
Conformational parameter for beta-turn.	*Protein Engineering* 1:289-294(1987)	-0.29
Polarity (p)	*Science* 185:862-864(1974)	-0.29

Hydrophobicity scale based on free energy of transfer (kcal/mole)	*Biophys J.* 47:61-70(1985)	-0.30
power to be at the C-terminal of a-helix;	*Molecular Simulation* Vol. 34, No. 9, August 2008, 1–48	-0.34
shape (position of branch point in a side chain);	*Molecular Simulation* Vol. 34, No. 9, August 2008, 1–48	-0.35
Normalized frequency for beta-turn.	*Biochemistry* 17:4277-4285(1978)	-0.39
turn, tendencies;	*Molecular Simulation* Vol. 34, No. 9, August 2008, 1–48	-0.39
coil tendencies;	*Molecular Simulation* Vol. 34, No. 9, August 2008, 1–48	-0.40
solvent-accessible surface area for native,	*Molecular Simulation* Vol. 34, No. 9, August 2008, 1–48	-0.40
Chou-Fasman method	*Molecular Simulation* Vol. 34, No. 9, August 2008, 1–48	-0.40
Conformational parameter for beta-turn (computed from 29 proteins)	*Adv. Enzym.* 47:45-148(1978)	-0.45
Conformational parameter for coil.	*Protein Engineering* 1:289-294(1987)	-0.47

List of Abbreviations

14-3-3	Family of conserved regulatory molecules
Å	Ångström
ANK repeat	33-residue motif consisting of two α-helices separated by loops
AQP0	Lens Aquaporin-0
ASIC	Acid-sensing ion channel
ATCV-1	Acanthocystis turfacea Chlorella Virus Type 1
C	Cavity
ClC	Chloride channel
CNG channel	Cyclic nucleotide gated channel
Cs^+	Ceasium ion
DNA	Desoxyribonucleic acid
DOPG	Dioleoylphosphatidylglycerol
DPPC	Dipalmitoylphosphatidylcholine
E. coli	*Escherichia coli*
EGFP	Enhanced green fluorescent protein
EsV-1	*Ectocarpus siliculosus* Virus 1
F	Filter
G	Gate
h	hour
H_v channel	Voltage-gated proton channel
HEK293	Human embryonic kidney 293 cell
HERG	Human eag-related gene
I/V-curve	Current-voltage relationship
K^+	Potassium ion
$[K^+]$	Potassium concentration
$[K^+]cav$	Potassium concentration in the cavity
KATP	ATP-sensitive potassium channel
Kesv	K^+ channel from *Ectocarpus siliculosus* Virus
kb	Kilobase
KcsA	K^+ channel from *Streptomyces lividans*
Kcv	K^+ channel Chlorella Virus

Kir2.1	Inward rectifier potassium channel 2.1
KirBac1.1	bacterial inwardly-rectifying K^+ channel
Kir channel	Inwardly rectifying potassium channel
K_v channel	Voltage-gated potassium channel
LGIC	Ligand-gated ion channel
Li^+	Lithium ion
M1 or M2	Transmembrane helices of KcsA
MD simulation	Molecular dynamics simulation
ml	Millilitre
mm	Millimetre
mM	Millimolar
mV	Millivolt
MT235	Phycodnavirus MT325, which infects Chlorella Pbi
MthK	K^+ channel from *Methanobacterium thermoautotrophicum*
MS channel	Mechanosensitive ion channel
MscL channel	Mechanosensitive channel of large conductance
μl	Mikrolitre
Na^+	Sodium ion
Na_v channel	Voltage-gated sodium channel
NaK	Na^+/K^+ conducting channel
NC64A	T*Chlorella* strain NC64A
nm	Nanometre
OD_{600}	optical density at 600 nm
P or P loop	Pore or Pore loop
pA	Picoampere
PBCV-1	*Paramecium bursaria* Chlorella Virus Type 1
PC	Phosphatidylcholin
PDB	Protein Database
pH	$pH = -\log_{10}(a_H)$
PI	Phosphatidylinositol
pK_a	$pK_a = -\log_{10}(K_a)$
PS	Phosphatidylserin

Rb$^+$	Rubidium ion
rpm	Revolutions per minute
S2	second TMD of 6TMD motif channels
S3	third TMD of 6TMD motif channels
S4	Fourth TMD of 6TMD motif channels; voltage sensor
TM	Transmembrane
TMD	Transmembrane domain
TRK1	Transport of potassium 1
TRP channel	Transient receptor potential channel
VGCC	Voltage-gated calcium channel
wt	wildtype

Amino acids

A	Ala	Alanine	N	Asn	Asparagine
C	Cys	Cysteine	P	Pro	Proline
D	Asp	Asparatic acid	Q	Gln	Glutamine
E	Glu	Glutaminic acid	R	Arg	Arginine
F	Phe	Phenylalanine	S	Se	Serine
G	Gly	Glycine	T	Thr	Threonine
H	His	Histidine	V	Val	Valine
I	Ile	Isoleucine	W	Trp	Tryptophan
K	Lys	Lysine	Y	Tyr	Tyrosine
L	Leu	Leucine	X		Unspecified or unknown amino acid
M	Met	Methionine			